AD-A071 099 NAVAL RESEARCH LAB WASHINGTON DC F/G 20/3
AN MHD INSTABILITY PRIMER.(U)
JUN 79 W MANHEIMER, C LASHMORE-DAVIES
UNCLASSIFIED NRL-MR-4000 NL

1 OF 2
AD A071099

NRL Memorandum Report 4000

An MHD Instability Primer

WALLACE MANHEIMER

Plasma Theory Branch
Plasma Physics Division

AND

CHRIS. LASHMORE-DAVIES

Theory Division
Culham Laboratory
Abingdon, England

June 29, 1979

NAVAL RESEARCH LABORATORY
Washington, D.C.

SECURITY CLASSIFICATION OF THIS PAGE (When Data Entered)

REPORT DOCUMENTATION PAGE

READ INSTRUCTIONS BEFORE COMPLETING FORM

1. REPORT NUMBER: NRL Memorandum Report 4000	2. GOVT ACCESSION NO. (14) 3. RECIPIENT'S CATALOG NUMBER: NRL-MR-4000
4. TITLE (and Subtitle): (6) AN MHD INSTABILITY PRIMER	5. TYPE OF REPORT & PERIOD COVERED: (9) Interim report on a continuing NRL problem.
	6. PERFORMING ORG. REPORT NUMBER
7. AUTHOR(s): (10) W. Manheimer and Chris. Lashmore-Davies*	8. CONTRACT OR GRANT NUMBER(s)
9. PERFORMING ORGANIZATION NAME AND ADDRESS: Naval Research Laboratory, Washington, D.C. 20375	10. PROGRAM ELEMENT, PROJECT, TASK AREA & WORK UNIT NUMBERS: NRL Problem H02-37
11. CONTROLLING OFFICE NAME AND ADDRESS: U.S. Department of Energy, Washington, D.C. 20545 (11) 24	12. REPORT DATE: June [illegible]79
	13. NUMBER OF PAGES: 143
14. MONITORING AGENCY NAME & ADDRESS (if different from Controlling Office) (12) 141 p.	15. SECURITY CLASS. (of this report): UNCLASSIFIED
	15a. DECLASSIFICATION/DOWNGRADING SCHEDULE

16. DISTRIBUTION STATEMENT (of this Report)

Approved for public release; distribution unlimited.

17. DISTRIBUTION STATEMENT (of the abstract entered in Block 20, if different from Report)

18. SUPPLEMENTARY NOTES

This research was sponsored by the U.S. Department of Energy.

*Theory Branch, Culham Laboratory, Abingdon, England.

19. KEY WORDS (Continue on reverse side if necessary and identify by block number)

MHD instability
Magnetic reconnection
Controlled thermonuclear fusion

20. ABSTRACT (Continue on reverse side if necessary and identify by block number)

This report is a simple, self-contained treatise on MHD instabilities in plasmas. It is the result of a one year work assignment for one of us (WMM) at the Culham Laboratory in Abingdon, England.

DD FORM 1 JAN 73 1473 EDITION OF 1 NOV 65 IS OBSOLETE S/N 0102-014-6601

SECURITY CLASSIFICATION OF THIS PAGE (When Data Entered)

251 950

CONTENTS

AN MHD INSTABILITY PRIMER

Introduction

This NRL memo report provides what we hope is a relatively simple, self contained description of MHD instabilities. It is the result of a one year sabbatical (Sept. 77 - Sept. 78) one of us (WMM) spent at Culham Laboratory in Abingdon, England. The principle purpose of this sabbatical was to learn the modern theory of MHD instabilities. During the year there, the two of us worked very closely in our attempt to learn this field. In this endeavor, we each received a tremendous amount of help from Dr. John Wesson, also of Culham.

Although there are many plasma physicists who have had much more experience in this area than we have, we feel that having just learned it ourselves makes us particularly sympathetic to the problems someone has in trying to learn about MHD instabilities for the first time. Indeed one of the problems of this field seems to be that it is extremely difficult for someone to learn it by reading the primary references. This has led to a situation where a relatively small number of researchers have gotten far ahead of the rest of the plasma physics community. Our feeling is that scientific endeavors will make more rapid progress if knowledge is broadly based. Thus we feel that there is a need to make contact between researchers in MHD and the rest of the community. Our intention here is to help provide this link up; in doing so we hope to provide a service not only for those who would like to learn this area, but also for those who already know it.

One deceptive aspect of MHD instabilities is that the simplest ones are extremely easy to understand. For instance the instabilities of a Z pinch to sausage and kind displacements have been described in such standard

Note: Manuscript submitted April 3, 1979.

texts as Jackson's Classical Electrodynamics. However more complicated instabilities, for instance in a plasma where both an axial and azimuthal field are present are much more difficult to visualize; but they are also much more interesting and fun to learn.

Although, as we will see, there is a tremendous variety of MHD instabilities, all those which we will study (and we cover most of the major ones) are driven by one of two mechanisms. First of all there may be a gravity (or something equivalent to a gravitational force) which is opposite to the density gradient. This can drive Raleigh-Taylor type instabilities. This is the fundamental driving force behind both ideal and resistive pressure driven modes in a reversed field pinch, ballooning modes in a tokamak, rotationally driven modes in a θ pinch and the mirror instability in a magnetic mirror whose field lines bulge outward away from the plasma. Second, a plasma which carries a current is potentially unstable because current elements traveling in the same direction attract each other and would like to all clump up together. Of course this is not so simple because the current flows through a conducting fluid and, as will be amply demonstrated, this imposes all sorts of constraints. Nevertheless, this mutual attraction of like current elements is the basic mechanism which drives free surface modes in a cylindrical or toroidal plasma; tearing modes in plane, cylindrical and tokamak geometry, and the internal $m = 1$ kink tearing mode in cylindrical or tokamak geometry.

There are other views we have on this area which affected the material we chose to cover. First of all, we de-emphasized both the energy principle and also modes in a plasma with a free surface. At least for one dimensional configurations (that is plasmas where all variation is in one direction), which we emphasize, it is really no simpler to utilize the energy principle

than it is to solve for the eigenfunction and eigenvalue. This is especially true now, where second order ordinary differential equations can be so easily solved numerically. However we could hardly write this memo and make no mention of the energy principle since it is widely used. Therefore one chapter is devoted to it.

As far as free surfaces are concerned, first of all it is rare that plasmas have free surfaces; usually experimental plots of say density or temperature profile usually show them going smoothely to zero with radius. Secondly, free surfaces are not particularly difficult to understand, but applying boundary conditions across them in their unperturbed and perturbed state can involve a great deal of mathematical complexity. Therefore, they do not seem to be worth expending a great deal of effort on in a manuscript like ours which attempts to emphasize physical principle, not mathematical detail. Hence we deal with free surfaces in only one chapter in which we drive some fundamental stability requirements for tokamak plasmas.

One thing which we attempt to emphasize however is magnetic reconnection. As we will see shortly, in ideal MHD, each magnetic field line maintains its integrity and behaves rather like a string which threads the fluid and cannot break. However there are flow patterns which force two magnetic field lines together. Often non ideal effects, for instance resistivity, can cause the field lines to break and reconnect. Not only is reconnection very much in vogue these days, it is also extremely interesting in its own right. Even if a plasma physicist does not want to work on tearing modes, it might still be worth learning about them for the sheer joy of it.

The outline of the remainder of this memo is as follows. Chapter II introduces MHD and Chapter III proves the energy principle. Chapter IV discusses free surface modes in a cylindrical. Chapter V looks at gravity

driven modes and shows how magnetic shear can stabilize them. Chapter VI shows how the presence of resistivity can destabilize gravity modes which have been shear stabilized. Chapter VII examines the tearing mode in slab geometry and shows how instabilities which are forbidden in ideal MHD are possible if magnetic reconnection is allowed. Chapter VIII looks at how all of these instabilities transform when going from slab to cylindrical geometry, and Chapter IX briefly discusses the additional complications of toroidal geometry.

II. Introduction to MHD

The Magnetohydrodynamic equations, which form the subject of this work are taken as

$$\frac{\partial \rho}{\partial t} + \nabla \cdot \rho \underline{V} = 0 \qquad \text{(II 1)}$$

(mass conservation),

$$\rho \frac{\partial \underline{V}}{\partial t} + \rho (\underline{V} \cdot \nabla) \underline{V} = - \nabla p + \frac{1}{c} \underline{J} \times \underline{B} \qquad \text{(II 2)}$$

(momentum conservation assuming scalar pressure)

$$\frac{1}{c} \frac{\partial \underline{B}}{\partial t} = - \nabla \times \underline{E} \qquad (a)$$

$$\nabla \cdot \underline{B} = 0 \qquad (b) \qquad \text{(II 3)}$$

$$\nabla \times \underline{B} = \frac{4\pi}{c} \underline{J} \qquad (c)$$

(Maxwells equations). In Maxwell's equations, the displacement current is neglected; instead the electric field is related to the current through Ohms law

$$\underline{E} + \frac{\underline{V}}{c} \times \underline{B} = \eta \underline{J} \qquad \text{(II 4)}$$

where $\underline{E} + \frac{\underline{V}}{c} \times \underline{B}$ is the electric field in the reference frame moving with the (nonrelativistic) fluid velocity and η is the resistivity. The only other quantity needed is the pressure. We will assume an adiabadic law

$$\left(\frac{\partial}{\partial t} + \underline{V} \cdot \nabla \right) \left(\frac{p}{\rho^\gamma} \right) \equiv \frac{d}{dt} \left(\frac{p}{\rho^\gamma} \right) = 0 \qquad \text{(II 5)}$$

Equations (II 1) through (II 5) constitute a complete description of the system. The unknowns are density, pressure and the three components of magnetic field, electric field, current density and fluid velocity, fourteen in all. Equations (II 1 and 5) are two scalar equations for ρ and p,

Eqs. (II 2, 3c and 4) are three vector equations for the three components of $\underline{v}$, $\underline{J}$ and $\underline{E}$, and finally Eq. (II 3 a and b) are equations for the solenoidal and irrotational parts of $\underline{B}$.

Usually, it is convenient to eliminate $\underline{E}$ and $\underline{J}$ directly by using Eqs. (II 3c and 4). Doing so, the momentum equation and Maxwell's equation become

$$\rho \frac{d\underline{v}}{dt} = -\underline{\nabla} p + \frac{1}{4\pi} (\underline{\nabla} \times \underline{B}) \times \underline{B} \tag{II 6}$$

and

$$\frac{\partial \underline{B}}{\partial t} = \underline{\nabla} \times (\underline{v} \times \underline{B}) - \frac{\eta c^2}{4\pi} \underline{\nabla} \times (\underline{\nabla} \times \underline{B}) \tag{II 7}$$

Much of our discussion will concern perfectly conducting Fluids ($\eta = 0$) so that Eq. (II 7) is

$$\frac{\partial \underline{B}}{\partial t} = \underline{\nabla} \times (\underline{v} \times \underline{B}) \tag{II 8}$$

Equations (II 1, 5, 6 and 7 or 8) form a complete description of the magnetized conducting fluid. Derivations of these equations as well as discussions of their validity and possible extensions (for instance including tensor pressure, thermal conduction, finite Larmor radius, etc.) have been discussed in many textbooks on plasma physics. We simply assume these equations describe the plasma and investigate their consequences; particularly we focus on how the magnetic field couples to the fluid motion.

Before doing this, it is worthwhile to quickly review what magnetic field lines and flux tubes are. Any vector field has streamlines. For the magnetic field, these are the solution of

$$\frac{dx}{B_x} = \frac{dy}{B_y} = \frac{dz}{B_z} \tag{II 9}$$

The field lines are then everywhere parallel to the magnetic field. Let us now imagine an element of area $\delta\underline{A}$ which is parallel to a field line at some point s on the field line. If the magnetic field at this point has strength B(s), the flux through this element of area is $\delta\phi = \underline{B}(s)\ \delta\underline{A} \equiv B(s)\cdot\delta A$. One can then imagine a tube of constant flux around the field line. If the flux is $d\phi$, the area of the flux tube as a function of distance along the field line is given by

$$\delta A(s) = \frac{\delta\varphi}{B(s)} \qquad \text{(II 10)}$$

The amazing thing about a flux tube is that in a perfectly conducting plasma ($\eta = 0$), which we will refer to as ideal MHD, a flux tube is convected with the flow. It is a simple matter to prove this from Eq. (II 7). Integrating Eq. (II 7) over a fixed area δA, we find

$$d(\delta\varphi) = dt \oint d\underline{s}\cdot(\underline{v}\times\underline{B}) = \oint (d\underline{s}\times\underline{v}dt)\cdot\underline{B} \qquad \text{(II 11)}$$

where $\oint ds$ is an integral around the closed line bounding $\delta\phi$. However $d\underline{s} \times \underline{v}\ dt$ is the area swept out by an element ds of the periphery of the flux loop. The term on the right hand side of Eq. (II 11) is then negative the flux swept out by the circumference in its trajectory. Therefore, the total flux through a surface area moving with the fluid does not change time, or

$$\frac{d\varphi}{dt} = 0 \qquad \text{(II 12)}$$

Perhaps a more direct way to see this is to note that if $\eta = 0$, Ohms law Eq. (II 4), simply says that E = 0 as one moves with the fluid. However in the inertial frame locally moving with the fluid, Maxwells equation says that the rate of change of the enclosed flux is minus the loop voltage, that is zero.

While the magnetic lines of force are well defined by Eq. (II 9), in general there is no unique way to define the motion of lines of $\underline{B}$ in a changing medium. However in a perfectly conducting fluid, the flux is frozen into the flow. Since the flux tubes can be regarded as bundles of field lines, one can equally look upon the field lines themselves as being carried along with the flow. We will now examine just what this means. Since $\nabla \cdot B = 0$, the field lines have no start or finish, but either close on themselves or else have infinite length. Since they are frozen into the flow, the field lines cannot reconnect, or in other words, the topological properties of the field is maintained. That is, the field line can stretch and bend, but it cannot change its topology.

Let us illustrate this for two dimensional motion. Say the field line initially is the dotted circle shown in Fig. (II 1a). Since the velocity field is a single valued function of $\underline{r}$ for all time, there is no way that two fluid elements initially far from each other can ever occupy the same point; to do so would mean the fluid elements pass through each other, implying a double valued velocity field. Therefore, while a complicated flow pattern can greatly contort the field line, to for instance the solid line in Fig. (II 1a), the field line can never cross itself, it always has a single inside and outside. Thus the topological properties of the field line are maintained. One possible flow pattern could distort two nearby field lines to a pattern shown in Fig. (II 1b). While the two points near A can be arbitrarially close, the field line still must maintain its integrity. However as we will see in later chapters, the presence of non ideal effects, for instance resistivity, can relax the topological constraint so that the field line can break and reconnect, forming that pattern in Fig. II 1c. Clearly the topology has changed from a simple closed curve topology to a

figure eight. That is there are two inner regions instead of one and two sets of closed field lines.

As another example the topological constraints on the field line motion, we will consider an example in three dimensions. Consider two field lines which are initially parallel to each other shown in Fig. (II 2a). (In order to distinguish which field line is in front of the other, each line is shown with finite width and different shading). Imagine a flow pattern which distorts the field line, but which renders this field line periodic in space with periodicity length L, and which has $v = 0$ along the dark field line.

Since the lighter field line is frozen into the flow, it cannot wind around the dark field line between $Z = 0$ and $Z = L$. For instance, if the fluid winds around the inner field line at say $Z = L/2$, but does not move at $Z = 0$ and $Z = L$, the shaded line winds around the dark line as shown in Fig. (II 2b). Between $Z = 0$ and $Z = L/2$, the shaded line winds around the dark line, but between $Z = L/2$ and $Z = L$ it unwinds. The total winding number of the shaded line around the dark, between $0<Z<L$, is preserved at zero.

However another type of fluid motion might give rise to the field lines shown in Fig. (II 2c). The topology of the shaded line is the same as shown in Fig. (II 2a and b). That is, if one pulled the field line at $Z = 0$ and $Z = L$, it would snap back to that shape in Fig. (II 2a). Notice though that near the point marked A, two parts of the field line are forced close together. Again, the presence of non-ideal effects could cause the field line there to break and reconnect as shown in Fig. II 2d where now two sets of field lines are produced, the main field line which now loops around the axis, and an additional circle which also loops the axis. Thus, in ideal

MHD if a field line does not wind around another initially, it never does. However if non-ideal effects (for instance resistivity) are allowed, the field lines may break and reconnect and then wind around another field line which it did not initially encircle. In other words, new magnetic axes can be generated.

To summarize, the field lines in a magnetized fluid can be regarded as strings which thread the fluid and go wherever the fluid goes. They can stretch and bend but cannot break or reconnect in ideal MHD. However if non-ideal effects are allowed, the field lines can break and reconnect. Obviously, however, since div·B = 0, a field line cannot break unless it reconnects instantaneously with another part of the field line (or with a different field line). As we will see, there are types of fluid motion which tend to force different portions of field lines together, as shown at points A in Fig. (II 1b and II 2c). In this case, often a very small amount of resistivity can cause reconnection at these points. In other words, given a choice between evolving toward a very complicated structure with the same topology, or a simple structure with different topology, a field line in a real plasma will often choose the latter.

We now turn to a study of the magnetic forces exerted on the plasma. The magnetic force per unit volume is given by

$$\underline{F}_m = \frac{1}{c}\,\underline{J} \times \underline{B} \qquad \text{(II 13)}$$

which is clearly always perpendicular to both $\underline{B}$ and $\underline{J}$. A more convenient form for $\underline{F}_m$ is

$$\underline{F}_m = \frac{1}{4\pi}\left(\nabla \times \underline{B}\right) \times \underline{B} = -\frac{1}{8\pi}\,\nabla B^2 + \frac{1}{4\pi}\left(\underline{B}\cdot\nabla\right)\underline{B} \qquad \text{(a)}$$

$$= -\frac{1}{8\pi}\,\nabla_\perp B^2 + \frac{B^2}{4\pi}\left(\underline{i}_b \cdot \nabla\right)\underline{i}_b \qquad \text{(b)}$$

(II 14)

In Eq. (II 14b) above $\underline{\nabla}_\perp$ means the portion of the gradient which is perpendicular to $\underline{B}$ and $\underline{i}_b$ is a unit vector in the direction of $\underline{B}$.

The two terms in Eq. (II 14b) have simple interpretation. The first term shows that the magnitude of B^2 acts like a pressure in a direction perpendicular to $\underline{B}$. That is a gradient in B^2 exerts a force which pushes the plasma toward regions of lower B^2. To interpret the second term, note that $(\underline{i}_b \cdot \underline{\nabla})\underline{i}_b = \underline{i}_R / R$ where R is the radius of curvature of the field line and $\underline{i}_R$ is a unit vector pointing toward the center of curvature. Thus if the field lines are bent, there is a force exerted on the plasma of magnitude $\frac{B^2}{4\pi R}$ and directed toward the center of curvature. This latter force acts rather as if the field line were a rubber band. If a stretched rubber band is bent, a force is exerted which tends to snap it back to a straight line. This then corresponds to the way a magnetic field line acts. The main difference is, of course, that a stretched bent rubber band exerts a strong force along its length as well as perpendicular to itself; the bent magnetic field line only exerts this force perpendicular to itself but not along its length. Fig. (II 3) illustrates the force exerted on the plasma by the two terms in Eq. (II 14b).

Clearly, before we can concern ourselves with MHD instabilities, a first step is an examination of MHD equilibria. In equilibrium, with $V = \frac{\partial}{\partial t} = 0$, the momentum conservation equation is

$$\underline{\nabla} p = \frac{1}{c} \underline{J} \times \underline{B} = -\frac{1}{8\pi} \underline{\nabla} B^2 + \frac{1}{4\pi} (\underline{B} \cdot \underline{\nabla}) \underline{B} \qquad \text{(II 15)}$$

There are several immediate consequences of Eq. (II 15). First of all, it is easy to show that the pressure must be constant along a field line; simply take dot product of Eq. (II 15) with $\underline{i}_b$ and get the result

$$(\underline{i}_b \cdot \underline{\nabla}) P = 0 \qquad \text{(II 16)}$$

so the pressure is constant along a field line. Therefore any open ended device, for instance a magnetic mirror, where field lines end on walls, cannot be in MHD equilibrium, at least for scalar pressure. It is for this reason that the research on open ended devises usually concerns itself principly with Vlasov equilibria and stability or else with tensor pressure.

For the remainder of this chapter we will concern ourselves with devices with enclosed field lines, for instance tokamaks, reversed field pinches, or infinitely long cylinders. As a field line goes around a toroidal machine, there are three possibilities; first, it may close on itself after one or more transits; second, it may trace out a surface, and third, it may ergodigally fill a volume, which may be either the entire volume of the torus or a portion of it. In MHD equilibrium, the pressure is constant along each magnetic line, surface or volume, whatever the case may be. Clearly, if the field lines fill the volume of the device, no MHD equilibrium is possible.

In the case of reverse field pinches or tokamaks, the field lines form surfaces. From Eq. (II 15), it is possible to show that the current lines are also in the flux surfaces. To do so, take the dot product with $\underline{J}$ which shows that P = constant along the lines of $\underline{J}$. However if P varies from one flux surface to the next, then lines of $\underline{J}$ must also lie in the surfaces of constant P that is the flux surfaces.

In a general toroidal equilibrium, it is usually convenient to choose as one co-ordinate surface,the flux surface. This gives rise to the Grad-Shafranov equation and is discussed in Appendix _____. For our purposes here, we only write the pressure balance equation in cylindrical geometry with variation only in r. These are

$$B_r = 0$$

$$0 = \frac{d}{dr}\left(p + \frac{B_z^2}{8\pi} + \frac{B_\theta^2}{8\pi} \right) + \frac{1}{4\pi} \frac{B_\theta^2}{r} \qquad \text{(II 17)}$$

Once p and B_z are given, Eq. (II 17) can be solved for the appropriate B_θ for equilibrium.

Having discussed the steady state equilibrium, we now proceed to a discussion of the dynamics by examining what sort of wave motion is allowed in a uniform, magnetized, current free conducting fluid. Denoting an unperturbed (equilibrium) quantity with a subscript zero and a perturbed quantity with no subscript, the linearized equations of motion are

$$\rho_0 \frac{\partial \underline{V}}{\partial t} = - \frac{\gamma p_0}{\rho_0} \underline{\nabla} \rho + \frac{1}{4\pi} \left(\underline{\nabla} \times \underline{B} \right) \times \underline{B}_0 \qquad \text{a)}$$

$$\frac{\partial \rho}{\partial t} + \rho_0 \underline{\nabla} \cdot \underline{V} = 0 \qquad \text{b)} \qquad \text{(II 18)}$$

$$\frac{\partial \underline{B}}{\partial t} = \underline{\nabla} \times \underline{V} \times \underline{B}_0$$

where we have made use of the adiabatic relation between ρ and p. Taking $\frac{\partial}{\partial t}$ of Eq. (II 18) and substituting from Eq. (II 18 b and c), we find a single vector equation for $\underline{V}$. Assuming $\underline{\nabla} = i\underline{k}$ and $\frac{\partial}{\partial t} = -i\omega$, it is

$$-\omega^2 \underline{V} = - c_s^2 \underline{k} (\underline{k} \cdot \underline{V}) + V_A^2 \, \underline{i}_z \times \left[\underline{k} \times \left\{ \underline{k} \times (\underline{V} \times \underline{i}_z) \right\} \right] \qquad \text{(II 19)}$$

where c_s is the sound speed, $c_s = \left(\gamma p_0 / \rho_0 \right)^{1/2}$ and V_A is the Alfven speed $V_A = B_0 / \sqrt{4\pi\rho_0}$. Also $\underline{B}_0$ is assumed to be in the z direction. Since the plasma is isotropic in the x-y plane, we may take $\underline{k}$ to be in the yz plane

without loss of generality. Then taking the component forms of Eq. (II 19), gives

$$\omega^2 V_x = k_z^2 V_A^2 V_x \qquad (a)$$

$$\omega^2 V_y = k_y c_s^2 (k_y V_y + k_z V_z) + (k_y^2 + k_z^2) V_A^2 V_y \qquad (b) \qquad \text{(II 20)}$$

$$\omega^2 V_z = k_z c_s^2 (k_y V_y + k_z V_z) \qquad (c)$$

As is clear from Eq. (II 20a), the x velocity decouples and this is the shear Alfven wave with dispersion relation

$$\omega^2 = k_z^2 V_A^2 = k^2 V_A^2 \cos^2\theta \qquad \text{(II 21)}$$

k being the magnitude of $\underline{k}$ and θ being the angle between $\underline{B}$ and $\underline{k}$. The other modes involve the coupled y and z motion. A straightforward calculation from Eqs. (II 20 b and c) gives the result

$$\frac{\omega^2}{k^2} = \frac{(V_A^2 + c_s^2) \pm \left((V_A^2 - c_s^2)^2 + 4 c_s^2 V_A^2 \sin^2\theta\right)^{1/2}}{2} \qquad \text{(II 22)}$$

For $\theta = 0$, the two roots are $\omega^2/k^2 = c_s^2$ and V_A^2, while for $\theta \approx \pi/2$, the two roots are $\omega^2/k^2 \approx c_s^2 + V_A^2$ and $\omega^2/k^2 \approx c_s^2 \cos^2\theta/(1 + c_s^2/V_A^2) \approx 0$. A polar plot ω/kV_A for the three roots is shown in Fig. (II 4) for the case of $V_A = 3c_s$. Figure (II 4) shows that waves in a magnetized fluid have some interesting properties. Since the shear Alfven wave (Eq. (II 21)) has $V_y = V_z = 0$, it does not compress the plasma. At $\theta = 0$, the sound wave does compress the plasma, but by following this root around to $\theta = \pi/2$ where $\omega = 0$, one can show

that there is no plasma compression there. On the other hand, at $\theta = 0$, the wave which has $\omega/k = V_A$ does not compress the plasma; however following the root around to $\theta = \pi/2$, where $\omega^2/k^2 = V_A^2 + c_s^2$, we see that the plasma is compressed. Thus if $V_A > c_s$, there is *no* such thing as a pure sound wave. What starts out as a compressional wave at $\theta = 0$ ends up as a shear wave at $\theta = \pi/2$, and visa versa. However if $c_s > V_A$, the sound wave is compressional at all angles.

We now give simple physical pictures first for the shear Alfven wave for $\theta = 0$ and then for the compressional Alfven (magnetosonic) wave at $\theta = \pi/2$. Imagine that each fluid element is displaced in the x direction an amount

$$x = x_0 \cos kz \tag{II 23}$$

Since the field line is frozen into the flow, Eq. (II 23) above is also the equation for a field line. The perturbed field $B_{x-x}\underline{i}$ is perpendicular to the equilibrium field, $B_o\underline{i}_z$, so there is no first order change in the magnitude of $\underline{B}$. Hence the only force on the fluid arises from the bending of the field line, as discussed after Eq. (II 14). If terms of order x_o^2 are neglected, the reciprocal of the radius of curvature of the field line is

$$\underline{R}^{-1} = -k^2 x_0 \cos kz \; \underline{i}_x \tag{II 24}$$

Therefore the force per unit volume on each fluid element is

$$\underline{F}_m = -\frac{B_o^2 k^2}{4\pi} \underline{i}_x x_0 \cos kz \tag{II 25}$$

which is just minus a constant times the displacement of the fluid element. That is, each fluid element performs simple harmonic oscillation with

frequency given by $\omega^2 = k^2 B_o^2/4\pi\rho_o$ perpendicular to the equilibrium magnetic field. The phase speed of this wave is the Alfven speed.

One can picture this oscillation in terms of the magnetic field lines constituting a series of strings which permeate the plasma. Imagine pulling on these strings with a tension of $B^2/4\pi$ per unit area. Then if the strings are bent, they will tend to snap back and oscillate about their equilibrium position with frequency $k^2B^2/4\pi\rho$.

Therefore as far forces perpendicular to themselves are concerned, the magnetic field lines are like strings with tension $B^2/4\pi$ per unit area. They are different however, in that unlike a stretched string there is no force along a magnetic field line.

We now turn to an examination of wave motion across a magnetic field. Say that B_o is in the z direction and the displacement and wave number are both in the y direction. In this case, the field lines remain straight and do not bend. Therefore, according to Eq. (II 14b), the force density on the plasma is minus the gradient of the scalar magnetic pressure. This perturbed magnetic pressure is

$$P_M = \frac{B_o B_z}{4\pi} = \frac{B_o^2}{8\pi}\,2\,\frac{B_z}{B_o} = \frac{2P_{Mo}}{\rho_o}\rho \qquad \text{(II 26)}$$

where we have used the fact that the field is frozen into the plasma so $\rho/\rho_o = B_z/B_{zo}$ (Also this can be easily verified from Eqs. (II 18b and c).). Hence the magnetic scalar pressure acts like a fluid with $\gamma = 2$. The perturbed fluid pressure is of course $\left(\gamma P_o/\rho_o\right)\rho$ so that the perturbed total pressure in the plasma is given by

$$P_{TOT} = \left(\frac{\gamma P_o}{\rho_o} + 2\,\frac{P_{Mo}}{\rho_o}\right)\rho \qquad \text{(II 27)}$$

Now it is clear that perpendicular to the field, waves propagate like sound waves, except that the magnetic field adds an extra 'springiness' to the plasma.

We conclude this chapter with a discussion of what sort of plasma motion an MHD instability is likely to generate. The modes we have discussed all have $\omega^2 > 0$. However for instability, obviously $\omega^2 < 0$. Now imagine that there is some physical effect which perturbs the system so as to drive the plasma toward instability. Clearly this effect will manifest itself by lowering ω^2. However if ω^2 is large to begin with, instability, in general, will not result, but instead just a lowering of the frequency. Clearly, the most likely place for instability is where $\omega^2 = 0$, or for incompressible flow with $\underline{k}\cdot\underline{B} = 0$, according to Fig. II 4 and the discussion following Eq. (II 22). In other words, if $k\cdot B \neq 0$, the unstable flow will couple to shear Alfven waves, which is a stabilizing effect; and if $\nabla\cdot V \neq 0$, it will couple to sound or magnetosonic waves, which is also stabilizing. In most of the rest of this book, we focus on perturbed plasma motion which is incompressible. This does not mean, of course, that the plasma is impossible to compress, but rather that the motions we consider have phase speed much less than the magnetosonic speed and are therefore decoupled from compressional motion. This is no different from any other fluid which is assumed to be incompressible. For instance with regard to paddling a canoe, water is incompressible; however sound does propagate through, and does compress it.

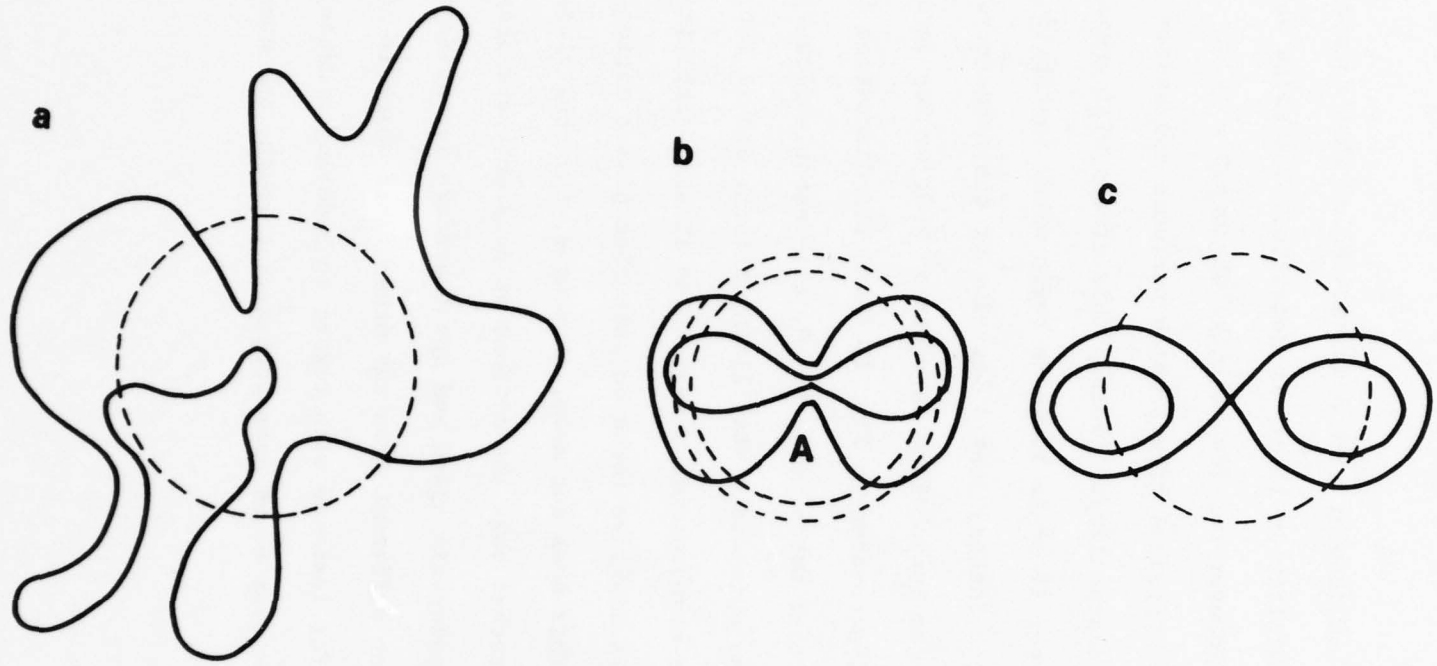

Fig. II 1(a) — A possible contortion of a field in two dimensions which preserve the topological constraint, (b) another motion which also preserves the topology by showing how field lines can be forced together, and (c) a field line pattern similar to 2(b), but where reconnection is allowed.

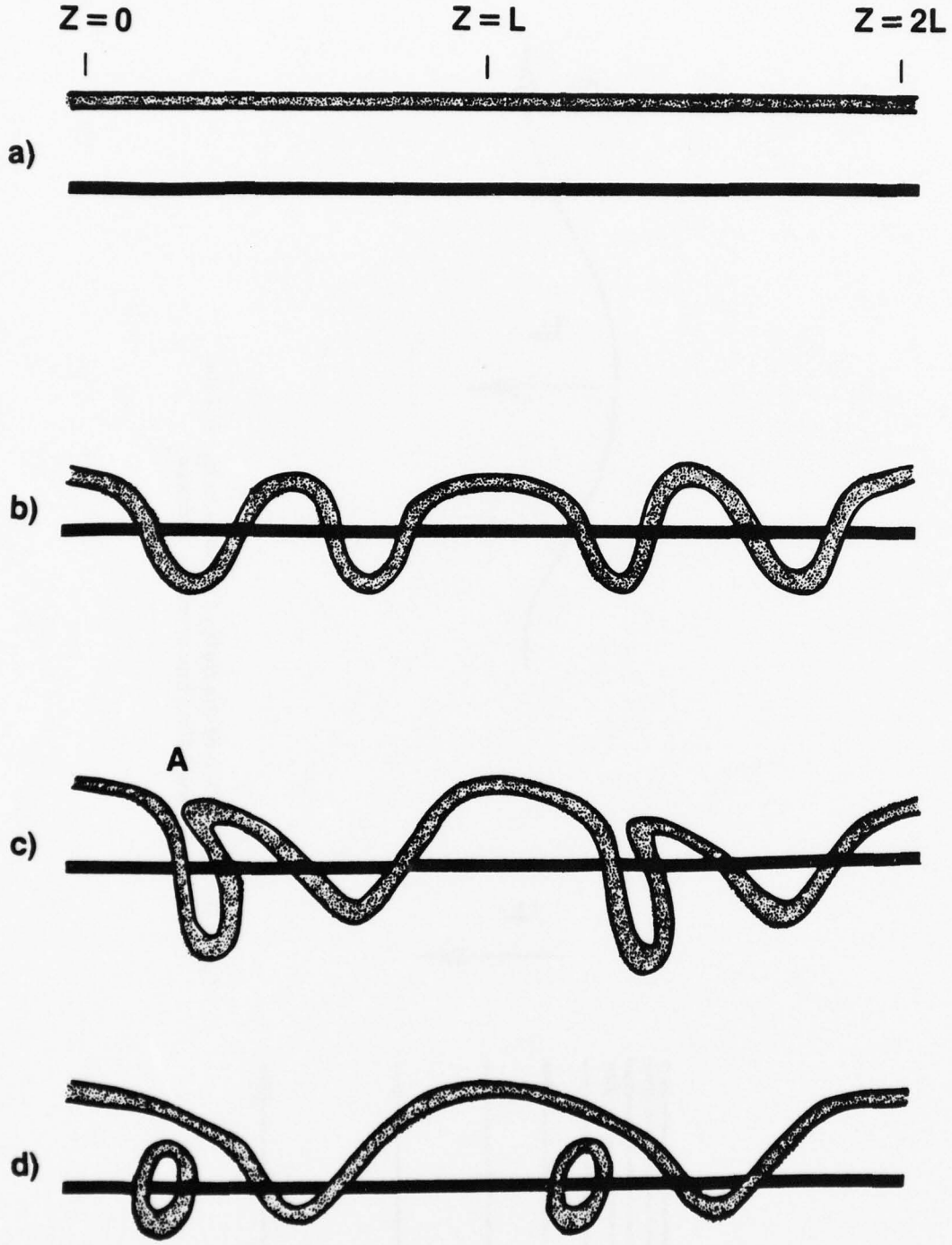

Fig. II 2 — (a) Two neighboring field lines, (b) distortion of one field line which preserves winding number, (c) distortion which preserves winding number but which forces field lines together, (d) field pattern similar to 2(d), but which allows reconnection. Note that winding number is no longer conserved, but dotted field line winds around dark one.

Fig. II 3 — Illustration of the force, a gradient in $B_\perp$, and the force a curved field line exerts on a plasma.

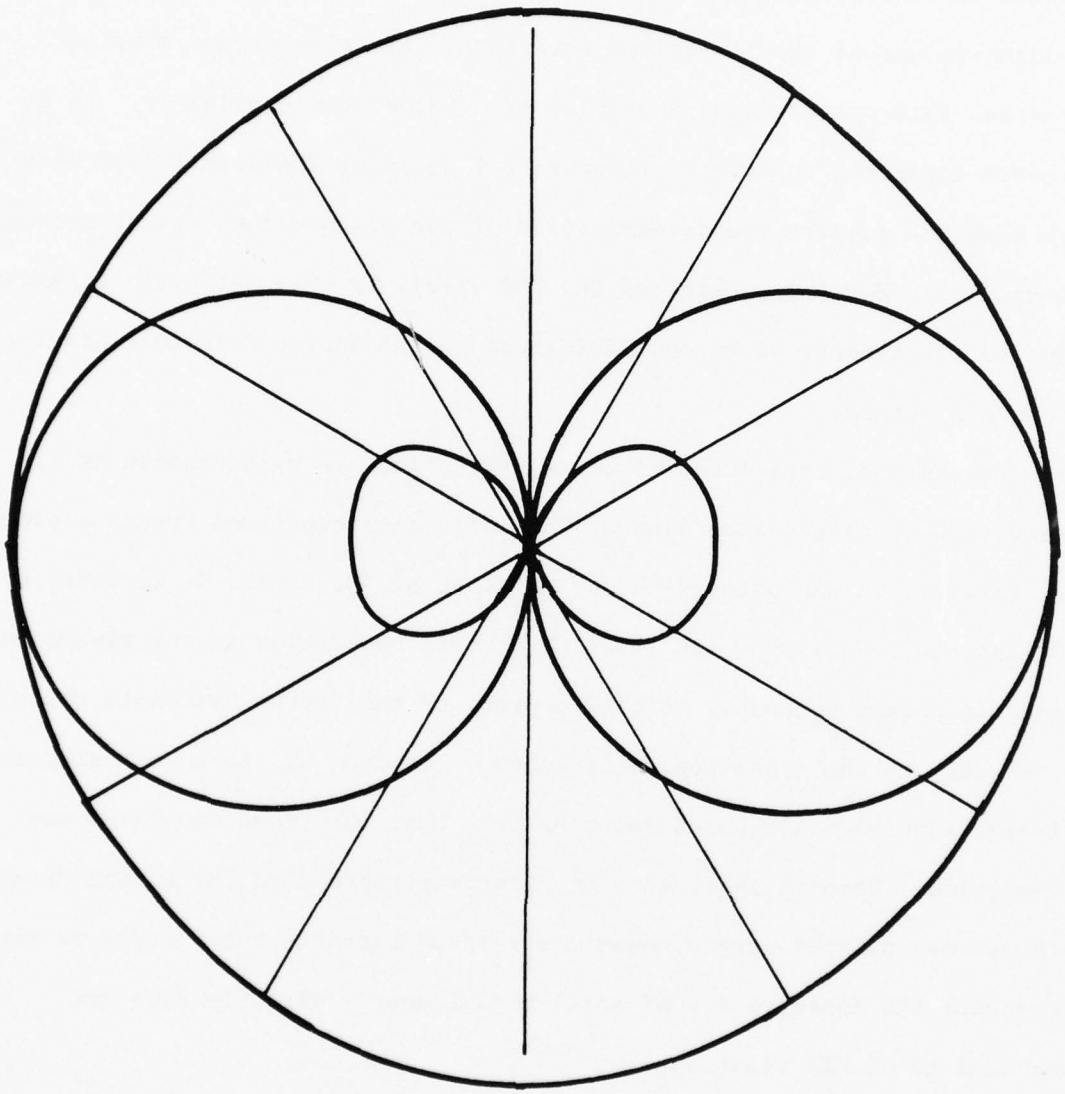

Fig. II 4 — A polar plot of phase velocity versus angle to the magnetic field for the three branches of MHD oscillation.

III. The Energy Principle

A complete solution of the linear stability of a plasma for a given magnetic field configuration requires the determination of eigen-functions and eigen-values of the linearized equations. For all but the simplest geometries this proves to be a problem of considerable complexity. It is therefore desirable to have a procedure for deciding the question of stability which does not require the determination of the eigen-values (or characteristic frequencies). For the problem of the MHD stability of a perfectly conducting plasma in the absence of an equilibrium flow, the Energy Principle provides just such a method.

The original derivation of the Energy Principle by Bernstein et al assumed that the eigen-functions of the linearized equations formed a complete set. However, it was pointed out by Laval et al (G. Laval, C. Mercier, and R. Pellat, Nucl Fusion 5, 156 (1965)) that this assumption is not always valid so that it became necessary to find a proof of the Energy Principle which did not rely on the completeness property. Laval et al, in a very elegant analysis, provided this proof assuming only that the linear operator was self-adjoint. Here we shall give an alternative proof of the Energy Principle which assumes neither completeness nor self-adjointness but instead we shall demonstrate the conservation of small signal energy directly from the linearized ideal MHD equations.

Before giving this proof let us say a few words about the small signal energy mentioned above. The small signal energy is defined entirely in terms of the fields of the linear theory and is not the same as the physical energy. It was Sturrock who first drew attention to the significance of the small signal energy (or "pseudo-energy" as he called it) for the problem of linear stability. It is not obvious that this small signal energy will be

conserved in a conservative system simply because the physical energy is conserved since the exact fields have been expanded in a series and truncated at the first order.

We shall now derive a generalization of the Poynting theorem from the linearized MHD equations and from this obtain the conservation of small signal energy. The proof of the Energy Principle is then completed using the arguments given by Laval et al.

Let us consider a plasma in which the pressure is isotropic and which is bounded by a rigid, perfectly conducting wall, where the boundary conditions are the following

$$\hat{n}\cdot\underset{\sim}{V} = 0; \quad \hat{n}\times\underset{\sim}{E} = 0; \quad \hat{n}\,\frac{\partial\underset{\sim}{B}}{\partial t} = 0$$

where $\hat{n}$ is the unit normal to the boundary. The analysis is easily generalized to other boundary conditions (e.g. plasma-vacuum boundary). The linearized equations of the ideal MHD model are

$$\rho_0 \frac{\partial \underline{V}}{\partial t} = -\nabla p + \frac{1}{c}\underline{J}\times\underline{B}_0 + \frac{1}{c}\underline{J}_0\times\underline{B} \qquad \text{(III. 1)}$$

$$\frac{\partial \rho}{\partial t} + \underline{\nabla}\cdot(\rho_0\underline{V}) = 0 \qquad \text{(III. 2)}$$

$$\underline{E} + \frac{1}{c}\underline{V}\times B_0 = 0 \qquad \text{(III. 3)}$$

$$\frac{\partial p}{\partial t} + (\underline{v}\cdot\underline{\nabla})p = \frac{\gamma p_0}{\rho_0}\left(\frac{\partial \rho}{\partial t} + \underline{v}\cdot\nabla\rho_0\right) \qquad \text{(III. 4)}$$

$$\underline{\nabla}\times\underline{E} = -\frac{1}{c}\frac{\partial \underline{B}}{\partial t} \qquad \text{(III. 5)}$$

$$\underline{\nabla}\times\underline{B} = \frac{4\pi}{c}\underline{J} \qquad \text{(III. 6)}$$

$$\nabla\cdot\underline{B} = 0 \qquad \text{(III. 7)}$$

where fields with subscript zero are equilibrium quantities and the linearized variables are written without subscripts. As already mentioned there is no equilibrium flow of the plasma. We now scalar multiply equation (III. 1) by $\underline{v}$ to obtain

$$\rho_0\,\underline{v}\cdot\frac{\partial \underline{v}}{\partial t} = -\underline{v}\cdot\underline{\nabla}p + \frac{\underline{v}}{c}\times(\underline{J}\times\underline{B}_0) + \frac{\underline{v}}{c}(\underline{J}_0\times\underline{B}) \qquad \text{(III. 8)}$$

using the relation

$$\underline{\nabla}\cdot(p\underline{v}) = p\,\underline{\nabla}\cdot\underline{v} + \underline{v}\cdot\underline{\nabla}p$$

equation (III. 8) can be written in the form

$$\frac{\partial}{\partial t}\left(\rho_0\frac{\underline{v}\cdot\underline{v}}{2}\right) = -\underline{\nabla}\cdot(p\underline{v}) + p\,\underline{\nabla}\cdot\underline{v} + \frac{\underline{v}}{c}\cdot(\underline{J}\times\underline{B}_0) + \frac{\underline{v}}{c}(\underline{J}_0\times\underline{B}) \qquad \text{(III. 9)}$$

Next, scalar multiple equation (III. 6) by $\frac{c}{4\pi}\underline{E}$, equation (III. 5) by $\frac{c\underline{B}}{4\pi}$

to obtain

$$\frac{c}{4\pi}\,\underset{\sim}{E}\cdot\underset{\sim}{\nabla}\times\underset{\sim}{B}-\frac{c}{4\pi}\,\underset{\sim}{B}\cdot\underset{\sim}{\nabla}\times\underset{\sim}{E}=\frac{\partial}{\partial t}\left(\frac{\underset{\sim}{B}\,\underset{\sim}{B}}{8\pi}\right)+\underset{\sim}{J}\cdot\underset{\sim}{E}$$

This can be written as

$$\frac{\partial}{\partial t}\left(\frac{\underline{B}\cdot\underline{B}}{8\pi}\right)+\underline{\nabla}\cdot\left(\frac{c\,\underline{E}\times\underline{B}}{4\pi}\right)+\underline{J}\cdot\underline{E}=0 \qquad \text{(III. 10)}$$

Substituting for $\underset{\sim}{E}$ from equation (III. 3) into the term $\underset{\sim}{J}\cdot\underset{\sim}{E}$ equation (III. 10) becomes

$$\frac{\partial}{\partial t}\left(\frac{\underline{B}\cdot\underline{B}}{8\pi}\right)+\underline{\nabla}\cdot\left(\frac{c\,\underline{E}\times\underline{B}}{4\pi}\right)=-\underline{V}\cdot\left(\underline{J}\times\underline{B}_o\right) \qquad \text{(III. 11)}$$

where we have made use of the vector identy $\underline{J}\,(\underline{V}\times\underline{B}_o)=\underline{V}\cdot(\underline{B}_o\times\underline{J})$. Adding equations (III. 9) and (III. 11), we obtain

$$\frac{\partial}{\partial t}\left(\frac{1}{2}\rho_o\,\underline{V}\cdot\underline{V}+\frac{B^2}{8\pi}\right)+\underline{\nabla}\cdot\left(\frac{c\,\underline{E}\times\underline{B}}{4\pi}+p\underline{V}\right) \qquad \text{(III. 12)}$$

$$=p\,\underline{\nabla}\cdot\underline{V}+\underline{V}\cdot\left(\underline{J}_o\times\underline{B}\right)$$

Now consider the term $p\underset{\sim}{\nabla}\cdot\underset{\sim}{V}$. With the aid of equations (III. 2) and (III. 4), we find

$$\underline{\nabla}\cdot\underline{V}=-\left\{\frac{1}{\gamma p_o}\frac{\partial p}{\partial t}+\frac{1}{\gamma p_o}\left(V\cdot\nabla\right)p_o\right\} \qquad \text{(III. 13)}$$

Substituting equation (III. 13) into (III. 12) we have

$$\frac{\partial}{\partial t}\left\{\frac{1}{2}\rho_o\,\underline{V}\cdot\underline{V}+\frac{\underline{B}\cdot\underline{B}}{8\pi}+\frac{1}{2}\frac{p^2}{\gamma p_o}\right\}+\underline{\nabla}\cdot\left(\frac{c}{4\pi}\,\underline{E}\times\underline{B}+p\underline{V}\right) \qquad \text{(III. 14)}$$

$$=\underline{V}\cdot\left(\underline{J}_o\times B\right)-\frac{p}{\gamma p_o}\left(\underline{V}\cdot\underline{\nabla}\right)p_o$$

In order to obtain the final form of the conservation equation we must introduce the linear displacement vector $\underset{\sim}{\xi}$ defined by

$$\frac{\partial\,\underset{\sim}{\xi}}{\partial t}=\underline{V} \qquad \text{(III. 15)}$$

This enables us to integrate equation (III. 5) in time to obtain $\underset{\sim}{B}$ in terms of $\underset{\sim}{\xi}$ thus

$$\underline{B} = \nabla \times (\underline{\xi} \times \underline{B}_0) \qquad \text{(III. 16)}$$

where we have, of course, made use of equation (III. 3). We can also obtain p in terms of $\underset{\sim}{\xi}$ by integrating equation (III. 13) in time to obtain

$$p = -(\underline{\xi} \cdot \nabla) p_0 - \gamma p_0 (\nabla \cdot \underline{\xi}) \qquad \text{(III. 17)}$$

Now consider the two terms on the right hand side of equation (III. 14). First,

$$\underline{V} \cdot (\underline{J}_0 \times \underline{B}) = - \underline{J}_0 \cdot \left(\frac{\partial \underline{\xi}}{\partial t} \times \underline{B} \right)$$

Since $\underset{\sim}{B}$ depends linearly on $\underset{\sim}{\xi}$ and $\underset{\sim}{J}_0$ is independent of time we may write

$$\underline{J}_0 \cdot \left(\frac{\partial \underline{\xi}}{\partial t} \times \underline{B} \right) = \frac{\partial}{\partial t} \left(\frac{1}{2} \underline{J}_0 \cdot [\underline{\xi} \times \underline{B}] \right)$$

so that

$$\underline{V} \cdot (\underline{J}_0 \times \underline{B}) = \frac{\partial}{\partial t} \left(\frac{1}{2} \underline{J}_0 \cdot [\underline{\xi} \times \underline{B}] \right) \qquad \text{(III. 18)}$$

Next, consider the second term

$$\frac{p}{\gamma p_0} (\underline{V} \cdot \nabla) p_0 = \frac{p}{\gamma p_0} \frac{\partial \underline{\xi}}{\partial t} \cdot \nabla p_0$$

Since p depends linearly on $\underset{\sim}{\xi}$ through equation (III. 17) and p_0 is independent of time we may again write

$$\frac{p}{\gamma p_0} (\underline{V} \cdot \nabla) p_0 = \frac{\partial}{\partial t} \left[\frac{1}{2} \frac{p}{\gamma p_0} \underline{\xi} \cdot \nabla p_0 \right] \qquad \text{(III. 19)}$$

We may now substitute (III. 18) and (III. 19) into equation (III. 14) to obtain

$$\frac{\partial}{\partial t}\left[\frac{1}{2}\rho_0 \underline{v}\cdot\underline{v} + \frac{\underline{B}\cdot\underline{B}}{8\pi} + \frac{1}{2}\frac{p^2}{\gamma p_0} + \frac{1}{2}\underline{J}_0\cdot(\underline{\xi}\times\underline{B})\right.$$

$$\left. + \frac{1}{2}\frac{p}{\gamma p_0}\left(\underline{\xi}\cdot\nabla\right)p_0\right] + \nabla\cdot\left[\frac{c}{4\pi}\underline{E}\times\underline{B} + p\underline{v}\right] = 0 \qquad \text{(III. 20)}$$

This is the required energy conservation relation and is the generalized Poynting theorem for linearized ideal MHD. The term inside the first set of parentheses is the total energy density of the perturbation per unit volume and the second set of parentheses represents the energy flow out of this unit volume. The energy flow terms will be easily recognized as the Poynting vector and the convection of the plasma internal energy by the perturbed plasma motion.

Equation (III. 20) is not yet in its most familiar form. Let us combine the pair of terms containing the perturbed pressure

$$\frac{1}{2}\frac{p^2}{\gamma p_0} + \frac{1}{2}\frac{p}{\gamma p_0}\underline{\xi}\cdot\nabla p_0 = \frac{1}{2}\frac{p}{\gamma p_0}\left(p + \underline{\xi}\cdot\nabla p_0\right)$$

Substituting for p from equation (III. 17) we obtain

$$\frac{1}{2}\frac{p^2}{\gamma p_0} + \frac{1}{2}\frac{p}{\gamma p_0}\underline{\xi}\cdot\nabla p_0 = \frac{1}{2}\left(\underline{\xi}\cdot\nabla\right)p_0 + \frac{1}{2}\gamma p_0\left(\nabla\cdot\underline{\xi}\right)^2 \qquad \text{(III. 21)}$$

Substituting (III. 21) into (III. 20) we obtain the final form for the small signal energy conservation equation

$$\frac{\partial}{\partial t}\left\{\frac{1}{2}\rho_0\underline{v}\cdot\underline{v} + \frac{\underline{B}\cdot\underline{B}}{8\pi} + \frac{1}{2}\underline{J}_0\cdot(\underline{\xi}\times\underline{B}) + \frac{1}{2}\gamma p_0\left(\nabla\cdot\underline{\xi}\right)^2 + \frac{1}{2}\left(\underline{\xi}\cdot\nabla p_0\right)\nabla\cdot\underline{\xi}\right\}$$

$$+ \nabla\cdot\left(\frac{c}{4\pi}\underline{E}\times\underline{B} + p\,\underline{v}\right) = 0 \qquad \text{(III. 22)}$$

We now integrate this equation over the whole plasma to obtain

$$\frac{\partial}{\partial t}\int\left\{\tfrac{1}{2}\rho_0\,\underline{v}\cdot\underline{v}+\frac{\underline{B}\cdot\underline{B}}{8\pi}+\tfrac{1}{2}\,\underline{J}_0\cdot\left(\underline{\xi}\times\underline{B}\right)+\tfrac{1}{2}\gamma p_0\left(\nabla\cdot\underline{\xi}\right)^2+\tfrac{1}{2}\left(\underline{\xi}\cdot\nabla p_0\right)\nabla\cdot\underline{\xi}\right\}d^3r$$

$$+\oint\left\{\frac{c}{4\pi}\,\underline{E}\times\underline{B}+p\,\underline{v}\right\}\cdot d\underline{S}=0$$

where $d\underline{S}\equiv\hat{n}S$ and S is the surface bounding the volume of integration. Since we have assumed a perfectly conducting, rigid wall in contact with the plasma the boundary conditions ensure that the surface integral vanishes. We are then left with the result that

$$\frac{\partial}{\partial t}\left(K+\delta W\right)=0 \tag{III. 23}$$

where $K\equiv\int\frac{1}{2}\,\rho_0\,\underline{v}\cdot\underline{v}\,dV$ is the total kinetic energy of the plasma δW is immediately identified as the potential energy of the perturbation and is given by

$$\delta W=\tfrac{1}{2}\int\left\{\frac{\underline{B}\cdot\underline{B}}{4\pi}+\underline{J}_0\cdot\left(\underline{\xi}\times\underline{B}\right)+\gamma p_0\left(\nabla\cdot\underline{\xi}\right)^2+\left(\underline{\xi}\cdot\nabla\right)p_0\,\nabla\cdot\underline{\xi}\right\}d^3r \tag{III. 24}$$

The form of δW given in equation (III. 24) is in agreement with that first given by Bernstein et al.

We can already draw a number of conclusions at this stage of the analysis with the aid of the equation for the conservation of energy. Since we assumed zero equilibrium flow, it follows that K is always positive definite. Taking as a definition of instability an unbounded increase of K in time, it is clear from equation (III. 23) that if $\delta W > 0$ the system must be absolutely stable. It is also clear from equation (III. 23) that in order to have instability $\delta W < 0$ such that $|\delta W|$ grows in time so as to

balance exactly the increase in K. To complete the proof of the Energy Principle we now follow the argument given by Laval et al in order to show that if a ξ and $B = \nabla \times \xi \times B_0$ can be found such that $\delta W < 0$ the plasma is unstable.

Equation (III. 1) can be written as

$$\rho_0 \frac{\partial^2 \underline{\xi}}{\partial t^2} = \underline{F}(\underline{\xi}) \tag{III. 25}$$

where

$$\underline{F}(\underline{\xi}) = \underline{\nabla}\left(\xi \cdot \nabla p_0\right) + \nabla\left(\gamma p_0 \nabla \cdot \underline{\xi}\right) + \frac{1}{c}\underline{J}_0 \times \underline{B} + \frac{1}{c}(\nabla \times \underline{B}) \times \underline{B}_0 \tag{III. 26}$$

The next step is to define the virial $I(\underline{\xi})$ defined by

$$I(\underline{\xi}) = \frac{1}{2}\int \rho_0 \underline{\xi} \cdot \underline{\xi}\, d^3 r \tag{III. 27}$$

Differentiating I twice with respect to time

$$\ddot{I} = \int \left(\rho_0 \dot{\underline{\xi}} \cdot \dot{\underline{\xi}} + \rho_0 \underline{\xi} \cdot \ddot{\underline{\xi}}\right) d^3 r \tag{III. 28}$$

The first term on the right hand side is twice the kinetic energy and the second term can be written in terms of $F(\underline{\xi})$ with the aid of equation (III. 25) giving

$$\ddot{I} = 2K + \int \underline{\xi} \cdot \underline{F}(\underline{\xi})\, d^3 r \tag{III. 29}$$

With the aid of some vector algebra it is straightforward to show that

$$\int \underline{\xi} \cdot \underline{F}(\underline{\xi})\, d^3 r = -2\delta W \tag{III. 30}$$

where δW is the potential energy defined in equation (III. 24). The final form of equation (III. 29) can now be written

$$\ddot{I} = 2K - 2\delta W \tag{III. 31}$$

We now assume that there is some displacement $\underset{\sim}{\eta}$ such that $\delta W(\underset{\sim}{\eta}) < 0$. We write this explicitly as

$$\delta W(\underline{\eta}) = -\omega^2 I(\underline{\eta}) \tag{III. 32}$$

where $\omega > 0$ and $I(\underset{\sim}{\eta})$, the virial, is, of course, positive definite. The displacement vector ξ, which is a solution of equation (III. 25), is now chosen to satisfy the following initial conditions

$$\underline{\xi} = \underline{\eta} \quad , \quad \dot{\underline{\xi}} = \omega \underline{\eta} \tag{III. 33}$$

Since the total energy Q of the perturbation must be a constant we may calculate its value with the aid of equations (III. 23). Thus

$$\begin{aligned} Q &= K + \delta W \\ &= I(\dot{\underset{\sim}{\xi}}) + \delta W(\underset{\sim}{\xi}) \\ &= \omega^2 I(\underset{\sim}{\eta}) + \delta W(\underset{\sim}{\eta}) \end{aligned}$$

so that $Q = 0$. Using this result we may now eliminate δW from equation (III. 31) to obtain

$$\ddot{I} = 4K \tag{III. 34}$$

We now relate $\ddot{I}$ to I and $\dot{I}$. By the definition of $\dot{I}$,

$$\dot{I}^2 = \left\{ \int \rho_0 \, \underline{\xi} \cdot \dot{\underline{\xi}} \, d^3\underline{r} \right\}^2 = \left\{ \int (\rho_0^{\frac{1}{2}} \underline{\xi}) \cdot (\rho_0^{\frac{1}{2}} \dot{\underline{\xi}}) \, d^3\underline{r} \right\}^2$$

Using Schwarz's inequality, we may write

$$\left\{ \int (\rho_0^{\frac{1}{2}} \underline{\xi}) \cdot (\rho_0^{\frac{1}{2}} \dot{\underline{\xi}}) \, d^3\underline{r} \right\}^2 \leq \left(\int \rho_0 \, \underline{\xi} \cdot \underline{\xi} \, d^3\underline{r} \right) \left(\int \rho_0 \, \dot{\underline{\xi}} \cdot \dot{\underline{\xi}} \, d^3\underline{r} \right)$$

and therefore $\dot{I}^2 \leq 4IK$. With the aid of equation (III. 34) the inequality becomes

$$\dot{I}^2 < I\ddot{I} \tag{III. 35}$$

Now $\ddot{I} > 0$ at $t = 0$. Integrating equation (III. 34) we obtain $\dot{I} = \dot{I}_o + \int_o^t 4K dt$ where the subscript zero indicates that the quantity has been evaluated at $t = 0$. We may evaluate the constant I_o with the aid of the initial conditions. Thus

$$\dot{I}_o = \int \rho_o \underline{\xi} \cdot \dot{\underline{\xi}} d^3\underline{r} = \omega \int \rho_o \underline{\eta} \cdot \underline{\eta} d^3\underline{r} = 2\omega I_o > 0 \qquad \text{(III. 36)}$$

We therefore find that $\dot{I}_o > 0$ so that $\dot{I} > 0$ for $t > 0$. Since $I\ddot{I} > 0$ for $t > 0$ we do not alter the sense of inequality (III. 35) by dividing throughout by this quantity, so that

$$\frac{\dot{I}}{I} < \frac{\ddot{I}}{\dot{I}} \qquad \text{(III. 37)}$$

Integrating for $t > 0$ we have

$$\ln I/I_o \leq \ln \dot{I}/I_o \qquad \text{(III. 38)}$$

Using inequality (III. 36) we obtain

$$\frac{\dot{I}}{I} > 2\omega \qquad \text{(III. 39)}$$

Again integrating for $t > 0$ we have

$$I \geq I_o \exp 2\omega t \qquad \text{(III. 40)}$$

Thus I grows at least as fast as $\exp(2\omega t)$ and since I is quadratic in $\underset{\sim}{\xi}$ it follows that the displacement $\underset{\sim}{\xi}$ will grow at least as fast as $\exp(\omega t)$. This then completes the proof that for any displacement which makes $\delta W < 0$ instability will always occur.

Let us conclude this chapter by considering, in very simple terms, the physical significance of the potential energy δW defined by equation (III. 24). We have seen that the plasma will be stable when $\delta W > 0$. The expression for δW then shows that the energy required to perturb the equilibrium

magnetic field (either field line bending or compression) is positive definite and therefore stabilizing. The third term is the expression for δW is also positive definite so that incompressible perturbations may be expected to be the most unstable. The second and fourth terms in the expression for δW are the potentially destabilizing ones. The driving mechanism in the first of these being due to the equilibrium current and is the second to the equilibrium pressure gradient. To apply the energy principle one can do one of two things. First of all, one can try various different displacements and see whether the δW can be made negative. For instance the well known stability requirement that $\int d\ell/B$ must decrease as the pressure decreases can be derived by examining the effect of a displacement which interchanges two adjacent flux tubes. Of course this only gives a necessary condition for stability; there may be other untried displacements which give instability. Alternatively one could attempt to minimize δW by applying the variational principle. If the minimum value of $\delta W > 0$, for a displacement which for instance has $\int |\xi|^2 d^3r = 1$, then the plasma is stable, and visa versa. Thus one can derive a necessary and sufficient condition for stability. This is the approach used by Newcomb (W.A. Newcomb, Annals of Physics, 10, 232 (1960)) in analyzing the stability of a diffuse linear pinch. For an illustration of the Energy Principle in a number of simple situations the interested reader may refer to the review of hydromagnetic stability by Kadomtsev. (B. B. Kadomtsev, Rev. Plasma Physics, Vol. 2, Edited by M. A. Leontovich, Consultants Bureau, New York (1966) p. 153).

IV. Free Surface Modes in a Cylindrical Plasma

A very important class of unstable modes occur when the plasma does not extend up to the wall of the metal chamber. In this case, the plasma has a free surface which can undergo unstable helical (or kink) perturbations. In this chapter, we work out the properties of two types of free surface modes, first where the current is carried on the surface, and second where the volume current density J_{oz} is uniform inside the plasma. The former instability is responsible for the famous Kruskal-Shafranov requirement for gross stability $q(a)>1$ where a is the radius of the free surface. The later instability is responsible for unstable displacements of the free surface wherever $q(a)<m/n$ where m and n are integers. Also $q(r) = rB_z/RB_\theta$, R being the major radius.

We begin with the former type of instability, that is where all the current flows along the free surface. Let us now define our model more precisely. We shall consider an infinitely long cylindrical plasma whose axis is taken to be the z direction. The plasma extends radially from r = 0 to r = a, beyond which there is a vacuum. For simplicity, assume the vacuum region extends to infinity and that the plasma surface current flows only in the z direction. Then, Maxwell's current equation gives the following boundary conditions for equilibrium magnetic fields

$$B_{oz}^{v} - B_{oz}^{p}\Big|_{r=a} = 0 \qquad \text{(IV 1)}$$

$$B_{o\theta}^{v} - B_{o\theta}^{p}\Big|_{r=a} = \frac{4\pi J_{zo}}{c} \qquad \text{(IV 2)}$$

where J_{oz} is the axial surface current and the superscripts V and p denote vacuum and plasma fields respectively. Assuming that $B_r = \frac{\partial}{\partial\theta} = \frac{\partial}{\partial z} = 0$ for the equilibrium we obtain the following equilibrium fields from Maxwell's equations

$$B_{oz}^{p} = B_{oz}^{v} \cong B_{oz} \tag{IV.3}$$

$$B_{o\theta}^{p} = 0 \tag{IV.4}$$

$$B_{o\theta}^{v} = \frac{4\pi a J_{oz}}{rc} \tag{IV.5}$$

Since the magnetic field is uniform in the plasma, then so must be the pressure. Then equilibrium pressure balance at the plasma vacuum interface is given by

$$p_o(a) = \frac{2\pi J_{oz}^2}{c^2} \tag{IV.6}$$

Let us now consider perturbations to this equilibrium, which are assumed to vary as $f(r) \exp\left(i\,(kz + m\theta) + \gamma t\right)$. (To make the transition from cylindrical to toroidal systems, we simply quantize k by taking $k = {}^{-n}/_{R}$ where R is the major radius of the torus). Here and henceforth we take $B_{\theta o}$, B_{zo}, J_{zo} and $m>0$. However the sign of k is arbitrary. In general there is only instability for $k<0$. The linearized equation of motion of the plasma can be written

$$\gamma \rho_o \underline{v} = \frac{1}{4\pi}\left(B_o \cdot \nabla\right) B - \nabla \tilde{p} \tag{IV.7}$$

where ρ_o is assumed to be uniform and $\tilde{P} = P + \frac{\underline{B}_o \cdot \underline{B}}{4\pi}$. In obtaining (IV. 7) we have used the fact that $\underline{B}_o$ is uniform in the plasma. Taking the divergence of Eq. (IV. 7) we obtain

$$\gamma \rho_o (\underline{\nabla} \cdot \underline{V}) = \frac{i k B_{oz}}{4\pi} \underline{\nabla} \cdot \underline{B} - \nabla^2 \tilde{P} \qquad \text{(IV. 8)}$$

We now assume that the motion is incompressible $\underline{\nabla} \cdot \underline{V} = \underline{\nabla} \cdot \underline{B} = 0$ so Eq. (IV. 8) reduces to the simple form

$$\nabla^2 \tilde{P} = 0 \qquad \text{(IV. 9)}$$

The solution of this equation which is bounded at the origin is

$$\tilde{P} = A I_m(kr) \qquad \text{(IV. 10)}$$

where A is an arbitrary constant and I_m is the modified Bessel function of the first kind.

We now also need to relate the perturbed velocity $\underline{V}$ to $\tilde{P}$. The equation for the perturbed magnetic field is

$$\gamma \underline{B} = \underline{\nabla} \times (\underline{V} \times \underline{B}_o) \qquad \text{(IV. 11)}$$

Using once more the incompressibility condition for B_o and Maxwell's equations, the above equation reduces to

$$\gamma \underline{B}_1 = (\underline{B}_o \cdot \underline{\nabla}) \underline{V} \qquad \text{(IV. 12)}$$

Substituting (IV. 12) into Eq. (IV. 7) we obtain $\underline{V}$ in terms of $\tilde{P}$

$$\underline{V} = \frac{\gamma \underline{\nabla} \tilde{P}}{\rho_o (\gamma^2 + k^2 c_A^2)} \qquad \text{(IV. 13)}$$

where $C_A^2 = B_{oz}^2/4\pi\rho_o$, the Alfven speed.

The perturbed field in the vacuum must satisfy $\nabla \cdot B^v = \nabla \times B^v = 0$. Putting $B^v = \underline{\nabla}\psi$, then ψ satisfies the equation

$$\nabla^2\psi = 0$$

so

$$\psi = C\, K_m(kr) \qquad \text{(IV. 14)}$$

where C is a constant and K_m is an arbitrary Bessel function of the second kind. The final step in the analysis is to match the perturbation in the plasma and vacuum. Since we have two arbitrary constants in Eqs. (IV. 10 and 14), two boundary conditions are necessary.

The first condition comes from the need to have pressure balance across the interface. Integrating the radial component of the equation of motion across the boundary, we have

$$p + p_o + \frac{\left(\underline{B}_o^p + \underline{B}^p\right)\cdot\left(\underline{B}_o^p + \underline{B}^p\right)}{8\pi} = \frac{\left(\underline{B}_o^v + \underline{B}^v\right)\cdot\left(\underline{B}_o^v + \underline{B}^v\right)}{8\pi} \qquad \text{(IV. 15)}$$

Since we require the linearized form of Eq. IV. 15, we note that the perturbed quantities are to be evaluated at the unperturbed boundary and the equilibrium quantities, at the perturbed boundary, which has been displaced a distance $\underline{\xi} = \underline{V}/\gamma$. We then find the following condition for pressure balance

$$\tilde{P}(a) = \left\{ \frac{\underline{B}_o^v \cdot \underline{B}^v}{4\pi} + \xi_r \frac{B_{oo}}{4\pi}\frac{\partial}{\partial r} B_{oo} \right\}_{r=a} \qquad \text{(IV. 16)}$$

where we have used the equilibrium pressure balance condition and the fact that equilibrium pressure was assumed uniform.

The second boundary condition results from the following observation. Since the plasma is assumed to have infinite conductivity the electric field

moving with the plasma must be identically zero, or

$$\underline{E}^P + \frac{\underline{V}}{c} \times \underline{B}_o^P = 0$$

If we now match fields in this frame; then, because the tangential component of electric field must be continuous in any reference frame, we must have

$$\underline{E}_t^v + (V \times B_o^v)_t = 0$$

where the subscript t denotes the tangential component. This is the second boundary condition. However it can be put in a more convenient form by adding the normal components of each term to the equation and taking the curl. With the aid of Maxwell's equations and a little vector algebra we obtain

$$\hat{\underline{n}} \cdot \frac{\partial \underline{B}^v}{\partial t} = \hat{\underline{n}} \cdot \underline{\nabla} \times (\underline{V} \times \underline{B}_o^v)$$

where $\hat{n}$ is the normal to the plasma surface. Since $\frac{\partial \underline{B}}{\partial t}$ and $\underline{V}$ are zero in equilibrium, we can replace n by the unperturbed normal i_r. Using $\underline{V} = \frac{\partial}{\partial t} \underline{\xi}$, we obtain

$$B_{1r}^v = \left\{ \underline{\nabla} \times (\underline{\xi} \times \underline{B}_o^v) \right\}_{r=a} \qquad \text{(IV. 17)}$$

The final form of the second boundary condition now becomes

$$B_{1r}^v = i \left(\frac{m}{r} B_{o\theta}^v + k B_{oz}^v \right) \xi \qquad \text{(IV. 18)}$$

We are now in a position to obtain the dispersion relation for the problem. Equations (IV. 10) and (IV. 13) give the result

$$\xi_r = - \frac{A k I_m'(kr)}{\rho_o (\gamma^2 + k^2 c_A^2)} \qquad \text{(IV. 19)}$$

where prime denotes derivative with respect to argument. Calculating the perturbed field in the vacuum from Eq. (IV. 4) and substituting Eq. (IV. 10 and 19) into Eq. (IV. 16), we find

$$\left\{ I_m(ka) - \frac{k I_m'(ka)}{\rho_o(\gamma^2 + k^2 C_A^2)} \frac{B_{o\theta}(a)}{4\pi} \frac{\partial B_{oo}}{\partial r}\Big|_{r=a} \right\} A$$

$$- \frac{i\, \underline{k} \cdot \underline{B}_o^v(a)}{4\pi} K_m(ka)\, C = 0 \qquad \text{(IV. 20)}$$

where $\underline{k} \cdot \underline{B}_o^v = \frac{m B_{o\theta}^v}{r} + k B_{oz}^v$. Then substituting from Eq. (IV. 19) and the expression for B_r^v (from Eq. (IV. 14)) into Eq. (IV. 18) results

$$\frac{i\, \underline{k} \cdot \underline{B}_o^v(a)\; I_m'(ka)}{\rho_o(\gamma^2 + k^2 C_A^2)} A + k K'(ka)\, C = 0 \qquad \text{(IV. 21)}$$

The condition for non trivial solution of Eqs. (IV. 20 and 21) gives the required dispersion relation

$$\gamma^2 = -k^2 C_A^2 + \frac{(k \cdot B_o^v(a))^2}{4\pi\rho_o} \frac{I_m'(ka)\, K_m(ka)}{I_m(ka)\, K_m'(ka)}$$

$$+ \frac{k (B_{oo}^v(a))^2}{4\pi\rho_o a} \frac{I_m'(ka)}{I_m(ka)} \qquad \text{(IV. 22)}$$

Since $I_m'(ka)/I_m(ka) > 0$ and $K_m'(ka)/K_m(ka) < 0$ it is only the third term on the right hand side of Eq. (IV. 22) which is destabilizing. In order to see when this term is larger than the other stabilizing terms, consider long wavelength $ka \ll 1$. Using the fact that

$$I_m'(ka)/I_m(ka) \approx m/ka$$

and

$$K_m'(ka)/K_m(ka) \approx -m/ka,$$

Eq. (IV. 22) can be written

$$-\gamma^2 = -k^2 C_A^2 - \frac{\left[k B_{oz} + \frac{m}{a} B_{o\theta}^{v}(a)\right]^2}{4\pi\rho_o} + \frac{m\left(B_{o\theta}^{v}(a)\right)^2}{4\pi a^2 \rho_o} . \quad \text{(IV. 23)}$$

The most unstable k value is

$$k = -\frac{m}{a}\,\frac{B_{o\theta}^{v}(a)}{2 B_{oz}} . \quad \text{(IV. 24)}$$

Substituting this into Eq. (IV. 23), we find that the maximum growth rate is

$$\gamma_{MAX}^2 = \frac{m}{a^2}\,\frac{B_{o\theta}^2(a)}{4\pi\rho_o}\left(-\frac{m}{2}+1\right) \quad \text{(IV. 25)}$$

so that the m = 1 surface mode is unstable, m = 0 and 2 are marginally stable and all higher m (long wavelength) are stable.

It is also of interest to write Eq. (IV. 23) in the form

$$\gamma^2 = -\frac{2k^2 B_{oz}^2}{4\pi\rho_o} - 2\,\frac{m}{a}\,\frac{B_{oz} B_{o\theta}^{v}(a)\, k}{4\pi\rho_o} - \frac{m}{a^2}\,\frac{\left(B_{o\theta}^{v}(a)\right)^2}{4\pi\rho_o}(m-1) \quad \text{(IV. 26)}$$

Since only the m = 1 mode is unstable we can immediately obtain the range of unstable wavelengths

$$0 < |k| < \frac{1}{a}\,\frac{B_{o\theta}^{v}(a)}{B_{oz}} .$$

For a torus, the minimum value of k is $\frac{1}{R}$, so a toroidal plasma is stable if

$$q(a) = \frac{a B_{oz}}{R B_{o\theta}^{v}(a)} > 1 \quad \text{(IV. 27)}$$

Equation (IV. 27) is the celebrated Kruskal-Shafranov limit on the q(a) value of a toroidal discharge.

Let us see what this condition implies for a tokamak plasma. The plasma and metal wall are shown in Fig. (IV. 1). The value of q at the plasma edge must be greater than unity. In the vacuum region between r = a and r = b, $B^{v}_{o\theta}(r)$ decreases as $1/r$ so that in the vacuum region q(r) increases as r^2, so that $q(b) > (b/a)^2$. Thus, depending on where the plasma boundary is, the value of q at the limiter must be somewhat greater than unity in order for the plasma to be stable to gross kink modes. This lower limit on q(a) implies an upper limit on current for stable configuration. Using $B^{\theta}_{ov}(r=b) = I/5r$ where I is in amps, B in Gauss and r in cm, the maximum current is

$$I < \frac{5a^2 B_{oz}}{R} \qquad \text{(IV. 28)}$$

We now turn to a discussion of the other type of free surface mode, that where the plasma has a uniform current up to r = a and vacuum outside. Also we assume $B_{oz} >> B_o$, R>>a, and treat the case where B_{oz} is constant. In equilibrium

$$0 = -\frac{dP_o}{dr} - \frac{1}{c} J_{zo} B_{\theta o} \qquad \text{(IV. 29)}$$

so the pressure profile is parabolic and vanishes at r = a, since $B_{\theta o} \sim r$ and J_{zo} is constant. We will see that this plasma is unstable for all m instead of just m = 1 as was the case for a surface current.

Before calculating the growth rate, let us show physically why this is so. As discussed in the last chapter, a perturbation is most likely to be unstable if $\underline{k} \cdot \underline{B}_o = 0$ since in this case, it does not couple to stable

shear Alfven waves. Right at the surface of the plasma, $\underline{k}\cdot\underline{B}_o = kB_{oz} + \frac{mB^v_{o\theta}(a)}{r}$, and as we just saw, the plasma is unstable when this nearly vanishes. However if $\underline{k}\cdot\underline{B}_o$ is zero at the plasma edge, it is equal to kB_{zo} inside the plasma. Thus, modes which are flute like (that is perpendicular to $\underline{B}_o$) on the plasma surface are not flute like in the plasma interior, and there is a strong coupling to shear Alfven waves there. This is the explanation of the stabilizing first term on the right hand side of Eq. (IV. 22). Clearly the thing responsible for this stabilizing effect is the fact that the magnetic field abruptly changes direction as one crosses the plasma boundary. However, if the axial current density is uniform, the poloidal magnetic field is a continuous function of radius so that a perturbation which is flute like on the plasma surface will be flute like in the plasma interior also. Thus we expect the plasma with uniform current to be <u>less</u> stable than the plasma with a surface current.

We now proceed to derive the properties of unstable modes in a plasma with a uniform axial current with $B_{zo} >> B_{\theta o}$ and $\frac{r}{R} << 1$, the so called tokamak ordering. Since the axial field is very large, one expects that the most unstable motion could not compress this field, implying two dimensional motion in the $r\theta$ plane, i.e., $v_z = B_z = 0$. We will assume this to be true for now and prove it a postiori. The perturbed magnetic field in the vacuum is unchanged and is given by Eq. (IV. 14).

The problem now is to derive an equation for the magnetic field inside the plasma. To do so, take the z component of the curl of the equation of motion. Using the fact the $\underline{J}_o$ is constant in the plasma, $\nabla\cdot J = \nabla\cdot B = 0$ and B_{oz} is constant, we find

$$\frac{\gamma}{r}\left(\frac{\partial}{\partial r} r \rho_0 V_\theta - i m V_r\right) = \frac{1}{c} \nabla \times \left(\underline{J} \times \underline{B}_0 + \underline{J}_0 \times B\right)\Big|_z$$

$$= \frac{1}{c} i k B_0 \underline{J}_z \qquad \text{(IV. 30)}$$

Relating J_z to B_z via Maxwells current equation, and using the fact that

$$\nabla \cdot B = \frac{1}{r}\frac{\partial}{\partial r} r B_r + \frac{im}{r} B_\theta = \nabla \cdot V = \frac{1}{r}\frac{\partial}{\partial r} r \rho V_r + \frac{im}{r} V_\theta = 0 \qquad \text{(IV. 31)}$$

we find

$$-\gamma\left(\frac{1}{r}\frac{\partial}{\partial r} r \rho_0 \frac{1}{im}\frac{\partial}{\partial r}(r V_r) + \frac{\rho_0 im}{r}\right) =$$

$$\frac{i F}{4\pi}\left(-\frac{1}{r}\frac{\partial}{\partial r}\frac{1}{im}\frac{\partial}{\partial r}(r B_r) - \frac{im}{r} B_r\right) \qquad \text{(IV. 32)}$$

where

$$F = \frac{m B_{\theta 0}}{r} - \frac{n B_{z0}}{R} \equiv \underline{k} \cdot \underline{B}_0 \qquad \text{(IV. 33)}$$

Note that for the case of constant current density $B_{0\theta}$ is proportional to r so F is constant. The other relation between B_r and V_r comes from Eq. (IV. 11). Taking the radial component, we find

$$V_r = \frac{\gamma B_r}{i F} \qquad \text{(IV. 34)}$$

Inserting Eq. (IV. 34) into Eq. (IV. 32), we find the single equation for B_r

$$\left(\frac{4\pi\rho_0 \gamma^2 + F^2}{m r}\right)\left[\frac{d}{dr} r \frac{d}{dr} r B_r - m^2 B_r\right] = 0 \qquad \text{(IV. 35)}$$

where we have assumped ρ_0 constant.

The factor outside is simply the dispersion relation for shear Alfven waves and cannot vanish for positive γ. The quantity in the square brackets must then be zero. Trying a solution $B_r = r^n$ and insisting that B_r be well behaved at the origin, we find

$$B_r = A r^{m-1} \qquad \text{(IV. 36)}$$

Of course A above and C from Eq. (IV. 14) can be simply related by requiring that B_r be continuous across the free surface. (Since the unperturbed fields are continuous across the free surface, all we need do is say that the perturbed radial field is continuous across the unperturbed free surface.) Using Eqs. (IV. 31 and 34) we also find

$$V_\theta = i V_r$$
$$B_\theta = i B_r \qquad \text{(IV. 37)}$$

The dispersion relation then follows from assuming pressure balance across the free surface, or

$$\left. \frac{B_{zo} B_z + B_{\theta o} B_\theta}{4\pi} \right|_V = \left. \frac{B_{\theta o} B_\theta}{4\pi} + p \right|_P \qquad \text{(IV. 38)}$$

where we have made use of the fact that $B_z^V = 0$ and that $|B_o|^2$ is continuous. In the vacuum, one can immediately derive

$$B_z = i \frac{K_m(ka)}{K_m'(ka)} B_r \qquad (a)$$

$$\text{(IV. 39)}$$

$$B_\theta = \frac{im}{r} \frac{K_m(ka)}{k K_m'(ka)} \qquad (b)$$

It remains only to calculate p in terms of B_r. This comes from the θ component of the momentum equation

$$\rho_o \gamma V_\theta = - \frac{im}{r} P + \frac{1}{c}\left[-J_r B_{oz} + B_r J_{oz} \right] . \qquad \text{(IV. 40)}$$

Now

$$J_r = \frac{c}{4\pi} \nabla \times B \Big|_r = \frac{ck}{4\pi} B_r \qquad \text{(IV. 41)}$$

where we have used Eqs. (IV. 37b and 36). Thus by using Eq. (IV. 41) and the expression for V_θ in terms of B_r from Eqs. (IV. 37a and 34), Eq. (IV. 40) relates p to B_r. Plugging into Eq. (IV. 38), we find the dispersion relation

$$\gamma^2 = \left\{ \frac{F}{\rho_o} \frac{B_{\theta o}}{2\pi r} - \frac{F^2}{2\pi \rho_o} \left(1 - \frac{m K_m(ka)}{kr K'_m(ka)} \right) \right\} \qquad \text{(IV. 42)}$$

Since $K_m/K'_m \quad 0$, the term proportional to F^2 is stabilizing. The term proportional to F can be destabilizing if $F > 0$, or $\frac{m B_{\theta o}}{r} > \frac{n B_{zo}}{R}$. Clearly the plasma can be unstable in the limit of $F \to 0$. Since B_{oz} is constant and $B_{o\theta}$ decreases as a function of r in the vacuum region, the plasma can be unstable if the singular surface, $F = 0$, falls just outside the plasma. If the singular surface falls inside the plasma $F(r = a) < 0$ so the plasma is stable. Also if the singular surface falls too far outside the plasma, the second term on the right of in Eq. (IV. 42) dominates the first and the plasma again is stable.

Let us see what this means for the current buildup of a tokamak plasma. As the current rises the value of q(a) decreases. Thus

$$F = \frac{m B_{\theta o}}{r} - \frac{n B_{zo}}{R} = \frac{m B_{\theta o}}{r} \left(1 - \frac{n q(a)}{m} \right)$$

starts out negative but as the current builds up it decreases. When the current reaches the value at which

$$q(a) = \frac{m}{n} \qquad \text{(IV. 43)}$$

F changes from negative to positive and the plasma is unstable to modes with values of m/n given in Eq. (IV. 43). However as the current increases, the mode becomes stable because of the stabilizing effect of the second term on the right of Eq. (IV. 42). Thus only certain values of total current give instability. In building up tokamak current, the idea then is to program its rise so that it passes through the unstable values very quickly. However the maximum plasma current will always still be limited by Eq. (IV. 28).

We close by determining the conditions under which the motion is two dimensional, as we have assumed. The velocity in the z direction comes from the A component of the momentum equation. Assuming $B_z = 0$, we find

$$\gamma \rho_o V_z = i k p$$

Inserting for p from Eq. (IV. 40) and taking the maximum value of γ , from Eq. (IV. 42), we find

$$\frac{V_z}{V_r} \sim \frac{kr}{2} \qquad \text{(IV. 44)}$$

so the motion basically is two dimensional as long as $kr/2 \ll 1$.

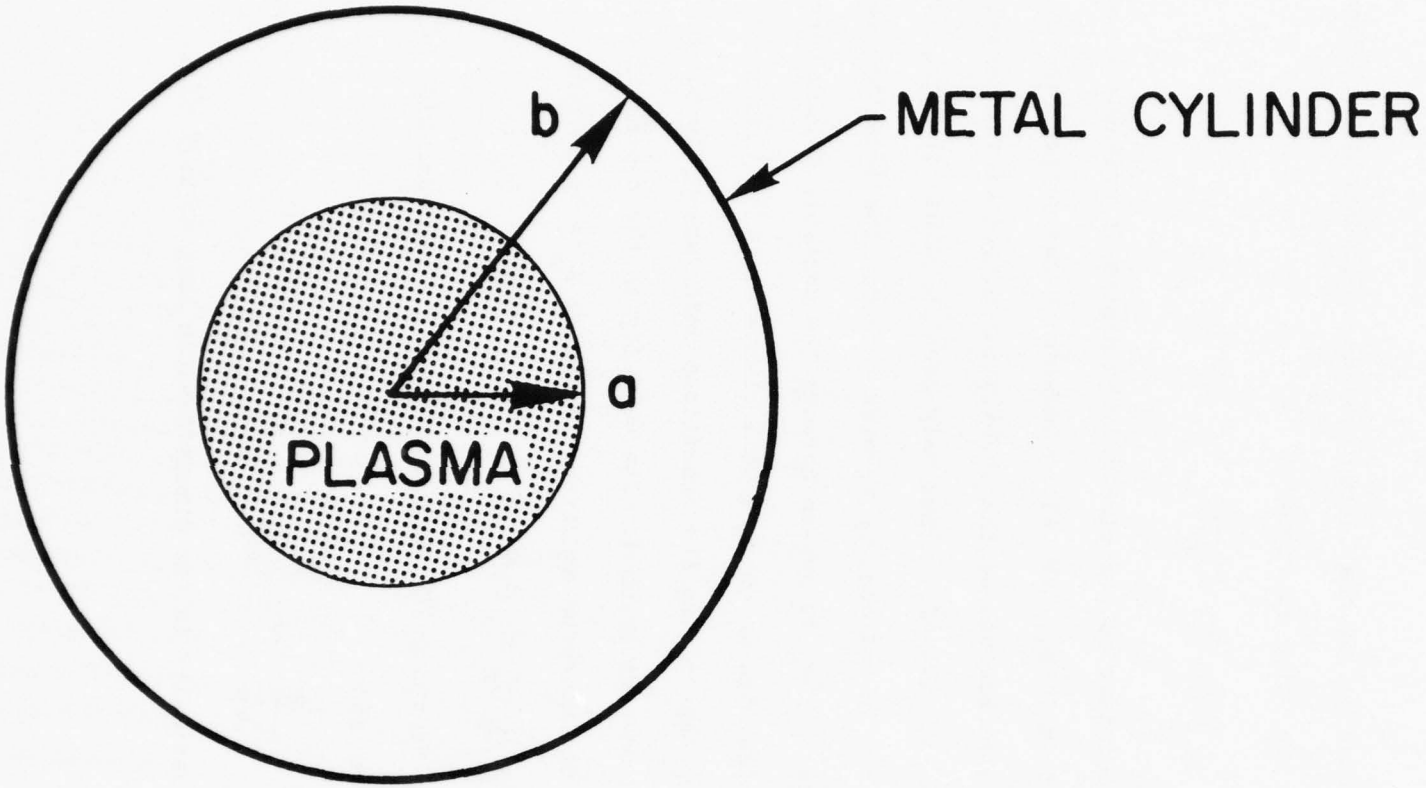

Fig. IV 1 — A cylindrical or toroidal plasma surrounded by a conducting wall.

V. Gravitational (g) Modes in Slab Geometry

This chapter discusses modes driven by a gravitational force in slab geometry. If gravity is present, the MHD equations for a perfectly conducting, incompressible fluid are

$$\frac{\partial \rho}{\partial t} + \underline{V}\cdot\underline{\nabla}\rho = 0 \qquad (a)$$

$$\rho\frac{\partial \underline{V}}{\partial t} + \rho\underline{V}\cdot\underline{\nabla}\underline{V} = -\underline{\nabla}p + \frac{\underline{J}}{c}\times\underline{B} - \rho g \qquad (b)$$

$$\frac{\partial \underline{B}}{\partial t} = -\underline{\nabla}\times\underline{V}\times\underline{B} \qquad (c)$$

$$\underline{\nabla}\times\underline{B} = \frac{4\pi}{c}\underline{J} \qquad (d)$$

$$\nabla\cdot V = 0 \qquad (e)$$

All variation is assumed to be in the x direction.

At this point we will digress briefly to consider what the significance of g is. First, and most obvious, g could correspond to a real physical force. Consider for instance a θ pinch implosion shown in Fig. V1. Clearly, as the theata pinch implodes, the plasma accelerates inward. In analyzing the local MHD stability of the imploding pinch, one could work in the reference frame in which the fluid is locally at rest. The inward acceleration is then described by an outward inertial force. Also if a Θ pinch plasma is rotating with angular velocity $\underline{\Omega}$, one could analyze its stability by working in a rotating reference frame. Then the inertial force is the sum of the centrifugal, $\Omega^2 r\underline{i}_r$ and coriolis, $2\Omega\times V$. The former is outward and acts like a gravitational force.

Less obvious, certainly less precise, but probably more useful, the acceleration g can be used to model complicated geometric aspects of the magnetic field. To see this, let us examine the right hand side of Eq. (1b) without a g term

$$-\nabla p + \frac{1}{4\pi}(\nabla \times B)\times B = -\nabla p - \frac{1}{8\pi}\nabla B^2 - \frac{1}{4\pi}(B\cdot\nabla)B \quad (\text{II}\text{-}2)$$

In slab geometry, the lines of B in equilibrium are assumed to be straight. Therefore any equilibrium variation in B^2 is balanced by a change in pressure. (That is $(B\cdot\nabla)B = 0$ in slab geometry in equilibrium). In a more realistic equilibrium, there are additional forces on the fluid which result from geometric aspects of B. For instance in cylindrical geometry, the lines of force are curved. In toroidal geometry, not only are the lines of force curved, there is also a change in the magnitude of the toroidal field resulting from the (geometric effect of the) decrease of field with major radius. The question is whether these additional forces on the fluid, which arise from geometric dependence of B, can be modeled with a gravitational force.

Of course there is clearly no way in which this simple gravitational acceleration can model all of the very complicated effects of field inhomogeniety and curvature. However, as we will see, in a collisionless plasma at least (collision frequency much less than ion cyclotron frequency) one can convincingly argue that many of the important effects of complicated field structure can indeed be approximately be modeled by gravity.

The force on a fluid element of course is just the sum of forces on all individual particles comprising the fluid element. If the field

lines are curved, having radius R, the particles feel an outward centrifugal force $MV_{\|}^2/R$ where $V_{\|}$ is the velocity parallel to the line of force, and $R^{-1} = -(\underline{B}\cdot\underline{\nabla})\underline{B}/B^2$. Thus the force on the particle resulting from the curvature of the field line is

$$\underline{F}_c = - \frac{M v_{\|}^2 (\underline{B}\cdot\underline{\nabla})\underline{B}}{B^2} \qquad (V\,3)$$

In addition to the force resulting from the curvature of the field lines, there is also a force arising from the gradient in magnitude of $\underline{B}$ perpendicular to B. Consider for instance a magnetic field in the z direction which increases in the x direction. The force in the negative x direction on the right hand side of the particle orbit is larger than the force in the positive x direction on the left hand side of the particle orbit, as shown in Fig. V2. Thus there is a net force in the negative x direction

$$\underline{F}_G = - \frac{M v_{\perp}^2}{2|B|} \underline{\nabla}|B| \qquad (V\,4)$$

(These average forces are calculated in much more detail in any standard plasma physics textbook. See for instance Schmidt, Physics of Hot Plasmas, or Krall and Trivelpiece, Plasma Physics.) The equivalent gravitational force g can now be calculated from Eq. (V 3 and 4). Of course in using Eq. (V4) for $\underline{F}_G$, one must only use that part of $\underline{\nabla}|B|$ which is due to geometric effects and not use that part which is balanced by a pressure gradient. This latter part, of course, is perfectly well described in a slab model.

For our purposes now, we simply model

$$g = \underline{i}_R \, V_T^2/R \qquad (V\,5)$$

where $\underline{i}_R$ is a unit vector pointing outward along the radius of curvature of the field line, and V_T is a typical thermal velocity (that is V_T is roughly either the ion thermal velocity or else $(M_e/M_i)^{1/2}$ times the electron thermal velocity).

After this digression on the significance of gravity, we return to a discussion of g modes as described by the linearized version of Eq. (V1). All variation is taken to be in the x direction and g also points in the x direction. The magnetic field points in the z direction and is taken to be uniform. The basic g mode is then very easily derived. Assuming a time dependence exp γt for perturbed quantities the linearized versions of Eq. (1) are

$$\gamma\rho + V_x \frac{\partial \rho_0}{\partial x} = 0 \qquad (a)$$

$$\gamma \rho_0 \underline{V} = -\underline{\nabla} p - \frac{1}{4\pi}\left\{ \underline{\nabla}(\underline{B}_0 \cdot \underline{B}) - (\underline{B}_0 \cdot \underline{\nabla})\underline{B} - (\underline{B} \cdot \underline{\nabla})\underline{B}_0 + \rho \underline{g} i_x \right\} \qquad (b)$$

$$\nabla \cdot V = 0 \qquad (V6)$$

where now perturbed quantities have no subscript and unperturbed quantities have a subscript zero. Let us further simplify by assuming a spatial dependence of exp i ky (that is no x or z dependence) for perturbed quantities. Then inserting from Eq. (V6a) into Eq. (V6b) and taking the x component, we find

$$\gamma^2 = -g \frac{\frac{\partial \rho_0}{\partial x}}{\rho_0} \qquad (V7)$$

Thus, if g and $\partial \rho_0 / \partial x$ have opposite signs the plasma is unstable. These are the classic instabilities one has if magnetic field lines are convex to the plasma like the classic magnetic mirror arrangement shown in

Fig.(V3). Here, the quantity g as approximated by Eq. (V5) is outward, or in the positive radial direction. The density gradient however is in the negative radial direction so that $g \frac{\partial \rho_o}{\partial x} < 0$ and the plasma is unstable. Notice also that this instability is extremely violent. Assuming that $L_n \equiv \left(\rho_o \frac{\partial \rho_o}{\partial x}\right)^{-1}$ is of order of R which is of order of the size of the plasma R, the growth time is of order R/V_T. That is the time for the mode to grow is roughly the time for the plasma to escape from the mirror trap traveling at the thermal velocity; in other words, there is no confinement of the plasma at all!

Clearly, in order to confine the plasma, some means must be devised to stabilize these modes. One possibility is to utilize a cusp (like minimum B) type configuration like that shown in Fig. (V4) so that $g \frac{\partial \rho_o}{\partial x} > 0$ everywhere. Another possibility is to find some way to stabilize these modes. One way to stabilize them is by magnetic shear. A discussion of this stabilization mechanism will occupy the remainder of this chapter. In order to set the stage for our calculation of shear stabilization of g modes, we begin by considering these modes when $k_z \neq 0$.

If perturbed quantities vary as exp i $(k_y y + k_z Z)$, then the x component of Eq.(V6b) becomes

$$\gamma \rho_o V_x = \frac{i k_z B_o}{4\pi} B_x - \frac{V_x}{\gamma} g \frac{\partial \rho_o}{\partial x} \qquad (V\,8)$$

To obtain B_x in terms of V_x, one uses the x component of Eq. (V1c). Inserting for B_x in terms of V_x, we find that the dispersion relation is

$$\gamma^2 = - \frac{k_z^2 B_o^2}{4\pi \rho_o} - \frac{g}{\rho_o} \frac{\partial \rho_o}{\partial x} \qquad (V\,9)$$

Notice that for $k_z^2 V_A^2 > g \frac{\partial \rho_o}{\partial x} / \rho_o$ the mode is stable. Clearly as k_z increases, the unstable g mode attempts to couple to a stable shear Alfven mode. Postulating a k_z sufficiently large that γ^2 given by Eq. (V9) is negative is, of course, not equivalent to stabilizing the system. In an unsheared field, the plasma is still free to pick a parallel wave number equal to zero. The basic idea behind shear stabilization is to remove this freedom by imposing an equilibrium variation on the direction of $\underline{B}$.

Let us now say that

$$\underline{B}_o(x) = B_o \left(\underline{i}_z + \frac{x}{L_s} \underline{i}_y \right) \qquad (V\,10)$$

where we imagine $x << L_s$. Since this additional x variation is imposed on the system, all perturbed quantities have the functional form

$$f(x) \exp(i k y + \gamma t)$$

where we have set $k_z = 0$. Notice however that the variation in a perturbed quantity is no longer perpendicular to $\underline{B}_o$. Indeed

$$(\underline{B}_o \cdot \nabla) f(x) \exp(i k y + \gamma t) = i k B_o \frac{x}{L_s} f(x) \exp(i k y + \gamma t) \qquad (V\,11)$$

Thus the presence of shear forces any perturbed quantity to vary parallel to $\underline{B}_o$ as long as $x \neq 0$. This forced variation parallel to $\underline{B}$ will tend to couple to shear Alfven modes and stabilize the plasma. We now proceed to calculate just how much shear is needed for stabilization.

In a sheared field, the equation for the perturbed x velocity is slightly, but not much more difficult to specify. Because of the inherent x dependence of $\underline{B}_o$, one can no longer assume that perturbations are independent of x. To begin, take the curl of the perturbed momentum equation

$$\gamma \nabla \times \rho_0 \underline{V} = \frac{1}{4\pi\gamma} \nabla \times \left\{ (\underline{B}_0 \cdot \nabla)(\nabla \times \underline{V} \times \underline{B}_0) + \left[(\nabla \times \underline{V} \times \underline{B}_0) \cdot \nabla \right] \underline{B}_0 \right\}$$

$$- g \nabla \times \left\{ \frac{1}{\gamma} V_x \frac{\partial \rho_0}{\partial x} \underline{i}_z \right\} \qquad (V\ 12)$$

where we have made use of the fact that $\underline{B} = \frac{1}{\gamma} \nabla \times \underline{V} \times \underline{B}_0$. Now consider the x component of Eq. (V 12). Recalling that $\frac{\partial}{\partial z} = 0$, a short calculation gives the result

$$\left[\rho_0 \gamma^2 + \frac{B_0^2}{4\pi} \left(\frac{x}{L_s} \right)^2 k^2 \right] V_z = 0 \qquad (V\ 13)$$

Equation (V 13) above dictates that either $V_z = 0$, or else the quantity in the square brackets vanishes. The latter case implies shear (stable) Alfven waves at each point x. Since these are not unstable, we assume the former, ie

$$V_z = 0 \qquad (V\ 14)$$

From the fact that $V_z = 0$, one can show easily from Eq.(V 1d) that also

$$B_z = 0 \qquad (V\ 15)$$

Thus the perturbation is two dimensional in the x-y plane. The incompressibility condition then relates V_x to V_y and B_x to B_y

$$\frac{\partial B_x}{\partial x} + ik B_y = \frac{\partial V_x}{\partial x} + ikV_y = 0 \qquad (V\ 16)$$

Then, taking the z component of Eq. (V 12) and making use of Eq. (V 16)

above, we find the following simple equation for V_x:

$$\frac{\partial}{\partial x}\left(\rho\gamma^2 + k^2\left(\frac{x}{L_s}\right)^2\frac{B_0^2}{4\pi}\right)\frac{\partial V_x}{\partial x} - k^2\left(\rho_0\gamma^2 + k^2\left(\frac{x}{L_s}\right)^2\frac{B_0^2}{4\pi} + g\frac{\partial\rho_0}{\partial x}\right)V_x = 0 \qquad (V\ 17)$$

Notice that the term in the parentheses on the right hand side is simply the local dispersion relation, Eq. (V 9), if one assumes $k_z^2 = k^2(x/L_s)^2$. However, this is no longer the dispersion relation in the sheared system. For instance if Eq. (V 9) were initially satisfied, disturbances near $x = 0$ would grow while those far from $x = 0$ would not. A strong x dependence would then be induced by the local growth, and eventually the first term of Eq. (V 17) would also be important. The problem then is to find the eigenfunctions and eigenvalues of Eq. (V 17). In the limit of $x \to \infty$, the equation approximately reduced to

$$\frac{\partial^2 V_x}{\partial x^2} \approx k^2 V_x \qquad (V\ 18)$$

with solution

$$V_x \approx \exp \pm kx \qquad (V\ 19)$$

clearly the proper boundary condition is that V_x approaches zero at both $x = \pm\infty$. Since

$$\rho_0\gamma^2 + k^2\left(\frac{x}{L_s}\right)^2\frac{B_0^2}{4\pi} \equiv Q > 0 \qquad (V\ 20)$$

as long as $\gamma^2 > 0$, Eq. (V 17) has no singular points on the real x axis. Therefore one could easily solve this equation numerically for the eigenvalues γ^2.

We now see what insights may be obtained analytically. One can immediately show that if $g\frac{\partial\rho_0}{\partial x} > 0$, no solution with $\gamma^2 > 0$ can satisfy

the boundary conditions. To do so, note that $\rho\gamma^2 + k^2(\frac{x}{L_s})^2 \frac{B_o^2}{4\pi} \equiv Q(x)$ is then greater than zero. Assume that at $x \to -\infty$, V_x is well behaved and also that $V_x > 0$. Then

$$\frac{\partial V_x}{\partial x} = \frac{1}{Q(x)} \int_{-\infty}^{x} k^2 G(x') V_x \, dx' \qquad (V\,21)$$

where

$$G(x) = Q(x) + g \frac{\partial \rho_o}{\partial x} \qquad (V\,22)$$

which is greater than zero since $g \frac{\partial \rho_o}{\partial x}$. Therefore $\frac{\partial V_x}{\partial x} > 0$ for all x so that the solution for V_x is a monotonically increasing function of x. Hence, it does not satisfy the proper boundary condition as $x \to +\infty$. Clearly, in order for V_x to satisfy the proper boundary condition as $x \to +\infty$,,there must be some region of x where $G(x) < 0$.

Now let us examine how an unstable eigenfunction can be constructed. If $g \frac{\partial \rho_o}{\partial x}$ is greater than zero the function is monotonically increasing, and as $x \to \infty$ it diverges as exp kx. Now depending upon the sign of G(x) (Eq. V 22), the equation has two fundamentally different types of behavior. If $G(x) > 0$, the solution for V_x is a monotonically increasing function of x as we have just discussed. On the other hand, if $G(x) < 0$, the solution for V_x is generally oscilliatory in x. The local wave number is given very roughly by $k(-G(x)/Q(x))^{1/2}$. If G(x) changes sign as x varies, we will denote the regions of $G(x) > 0$ as monotonic regions and the regions where $G(x) < 0$ as oscilliatory regions. We have just shown that the regions $x \to \pm \infty$ are monotonic.

If $g \frac{\partial \rho_o}{\partial x} < 0$, there is an oscilliatory region specified by

$$x_{as}^2 < \frac{4\pi L_s^2}{k^2 B_o^2}\left(-g\frac{\partial \rho_o}{\partial x} - \gamma^2\right) \qquad (V\ 23)$$

Since the wave number of the oscillation in the oscilliatory region is given roughly by $k(-G(x)/Q(x))^{1/2}$, it is clear that increasing γ increases the wavelength in the oscilliatory region. Let us imagine that a $\gamma \equiv \gamma_-$ can be found such that $V_x = 0$ at $x = x_{os}$. Then, since $x > x_{os}$ is a monatonic region, the solution for V_x for $x > x_o$ diverges toward minus infinity as $x \to +\infty$ as shown in curve A in Fig. (V 5). As γ is increased, the wavelength in the oscilliatory region increases so that the solution for V_x will not curve downward as much here. Thus for a sufficiently large $\gamma \equiv \gamma_+$, the solution for V_x diverges toward positive infinity as $x \to \infty$ as shown in Fig. (V 5) curve B. Clearly, there exists some $\gamma \equiv \gamma_o$ where $\gamma_- < \gamma_o < \gamma_+$ for which the solution to Eq. (V 17) assymptotes to zero for through positive values of V_+ as shown in Fig. (V 5) curve C. This then is an unstable eigenfunction with eigenvalue γ_o.

One can now deduce the following criterion for determining whether Eq. (V 17) has unstable eigenvalues. First select a γ and assume V_x is well behaved as $x \to -\infty$ and integrate the equation towards plus infinity. If there is one zero of V_x before the solution diverges at $x = +\infty$, then there will be one eigenfunction with a growth rate larger than this assumed γ. Similarly, if there are two zeros of V_x before the solution diverges for $x \to +\infty$, there are two eigenfunctions with growth rate larger than the assumed γ; and so on. Clearly, the more nodes to the eigenfunction, the smaller is γ. The equation, and this technique of determining a sequence of eigenvalues is closely related to the Sturm - Liousville equation described in

Morse and Feshback, Methods of Theoretical Physics, Vol. I, Chapter VI or almost any advanced calculus textbook.

Now it is possible to derive very quickly an approximate criterion for shear stabilization of g modes. In order that $V_x(x_{os}) \approx 0$, it is necessary that there be roughly one half a wavelength of oscillation in the oscilliatory region. Approximating the wave number of this oscillation by the square root maximum value of k^2G divided by the square root of the maximum value of Q, we find instability if

$$\frac{2}{\pi} x_{os} k \left[-g \frac{\partial \rho_0}{\partial x} \Big/ k^2 \frac{x_{os}^2}{L_s^2} \frac{B_0^2}{4\pi} \right]^{1/2}$$

$$= \frac{2}{\pi} \left[-g \frac{\partial \rho_0}{\partial x} \right]^{1/2} \frac{L_s \sqrt{4\pi}}{B_0} \gtrsim 1 \qquad (V\,24)$$

For L_s much larger than specified by Eq. V 24, the mode grows with growth rate given roughly be Eq. (V 7).

Equation (V 25) is then a condition for shear stabilization of g modes which have scale length of order x_{os}. One might think that by localizing the mode very close to x = 0, and by greatly decreasing the growth rate, the wavelength of the oscillation for V_x in the oscilliatory region could

be significantly reduced so that unstable eigenfunctions could be constructed even if Eq. (V 25) is violated. This possibility will now be examined.

For very small x and γ, the equation for V_x can be written as

$$\frac{\partial}{\partial x}\left(\rho\gamma^2 + k^2\left(\frac{x}{L_s}\right)^2 \frac{B_o^2}{4\pi}\right)\frac{\partial V_x}{\partial x} - k^2 g \frac{\partial \rho_o}{\partial x} V_x = 0 \qquad (V\,26)$$

In Eq. (V 26) above, the γ^2 is retained in the left hand term so that the solution is non singular at x = 0. However clearly, for

$$x^2 >> L_s^2 \frac{4\pi\rho\gamma^2}{k^2 B_o^2} \qquad (V\,27)$$

the γ term in Eq. (V 26) is not important. Therefore, we can neglect γ, but restrict ourselves to the range of x denoted by Eq. (V 27). By considering the limit $x \to 0$ we can see how the solution behaves for small x and γ, and particularly, we can see whether the solution has a node. (Naturally one cannot connect the solution at positive x to the solution at negative x in this way, because to do so one must also have the solution in the region where Eq. (V 27) is violated.)

If $\gamma = 0$ in Eq. (V 25), one can solve by assuming $V_x = x^n$. (Appendix ___ is a review of some aspects of power series solutions of second order differential equations). In this case one can solve for n and find

$$n = -\tfrac{1}{2} \pm (1 + 4\Psi)^{1/2} \qquad (V\,28)$$

where

$$\Psi = 4\pi g \frac{\partial \rho_o}{\partial x} L_s^2 / B_o^2 \qquad (V\,29)$$

The condition for the exponent n to be complex is simply

$$\Psi < -\tfrac{1}{4} \qquad (V\,30)$$

However if n is complex, $n = n_r + in_i$ the behavior of V_x is oscilliatory, and the wavelength of oscillation approaches zero as $x \to 0$, that is

$$V_r = x^{n_r} \exp(i n_i \ln x)$$

Thus there are an infinity of nodes of V_r in the limit of $x \to 0$. This means that there are an infinity of unstable eigenfunctions. The growth rates of these eigenfunctions approach zero as the number of nodes increase. The condition for such localized unstable modes is given by Eq.(V 30), while the approximate condition for stabilizing modes spread over x_{os} is given by Eq. (V 24). Notice that the equations have roughly the same form except that about three times as much shear (that is L_s smaller by one third) is required to stabilize modes localized over x_{os} than is required to stabilize modes localized right at the position $x = 0$. A condition for the occurrence of unstable modes is then given by Eq. (V 30).

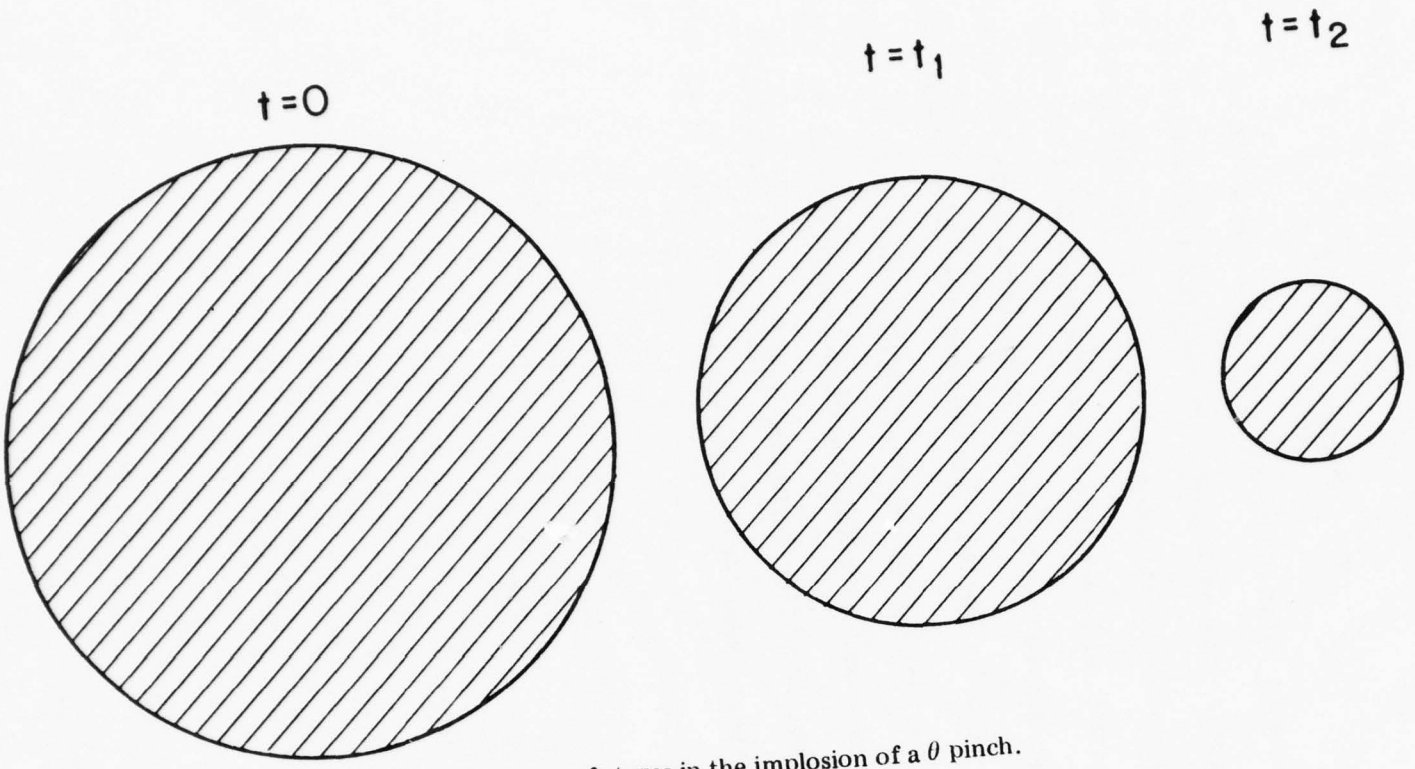

Fig. V 1 — Schematic of stages in the implosion of a θ pinch.

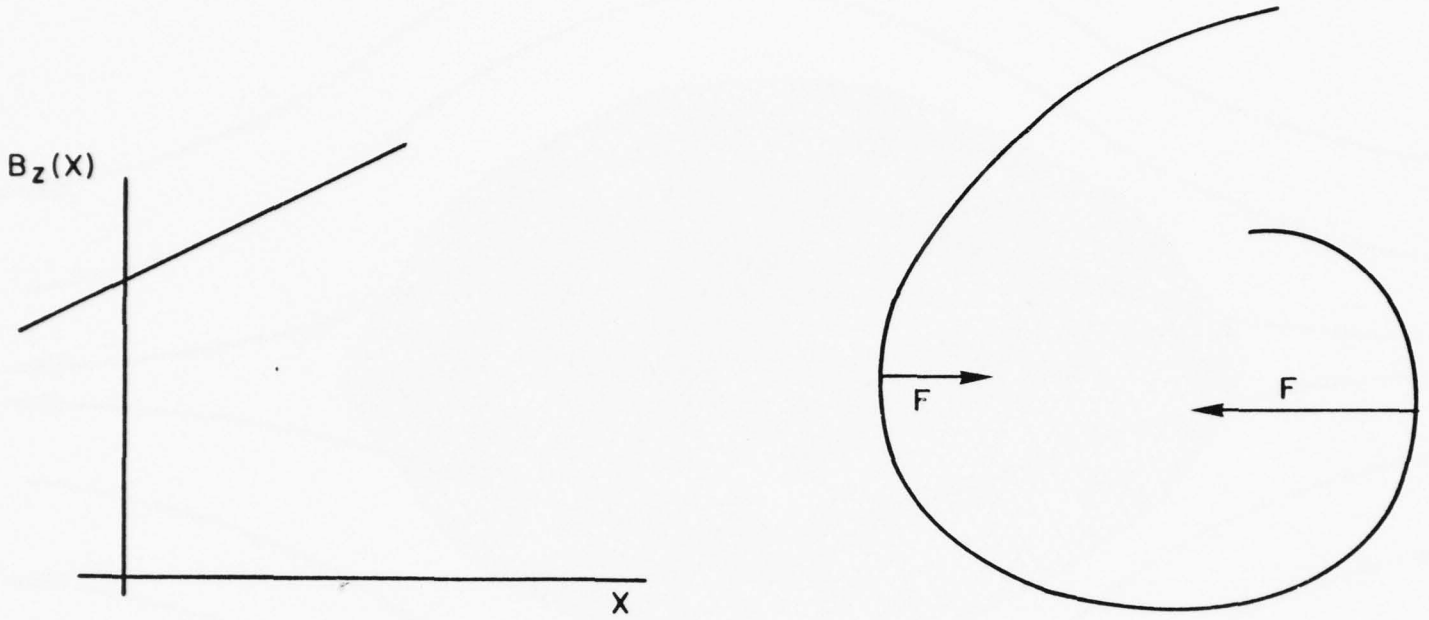

Fig. V 2 — Schematic showing how a gradient in B exerts an average force on a charged particle as it traverses its larmor orbit.

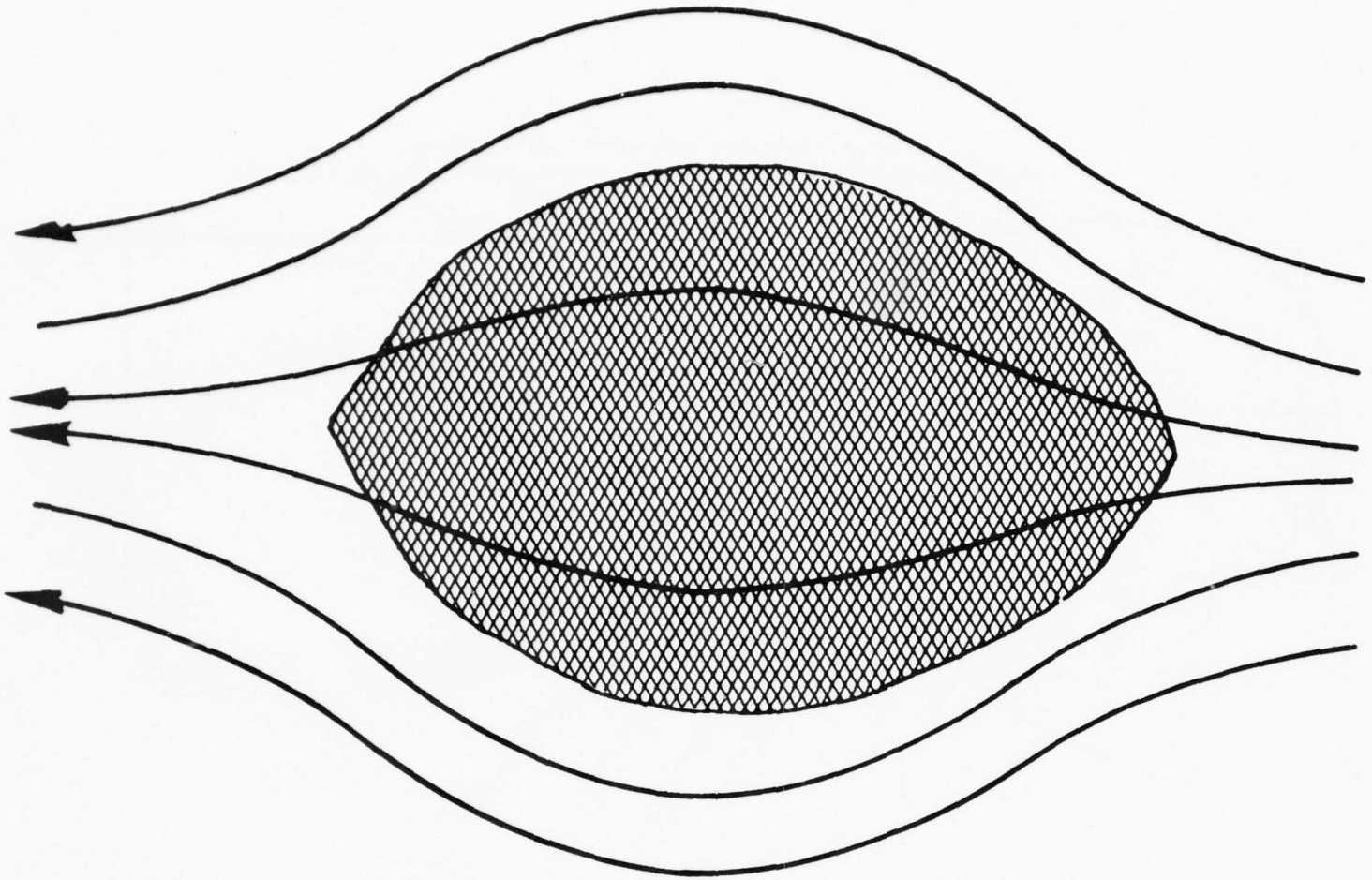

Fig. V 3 — Picture of a plasma confined in a magnetic configuration with unfavorable curvature.

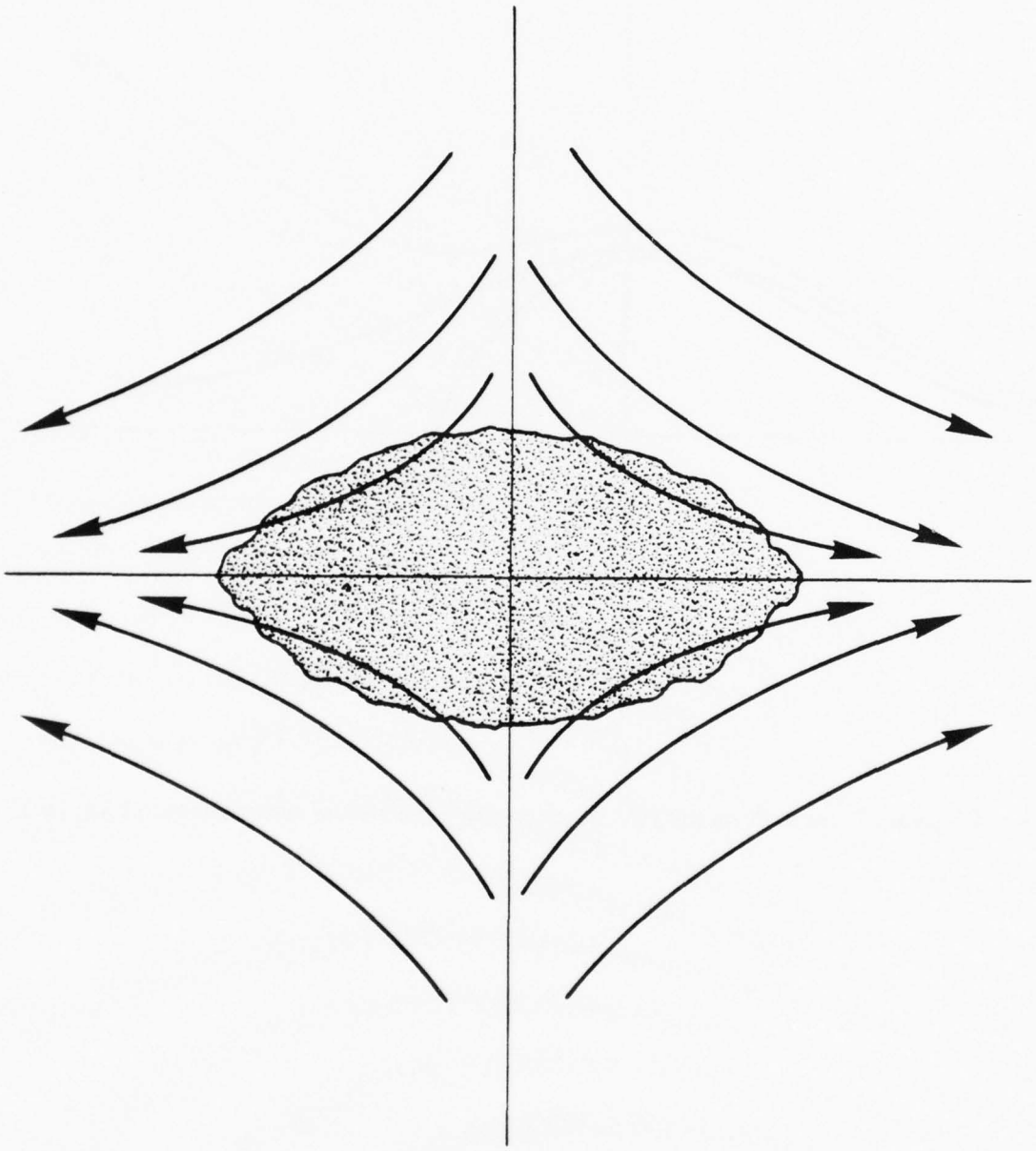

Fig. V 4 — Picture of a plasma confined in a magnetic configuration with favorable curvature.

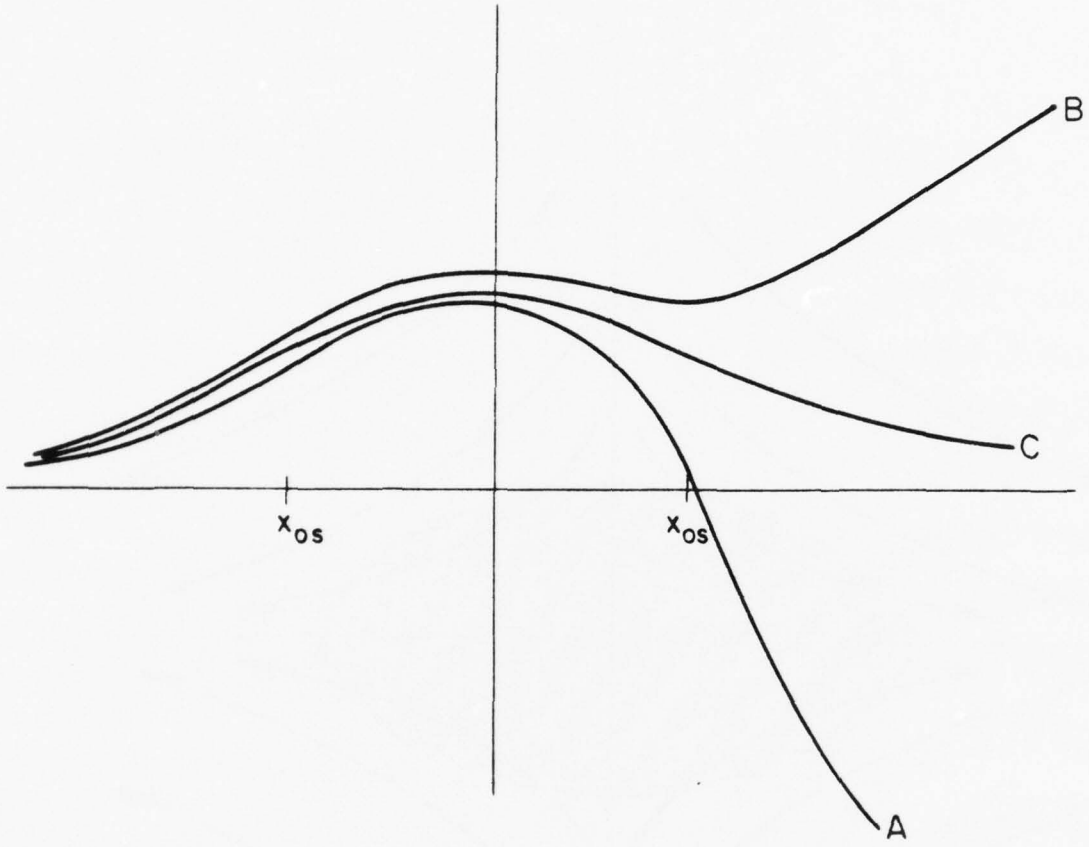

Fig. V 5 — Diagram of how to form the eigenfunction and calculate the eigenvalue (γ) of Eq. (V 17).

VI. Resistive g Modes

In the previous chapter it was shown how shear in the magnetic field produces a stabilizing effect on instabilities driven by a gravitational field g. In this chapter we shall again consider the stability of a plasma supported against gravity by a sheared magnetic field, but with the addition of a further physical effect, namely resistivity. For the g modes of the previous chapter the ideal MHD model was used for which the field and fluid are frozen together. However, for the instabilities to be described in this chapter, the magnetic field and fluid become decoupled due to the presence of resistivity. It will be found that the instability is again localized at the resonant surface where $k \cdot B = 0$, which, as we will see, is the only place where a small resistivity can introduce a significant amount of decoupling in motion of field and fluid. The net effect of resistivity on g modes is to nullify the stabilizing effect of magnetic shear. An ideal g mode which was stabilized by the presence of magnetic shear will be shown to be unstable - albiet at a reduced growth rate - when the presence of a small amount of resistivity is allowed for. Thus, if the effect of magnetic shear is compared to a dyke, then resistivity turns the dyke into a leaky one.

Let us now describe the resistive g mode in slab geometry, as in Chapter V. The magnetic field is taken as

$$\underline{B}_o(x) = B_o \hat{z} + B_o \frac{x}{L_s} \hat{y}$$

where B_o is a constant. The gravitational acceleration is in the x direction and all equilibrium fluid quantities also vary in only the x direction. We treat the plasma as an incompressible, weakly resistive fluid. The linearized equations of motion are

$$\rho_0 \frac{\partial \underline{V}}{\partial t} = -\underline{\nabla} p + \frac{1}{4\pi}(\underline{\nabla}\times\underline{B})\times\underline{B}_0 + \frac{1}{4\pi}(\underline{\nabla}\times\underline{B}_0)\times\underline{B} + \rho g \qquad (VI\ 1)$$

$$\frac{\partial \underline{B}}{\partial t} = \underline{\nabla}\times(\underline{V}\times\underline{B}_0) - \frac{\eta c^2}{4\pi}\nabla\times(\nabla\times B) \qquad (VI\ 2)$$

$$\frac{\partial \rho}{\partial t} = -(V\cdot\nabla)\rho_0 \qquad (VI\ 3)$$

$$\nabla\cdot V = 0 \qquad (VI\ 4)$$

Note that we have treated the resistivity as uniform in obtaining Eq. (VI. 2). Since the equilibrium varies only with x, we know that the eigenfunction of all perturbed quantities varies as f(x) exp ($\gamma t = iky$). We then find the V_z and B_z decouple from the remaining variable so that only the x and y components of Eq. (VI. 1 and 2) are required. (The variables V_z and B_z describe the properties of shear Alfven waves so that we may put both of these variables equal to zero when analyzing the behavior of linearly independent resistive g modes).

The x and y components of Eq. (VI 1 and 2) give

$$\gamma\rho_0 V_x = -\frac{\partial p}{\partial x} + \frac{B_0}{4\pi}\frac{x}{L_s} ikB_x - \frac{1}{4\pi}\frac{\partial}{\partial x}\left(B_0 \frac{x}{L_s} B_y\right) + \rho g \qquad (VI\ 5)$$

$$\gamma\rho V_y = -ikp + \frac{B_x}{4\pi}\frac{\partial}{\partial x}\left(B_0 \frac{x}{L_s}\right) \qquad (VI\ 6)$$

$$\gamma B_x = ikB_0 \frac{x}{L_s} V_x + \frac{\eta c^2}{4\pi}\left(\frac{\partial^2}{\partial x^2} - k^2\right) B_x \qquad (VI\ 7)$$

$$\gamma B_y = -B_0 \frac{\partial}{\partial x}\left(\frac{x}{L_s} V_x\right) + \frac{\eta c^2}{4\pi}\left(\frac{\partial^2}{\partial x^2} - k^2\right) B_y \qquad (VI\ 8)$$

We now simplify the problem by expressing all variables in terms of either V_x or B_x. Using Eqs. (VI. 6 and 4) we find

$$p = \frac{\gamma \rho_0}{k^2} \frac{\partial V_x}{\partial x} - \frac{i B_0}{4\pi k L_s} B_x \qquad \text{(VI 9)}$$

Substituting Eqs. (VI. 3 and 9) into Eq. (VI. 5) and using Maxwell's equation $\nabla \cdot B = 0$, gives

$$-\frac{\partial}{\partial x} \gamma^2 \rho_0 \frac{\partial V_x}{\partial x} + k^2 \left(\rho_0 \gamma^2 + g \frac{\partial \rho_0}{\partial x} \right) V_x = -i \gamma k \frac{B_0}{4\pi} \frac{x}{L_s} \left(\frac{\partial^2}{\partial x^2} - k^2 \right) B_x \qquad \text{(VI 10)}$$

We must now solve the pair of equations (VI. 7) and(VI. 10). Notice that with $\eta = 0$ in Eq. (VI. 7), the equations describing g modes in ideal MHD results.

Before solving these equations with $\eta \neq 0$, let us consider the effect of resistivity on the stability of the system. As already mentioned, the instability will be localized around the resonant surface $\underline{k} \cdot \underline{B}_0 = 0$. This is also the position where the motion of the fluid and field can most easily decouple. The form of Ohm's law which has been used to give Eq. (VI. 2) is

$$\eta \underline{J} = \underline{E} + \frac{\underline{V}}{c} \times \underline{B}_0 \qquad \text{(VI 11)}$$

For $\eta = 0$ the condition of frozen in field lines is simply

$$\underline{E} = -\frac{\underline{V}}{c} \times \underline{B}_0 \qquad \text{(VI 12)}$$

On the other hand, the opposite extreme to this is clearly when the fluid moves freely through the field lines, i.e., $V \neq 0$ but $E \approx 0$. In this case, Eq. (VI. 11) gives

$$J_z = \left. \frac{\underline{V}_1 \times \underline{B}_0}{\eta c} \right|_z = \frac{x}{c L_s} B_0 \frac{V_x}{\eta} \qquad \text{(VI 13)}$$

One part of the force exerted on the plasma is then

$$\underline{F} = \frac{\underline{J}}{c} \times \underline{B}_0 = -i_x B_0^2 \left(\frac{x}{L_s}\right)^2 \frac{V_x}{\gamma c^2} \qquad (VI\ 14)$$

From the negative sign, we see that the force is a restraining force and furthermore, for $x \neq 0$ and small η, this force is very large. This only means, of course, that the plasma does not slip through the field lines, rather the field remains frozen into the flow. However for $x = 0$ (that is $k \cdot B = 0$), the restraining force becomes small and the plasma can leak through the field. We therefore see the importance of the resonant surface and the reason that resistivity can be important at this point, but unimportant everywhere else in the plasma.

Let us assume that in the viscinity of the resonant surface the plasma flow is decoupled from the field, so that Eq. VI. 7 becomes

$$\left(\frac{\partial^2}{\partial x^2} - k^2\right) B_x = -\frac{4\pi i k}{\gamma c^2} B_0 \frac{x}{L_s} V_x \qquad (VI\ 15)$$

As we will see shortly, one simplifying feature of resistive g modes, as compared to for instance tearing modes (next chapter), is that resistive g modes are localized about the resonant surface. Therefore, for resistive g modes, (Eq. (VI. 5) can be taken to apply everywhere.

Substituting Eq. (VI. 15) into Eq. (VI. 10), we obtain

$$-\frac{\partial}{\partial x} \rho_0 \gamma^2 \frac{\partial V_x}{\partial x} + k^2 g \frac{\partial \rho_0}{\partial x} V_x + \frac{\gamma k^2 B_0^2 x^2}{\gamma c^2 L_s^2} V_x \qquad (VI\ 16)$$

The problem is now reduced to the solution of a single second ordinary differential equation, the quantum mechanical harmonic oscillator in fact. Since we are interested in solutions localized around $x = 0$, we neglect the

dependence of ρ_o on x and also neglected $k^2 B_x$ compared to $\frac{\partial^2 B_x}{\partial x^2}$ in Eq. (VI. 5). Finally we have assumed that the growth rate γ is much less than the growth rate in an unsheared field $\left(g/\rho_o \frac{\partial \rho_o}{\partial x}\right)^{1/2}$. Introducing the constants

$$A = \frac{\gamma \eta \rho_o L_s^2}{k^2 B_o^2} \qquad \text{(VI 17a)}$$

and

$$B = -\frac{g}{\gamma} \frac{d\rho_o}{dx} \eta \frac{L_s^2}{B_o^2} \qquad \text{(VI 17b)}$$

Eq. (VI. 16) can be rewritten

$$A \frac{d^2 V_x}{dx^2} + \left(B - x^2\right) V_x = 0 \qquad \text{(VI 18)}$$

Introducing a change in variables

$$x' = A^{-1/4} x$$

Eq. (VI. 8) becomes

$$\frac{d^2 V_x}{dx'^2} + \left(\frac{B}{A^{1/2}} - x'^2\right) V_x = 0 \qquad \text{(VI 19)}$$

The solutions to Eq. (VI. 19) which vanish at $x = \pm \infty$ are the Hermite functions

$$V_x = H(x') \exp - x'^2/2 \qquad \text{(VI 20)}$$

and the eigenvalues are

$$\frac{B}{A^{1/2}} = 2n+1 \qquad \text{(VI 21)}$$

Notice that there can only be a real eigenvalue γ, for $B > 0$. From the definition of B, Eq. (VI. 17.b), this means $g\rho_o' < 0$; that is density gradient is opposite to g so that the g mode in an unsheared field is unstable.

Equation (VI. 21) is the dispersion relation for the resistive g mode. Substituting for A and B, we find

$$\gamma = \left\{ \frac{1}{2n+1} \left(-g \frac{\partial \rho_o}{\partial x}\right) \frac{k L_s}{B_o} \right\}^{2/3} \left(\frac{\eta c^2}{\rho_o}\right)^{1/3} \qquad \text{(VI 22)}$$

This shows the characteristic dependence of the growth rate of the resistive g mode on the one third power of resistivity. Notice also that this mode cannot be removed by shear. As L_s decreases (increasing shear), the growth rate is reduced but there is no critical value at which it vanishes. Hence the earlier analogy with a "leaky dyke".

Finally, let us use the above solution to check the validity of the approximation which enabled us to carry out this analysis. This was the neglect of the γB_x compared with $\frac{\eta c^2}{4\pi} \frac{\partial^2 B_x}{\partial x^2}$ in Eq. (VI. 7). This approximation is only expected to be valid over a small distance, (say x_c) where x_c is given approximately from Eq. (VI. 16) by the condition

$$-k^2 g \frac{\partial \rho_0}{\partial x} V_x \approx \gamma \frac{k^2 B_0^2}{\eta} \left(\frac{x_c}{L_s}\right)^2 V_x$$

or

$$x_c \approx \left(\frac{-g \frac{\partial \rho_0}{\partial x} \eta L_s^2}{\gamma B_0^2} \right)$$

Using this to compare the orders of magnitude of the neglected term γB_x $\frac{\eta c^2}{4\pi} \frac{\partial^2 B_x}{\partial x^2}$, we find

$$\frac{\gamma B_x}{\frac{\eta c^2}{4\pi} \frac{\partial^2 B_x}{\partial x^2}} \sim 4\pi \gamma x_c^2 \sim \frac{4\pi\gamma}{\eta} \left(-g \frac{\partial \rho_0}{\partial x}\right) \frac{\eta L_s^2}{\gamma B_0^2}$$

From the expression for g given in the previous chapter

$$g \sim \frac{P_0}{\rho_0 R} \sim \frac{P_0 B_0^2}{\rho_0 r (B_z^2 + B_\theta^2)}$$

where R, the radius of the field line is $r(B_z^2 + B_\theta^2)/B_\theta^2$, and $L_s \sim Rq$ (R is the major radius of the torus), the condition for validity becomes

$$\frac{4\pi P}{B_{z0}^2 + B_{\theta 0}^2} \ll 1 \qquad \text{(VI 23)}$$

This condition is well satisfied in all current tokamaks and pinches.

VII. The Tearing Mode

In this chapter we turn to a discussion of one of the most important, and interesting modes in all of MHD theory, the tearing mode. This mode is quite different from the resistive g mode. There, resistivity allowed the plasma to slip through the sheared field, rather like (but much slower than) the case where there was no shear. The tearing mode is a totally different type of fluid motion and it is allowed only because of the presence of resistivity. In the resistive g mode, the fastest growing mode had V_x an even function of x. For the tearing mode however, V_x is an odd function of x so that for a particular y, two fluid elements on opposite sides of the singular surface are flowing either towards each other or away from each other.

Before actually discussing the tearing mode, it is worthwhile to examine this type of motion. By doing so, we will show that if magnetic field lines can reconnect, certain restraining forces disappear so that the equilibrium is more likely to be unstable. Let us consider two dimensional incompressible motion in the xy plane where initially

$$\underline{B} = B_0 \frac{x}{L_s} i_y \qquad (\text{VIII } 1)$$

Then specify the following velocity profile in the x direction

$$V_x = \begin{cases} -V_0 \cos ky & \delta < x \\ -V_0 \frac{x}{\delta} \cos ky & 0 < x < \delta \end{cases} \qquad (a) \quad (\text{VIII } 2)$$

$$V_x(-x) = -V_x(x) \qquad (b)$$

where δ is taken to be very small. Using the fact that the flow is two

dimensional and incompressible, we find

$$V_y = \begin{cases} 0 & \delta < x \\ \frac{V_0}{\delta} \sin ky & 0 < \delta < x \end{cases} \qquad \text{(a)} \qquad \text{(VII 3)}$$

$$V_y(-x) = V_y(x) \qquad \text{(b)}$$

Thus in the separation layer $|x| < \delta$, there is very rapid flow in the y direction. The velocity stream lines are as shown in Fig. (VII 1). The two fluids on opposite sides of the singular surface x = 0 stream towards each other for y > 0, recoil near x = 0 and then stream away from each other at some $y < \pi/k$. Similarly two fluid elements streaming towards each other at y < 0 recoil and stream away somewhere around $y > -\pi/k$. The fluid exactly at y = 0 initially, does not stream away toward either positive or negative y, but piles into the stagnation point at x = y = 0. We will call this type flow a tearing flow or tearing motion.

Now imagine that the fluid is magnetized with the field given by Eq. (VII 1). In ideal MHD, the magnetic field is frozen into the flow. This allows us to see just how the magnetic field reacts to the flow pattern shown in Fig. (VII 1). In Fig. (VII 2a) is shown a portion of two magnetic field lines $-\frac{\pi}{2k} < y < \frac{\pi}{2k}$ initially at x and -x where $|x| > \delta$ at time t = 0. On one of these field lines in Fig. (VII 2a) are a series of dots (A-A'). Since the field is frozen into the flow, it must always pass through these dots no matter where they go. Thus by following the position of these dots, we can construct the field line at later times. The field line for positive x can of course be drawn in an analogous way. Since $V_x = V_y = 0$ at $y = \pm \frac{\pi}{2k}$, the points A and A'

do not move, while the other points B-E move toward $x = -\delta$ with progressively higher velocity. Thus at a later time the field lines bulge as shown in Fig. (VII 2b). Now consider a still later time when points D, E and D′ have entered the separation region $-\delta < x < 0$. Point D shoots upward, D′ downward and E remains on the line $y = 0$, always approaching the separation point $x = y = 0$. Thus the field lines are distorted as shown in Fig. (VII 2c). At a later time this distortion is further accentuated and the field line looks as shown in Fig. (VII 2d). Notice that the field lines get very twisted and contorted by this type of motion.

This contortion of the field line strongly affects the fluid motion. The field line is sharply curved at the points marked with a * on the right hand side of Fig.s (VII c and d). However, as we have seen in Chapter III, a curved field line exerts a tension along the line rather like a rubber band. Thus the magnetic forces at the starred points in Figs. (VII 2c and d) (and of course at the analogous points on the left hand graph) are trying hard to snap the line back into its original shape. That is, the magnetic forces provide a strong restoring force which tends to prevent the type of fluid motion given by Eq. (VII 2 and 3).

Now, let us examine what effect non zero resistivity has on this motion. If the plasma has resistivity, the field lines can break and reconnect. Notice also that in addition to the sharp corners induced at the stars in Fig. (VII 2c and d), there are also long lines of weak, oppositely directed fields forced right next to each other near the singular surface $x = o$. Thus if resistivity, and thereby magnetic diffusion is allowed, the field lines, rather than looking like those in Fig. (VII 2c and d) would look like that shown in Fig. (VII 3).

Notice that the field pattern in Fig. (VII 3) does not have nearly as many sharp corners as that in Fig. (VII 2 c or d). Thus, it provides a much weaker restraining force against the tearing motion described by Eq. (VII 2 and 3). Indeed, as we will see in this chapter, configurations which are stable to tearing motion in ideal MHD can be unstable if the resistivity is non zero.

We now continue by writing out the equations for the linear stability of the system. We assume that $\underline{B}_o = B_o i_z + B_{oy}(x) iy$ where $B_{oy} = o$ at $x = 0$. The procedure is exactly the same as in Chapter V, namely take the x component of the curl of the momentum equation to show that $V_z = 0$. The z component of Eq. (V 1c) then shows that $B_z = 0$. Then take the z component of the curl of the momentum equation, use the fact that V and B are two dimensional and incompressible, and arrive at the result

$$\gamma\left[\frac{\partial}{\partial x}\frac{\rho_o}{ik}\frac{\partial V_x}{\partial x} + ik\rho_o V_x\right] = -\frac{1}{4\pi}\left[-B_{oy}\frac{\partial^2 B_x}{\partial x^2} + B_x\frac{\partial^2 B_{oy}}{\partial x^2} + k^2 B_{oy} B_x\right] \qquad \text{(VII 4)}$$

assuming, as usual that perturbed quantities vary as $\exp(\delta t + iky)$. Notice that Eq. (VII 4) combined with the x component of Eq. (V 1c) would give Eq. (V 17) except that in the former g is assumed to vanish, while in the latter, the second derivation of the current) is assumed zero.

If the resistivity is present, the equation relating B_x to V_x is

$$\gamma B_x = ik B_{oy} V_x + \frac{\eta c^2}{4\pi}\left(\frac{\partial^2 B_x}{\partial x^2} - k^2 B_x\right) \qquad \text{(VII 5)}$$

Let us first prove that this configuration is stable in ideal MHD (i.e. if $\eta = 0$). Substituting $B_x = ikB_{yo}V_x/\gamma$ into the right hand side of Eq. (VII 4),

we find the result

$$\frac{\partial}{\partial x}\left(\frac{\rho_o \gamma^2}{k^2} + \frac{B_{oy}^2}{4\pi}\right)\frac{\partial}{\partial x} V_x = \left(\frac{k^2 B_{oy}^2}{4\pi} + \rho\gamma^2\right) V_x \qquad \text{(VII 6)}$$

Notice that for real γ, the right hand side of Eq. (VII 6) is positive for all x. Thus, as discussed in Chapter V, V_x is a monotonically increasing function of x for all x as long as V_x and $\frac{\partial V_x}{\partial x}$ are both positive in the limit of $x \to \infty$. Hence there is no way to have a solution for V_x which approaches zero as $x \to \pm \infty$, so the plasma is stable in ideal MHD.

Another way to understand this ideal MHD stability is as follows. According to Maxwells equation an electric field

$$E_z = -\frac{\gamma}{ick} B_x \qquad \text{(VII 7)}$$

is induced by the fluid motion. However, we also have

$$E_z = -\frac{1}{c} V_x B_{oy} \qquad \text{(VII 8)}$$

so that any non zero E_z induces an infinitely large V_x near the singular point $x = B_{yo} = 0$. The only possible resolution in ideal MHD is of course $\gamma = 0$, or stability for the fluid. If the resistivity is non zero, then near the singular point the electric field can be balanced not only by fluid flow, but by Ohmic dissipation.

Let us now imagine that the resistivity is very small, but non-vanishing, and that its presence gives rise to instabilities whose growth rate vanishes in some way as $\eta \to 0$. Then, away from the singular point we expect the plasma to be described by the Ideal MHD equations with zero γ, or setting the right hand side of Eq. (VII 4) equal to zero,

$$\frac{d^2 B_x}{dx^2} = \left(k^2 + \frac{1}{B_{oy}} \frac{d^2 B_{oy}}{dx^2}\right) B_x \qquad \text{(VII 9)}$$

Let us briefly discuss the significance of the neglect of γ. Neglecting the growth rate in the momentum equation simply means

$$\frac{1}{c}\,(\underline{J} \times \underline{B}_o) + \frac{1}{c}\,(J_o \times B) - \nabla p = 0,$$

or equivantly

$$\nabla \times \left\{ \underline{J} \times \underline{B}_o + \underline{J}_o \times B \right\} = 0.$$

That is away from the singular region, the perturbed plasma is in a state of ideal MHD pressure balance equilibrium. Imagine that the tearing mode we consider grows with growth rate much less than kV_A where V_A is a characteristic Alfven speed in the outer region. Then if the plasma configuration is not in pressure balance equilibrium, magnetosonic waves and/or shocks with frequency $\omega \sim kV_A$ will be generated. Once these magnetosonic disturbances damp out, pressure balance will be attained. Our fundamental assumption then is that the time scale for maintaining this pressure balance is much less than the characteristic growth time of the tearing mode. Therefore, in the outer region, pressure balance applies for all time and this outer region is described by Eq. VII 9.

There are two difficulties in describing the entire system with Eq. (VII 9) above. First of all there is no eigenvalue γ, so that a solution which satisfies the proper boundary condition at $x = -\infty$ in general will not satisfy the boundary condition at $x = +\infty$. Stated another way, if the solution satisfies the boundary conditions at both $x = -\infty$ and $x = +\infty$, in general there will be a discontinuity in slope at the position where the two solutions meet (assuming the solutions are normalized so that there is no discontinuity in B_x itself). Secondly, the equation is singular at $x = 0$ where $B_{oy} = 0$. As shown in Appendix ___, the two linearly independent solutions, denoted ψ_1 and ψ_2 behave for small x as

$$\psi_1 = x$$
$$\psi_2 = C_1 + C_2 x \ln x \qquad \text{(VII 10)}$$

The idea then is that Eq. (VII 9) applies for all x except a very narrow range around $x = 0$, (the outer region). The solution of Eq. (VII 9) in the outer region has a discontinuity in slope at $x = 0$. In a very narrow range around $x = 0$ (the inner region), inertia and resistivity both come into play and smoothly connect the two outer solutions.

Before actually calculating the growth rate we consider more carefully just what drives instability and calculate qualitative expressions for the growth rate. Let us calculate the power liberated by the fluid in its motion. Imagine the fluid is acted upon by a force density $\underline{F}$ and that the fluid velocity is $\underline{V}$. Then the power P going into the fluid is

$$P = \int d^3x \quad \underline{V}^* \cdot \underline{F} \quad + c.c. \qquad \text{(VII 11 .)}$$

However for incompressible motion,

$$\underline{V} = \text{curl } \underline{R} \qquad \text{(VII 12)}$$

so that the power going into the fluid is

$$P = \int d^3x \ \text{curl}\, \underline{R} \cdot \underline{F} = \int d^3x \ \underline{R} \cdot \text{curl}\, \underline{F} \qquad \text{(VII 13)}$$

where we have assumed the solution is well behaved at $x = \pm \infty$ and that the velocities at $x = 0^+$ are somehow smoothly connected to those at $x = 0^-$. For two dimensional incompressible motion

$$\underline{R} = \frac{V_x}{ik} \underline{i}_z$$

so that

$$P = \int d^3x \left(\frac{V_x^*}{-ik} \right) \cdot \left(\nabla \times F \right)_z + \text{c.c.} \qquad \text{VII 14}$$

In ideal MHD, V_x is related to B_x by Eq. (VII 6), with $\eta = 0$, and the right hand side of Eq. (VII 4) is an expression for the z component of the curl of the force density. Putting these together we find

$$P = -\frac{1}{4\pi} \int d^3x \ \frac{\gamma}{k^2} B_x \left\{ -\frac{d^2 B_x}{dx^2} + k^2 B_x + \frac{\frac{d^2 B_{oy}}{dx^2}}{B_{oy}} B_x \right\} + \text{c.c.} \qquad \text{(VII 15)}$$

where we have assumed that B_x is real. The quantity in the curly brackets is just Eq. (VII 10) and is zero in the outer region. However, Eq. (VII 10) is not satisfied everywhere in the plasma, but only in the outer region. Thus power can be dissipated by the fluid in the inner region.

The outer region solutions for large x generally have a discontinuous derivative at $x = 0$, but as is apparent from Eqs. (VII 11 a and b), B_x itself is well behaved and continuous. This means that in the inner region, $\frac{\partial^2 B_x}{\partial x^2}$ is very large so that it is the dominant term in Eq. (VII 5). Hence the power per unit area dissipated in the inner region is given by

$$P = \frac{\gamma}{4\pi k^2} B_x^2 (x=0) \ \Delta + \text{c.c.} \qquad \text{(VII 16)}$$

where

$$\Delta = \frac{1}{B_x(x=0)} \left\{ \left.\frac{dB_x}{dx}\right|_{x=0^+} - \left.\frac{dB_x}{dx}\right|_{x=0^-} \right\} \qquad (VII\ 17)$$

Thus if Δ is positive, energy is dissipated by the fluid in the inner region, and we expect that the plasma is unstable. Clearly the potential energy driving this dissipation comes from the outer region. This is obvious because B_{oz} is not involved in the motion and B_{oy} is zero at the singular point, so there is no free energy in the inner region. In Chapters VIII and XII we will discuss other aspects of the free energy which drives the tearing mode.

The basic picture of a tearing mode is then that energy is released in the outer region and dissipated in the inner region. The condition for release of energy in the outer region, and therefore the condition for instability is

$$\Delta > 0. \qquad (VII\ 18)$$

As is shown in Appendix ___, for the sheet current at $x = \pm a$, and the profile

$$B_{oy} = B_{oy} \tanh ka, \qquad (VII\ 19)$$

the Δ's are given respectively by

$$\Delta = 2k\left(\frac{1 - ka - ka\tanh ka}{ka - (1-ka)\tanh ka}\right) \qquad (VII\ 20)$$

$$\Delta = a\left(\frac{1}{ka^2} - k\right) \qquad (VII\ 21)$$

Hence for sufficiently small k, each current distribution is potentially unstable to tearing modes.

One other interesting aspect of the instability criterion $\Delta > 0$ is the following. If $\Delta = 0$, the MHD solutions for $\gamma = 0$ connect smoothly to each other through the singularity. Thus if $\Delta = 0$ there is another MHD equilibrium ($B = \underline{B}_o + \underline{B}$) which can be arrived at from the original equilibrium with no expenditure of energy. Hence the condition for tearing mode instability is that there be a neighboring equilibrium of the magnetic structure which has the same energy as the initial equilibrium. This aspect will be important later on when we discuss the nonlinear theory.

Now that we have the condition for instability, we continue by estimating the size of the inner region and the growth rate. To start, we will eliminate the $\frac{d^2B_x}{dx^2}$ term in Eq. (VII 4) by using Eq. (VII 5). The result is

$$\frac{\partial}{\partial x}\rho_o \frac{\partial v_x}{\partial x} - k^2 \rho_o v_x - \frac{k^2 B_{oy}^2(x)}{\pi c^2 \gamma} v_x = -ik\left[\frac{-B_{oy}}{\pi c^2} + \frac{B_{oy}''}{4\pi\gamma} + \frac{k^2 B_{oy}}{4\pi\gamma^2}\right] B_x \qquad (VII\ 22)$$

where we have neglected $k^2 B_x << \frac{\partial^2 x}{\partial x^2}$ in Eq. (VII 5). Within the inner region, B_x is nearly constant as we have discussed previously, and $B_{oy} \approx B_o \frac{x}{L_s}$. Thus Eq. (VII 22) is an inhomogeneous differential equation for V_x in terms of the now constant B_x. Clearly the characteristic length scale on which V_x varies in the inner region is

$$L_c = \left(\frac{\rho_o \pi c^2 \gamma L_s^2}{k^2 B_o^2}\right)^{1/4} \qquad (VII\ 23)$$

To derive the growth rate, let us assume that the energy released in the outer region is dissipated by Ohmic heating in the inner region. Recall that $\frac{\partial B_x}{\partial x}$ is discontinuous across the inner region. Since

$B_y = -\frac{1}{ik}\frac{\partial B_x}{\partial x}$, B_y is then itself discontinuous across this region. Thus there is a strong current in the z direction which flows in the inner region. A rough estimate of the magnitude of this current is

$$J_z = \frac{c}{4\pi}\frac{B_y^+ - B_y^-}{L_c} \simeq \frac{c}{4\pi ik} B_x(x=0)\frac{\Delta}{L_c} \qquad (VII\ 24)$$

The power dissipated per unit area is then $\eta J_z^2 L_c$. Equating the Ohmic power dissipated in the inner region with the power released by the fluid in the outer region, we find

$$\frac{\eta c^2 \Delta^2 B_x^2(x=0) L_c}{16\pi^2 k^2 L_c^2} \simeq \frac{\gamma}{4\pi k^2}\Delta \qquad (VII\ 25a)$$

or

$$\gamma \simeq \left(\frac{1}{4\pi}\right)^{4/5}(\eta c^2)^{3/5}\,\Delta^{4/5}\left(\frac{k^2 B_o^2}{\rho_o L_s^2}\right)^{1/5} \qquad (VII\ 25b)$$

and

$$L_c \simeq \left(\frac{\rho_o L_s^2}{4k^2 B_o^2}\right)^{1/5}(\eta c^2)^{2/5}\left(\frac{\Delta}{4\pi}\right)^{1/5} \qquad (VII\ 25c)$$

Notice that once again, as for the case of the resistive g mode, the growth rate is proportional to a fractional power of the resistivity. This means that even if $\underline{\nabla} \times \eta \underline{\nabla} \times B_o \neq 0$, so that the plasma is not initially in equilibrium, the time for the relaxation of the plasma due to tearing modes, $t \sim \eta^{-3/5}$ is quicker than the time scale for relaxation of the assumed equilibrium due to resistive diffusion $t_r \sim \eta^{-1}$.

We now conclude this chapter by actually calculating the growth rate and also Ohmic and kinetic power dissipated in the inner region. Here the velocity is the solution of Eq. (VII 22). We now make a slight simplification and assume that the current sheet is symmetric so that B_{oy}'' also vanishes at

the singular surface. In this case, in the limit of $\eta \to 0$ the dominant term on the right handside of Eq. (VII 22) is the $-\frac{B_{oy}}{\eta c^2}$ term since it diverges as η^{-1} as $\eta \to 0$, whereas the other two terms diverge as $\eta^{-3/5}$ according to Eq. (VII 25b).

The idea now is to solve Eq. (VII 22) for V_x in the inner region. The growth rate is then calculated by insisting that the inner region solution matches with the outer region solutions for large x. If the inner region is narrow on the length scale which B_x varies on, then B_x on the right hand side of Eq.(VII) can be regarded as constant. This is equivalent to the constant ψ approximation first introduced by Furth, Killeen and Rosenbluth (Physics of Fluids, 6, 459 (1963)).

Making these approximations, Eq. (VII 22) reduces to

$$\rho_o \frac{\partial^2 V_x}{\partial x^2} - k^2 \rho_o V_x - \frac{k^2 B_o^2 x^2}{\eta c^2 \gamma L_s^2} V_x = i k \frac{B_o x}{\eta c^2 L_s} B_x(x=0) \qquad (VII\ 26)$$

assuming ρ_o does not vary substantially in the inner region. The solution for V_x from Eq. (VII 26) is that linear combination of homogeneous solutions and the particular solutions which satisfy the appropriate boundary conditions, that is $V_x \to 0$ as $x \to \pm \infty$. We first look at the solution to the homogeneous equation

$$\rho_o \frac{d^2}{dx^2} V_x = \left(k^2 \rho_o + \frac{k^2 B_o^2 x^2}{\eta c^2 \gamma L_s^2} \right) V_x$$

Since the quantity in parentheses is positive, the solution for V_x which is positive at $x \to -\infty$ is a monotonically increasing function of x and therefore cannot possibly satisfy the boundary conditions. Therefore the appropriate solution to Eq. (VII 26) is the particular solution alone. In general this can easily be calculated numerically. Here we give an approximate analytic solution. In the limit of $\eta \to 0$, the particular

solution for large x is

$$V_x = \frac{i\gamma L_s B_x}{k B_{0x}} = \frac{i\gamma}{k B_{0y}} B_x \qquad (VII\ 27)$$

which is the MHD solution. We now proceed to calculate the particular solution for all x. Assuming that the inner region width is much less than 1/k, Eq. (VII 26) can be simplified to

$$\frac{d^2 V_x}{dx^2} - \frac{x^2}{L_c^4} V_x = \frac{i\gamma B_x(x=0) L_s x}{k B_0 L_c^4} \qquad (VII\ 28)$$

At large x, the particular solution is given by Eq. (VII 27) while for small x it is the solution to

$$\frac{d^2 V_x}{dx^2} = \frac{i\gamma B_x(x=0) L_s}{k B_0 L_c^4} x \qquad (VII\ 29)$$

Let us assume a solution for V_x of the form

$$V_x = i \frac{Ax}{1 + Cx^2} \qquad (VII\ 30)$$

For large x, this matches with Eq. (VII 27) if

$$\frac{A}{C} = - \frac{\gamma L_s B_x(x=0)}{k B_0} \qquad (VII\ 31)$$

Expanding Eq. (VII 30) for small x and taking the second derivative, we find that Eq. (VII 30) matches the solution for small x if

$$AC = - \frac{\gamma L_s}{6 k B L_c^4} B_x(x=0) \qquad (VII\ 32)$$

Solving for A and C, we find an approximate particular solution to Eq. (VII 28) which matches the approximate solution for both large x and

small x is

$$V_x = i \frac{\frac{\gamma L_s x B_x(x=0)}{\sqrt{6}\, k B_0 L_c^2}}{1 + \frac{x^2}{\sqrt{6} L_c^2}} \qquad \text{(VII 33)}$$

Thus we now have an approximate solution for V_x in the inner region. The final task is to use Eq. (VII 5) to compute the eigenvalue γ. The trick is to insure that the Δ generated by the inner region solution is the same Δ generated by the outer region solution, for instance Eqs. (VII 20 or 21). To calculate the delta generated by the inner solution, we utilize Eq. (VII 5) (with $k^2 B_x$ neglected on the right hand side). Inserting V_x from Eq. (VII 33), this is

$$\frac{d^2 B_x}{dx^2} = \frac{4\pi}{\eta c^2} \left[\frac{\gamma}{1 + \frac{x^2}{\sqrt{6} L_c^2}} \right] B_x(x=0) \qquad \text{(VII 34)}$$

Integrating Eq.(VII 34) from $x = -\infty$ to $x = +\infty$ (that is across the inner region), we find

$$\frac{1}{B_x(x=0)} \left. \frac{dB_x}{dx} \right|_{-\infty}^{\infty} = \frac{4\pi\gamma}{\eta c^2} (6)^{1/4} \pi L_c \qquad \text{(VII 35)}$$

Inserting for L_c from Eq. (VII 23), we see that the growth rate is given to within numerical factors by the approximate expression, Eq. (VII 25b).

We now calculate the Ohmic power dissipated in the singular layer, and the kinetic power dissipated there also. The Ohmic power dissipated per unit area is ηJ_z^2 integrated across the singular layer. Now since

$$E_z = -\frac{1}{c} V_x B_{0y} + \eta J_z \qquad \text{(VII 36)}$$

but is also equal to $-\gamma B_x/ikc$; we find that the Ohmic power dissipated is

$$P_\Omega = \int_{-\infty}^{\infty} \frac{dx}{\eta c^2} \left| \frac{-\gamma}{ik} B_x + V_x B_{oy} \right|^2 \qquad \text{(VII 37)}$$

Substituting for V_x, we find that

$$P_\Omega = \int_{-\infty}^{\infty} \frac{dx}{\eta c^2} \frac{\gamma^2 B_x^2(x=0)}{\left(1 + \frac{x^2}{\sqrt{6} L_c^2}\right)^2} \qquad \text{(VII 38)}$$

The power dissipated into kinetic energy is somewhat more difficult to define because there is kinetic power in both the inner and outer region. However, as is apparent from Fig. (VII 1) and also from Eq. (VII 3), the y velocity is much larger than the x velocity in the inner region, but much smaller than it in the outer region. Therefore, we will define $\frac{1}{2}\rho V_y^2$ as the kinetic energy dissipated in the layer. Using the fact that $\nabla \cdot V = 0$, the kinetic power dissipated in the layer is then given by

$$P_K = \frac{\gamma\rho}{k^2} \int_{-\infty}^{\infty} \left|\frac{dV_x}{dx}\right|^2 dx = \frac{\rho \gamma^3 L_s^2 B_x^2(x=0)}{6 k^2 B_o^2 L_c^4} \int_{-\infty}^{\infty} dx \left\{ \frac{1 - \frac{x^2}{\sqrt{6} L_c^2}}{\left(1 + \frac{x^2}{\sqrt{6} L_c^2}\right)^2} \right\}^2 \qquad \text{(VII 39)}$$

where we have made use of Eq. (VII 33) for V_x. The integrals in Eqs. (VII 38 and 39) are forms (or slight variations of forms) which can be found in tables of definite integrals for instance

Using the expression for γ and L_c, we find

$$\frac{P_K}{P_\Omega} = \frac{1}{16}$$

Therefore, in a tearing mode, most of the energy liberated by the fluid in the outer region is dissipated into Ohmic heating of the inner region, with very little going into fluid motion in the inner region.

To summarize, the tearing mode just becomes unstable when there is a second magnetic equilibrium which is accessible from the first with no expenditure of energy.

The instability develops by the fluid releasing magnetic energy in the outer region, and dissipating it principally via Ohmic heating in a narrow inner region near the singular surface. This dissipation near x = 0 manifests itself by a change in the magnetic field topology, that is, island formation. If $B_y << B_o$, the equations for the field lines in the xy plane is

$$\frac{dx}{B\cos ky} = \frac{dy}{B_o \frac{x}{L_s}}$$

where B_x is taken as Bcosky. The equation for the field line is then

$$x = \left(K + \frac{2L_s B}{B_o k} \sin ky\right)^{1/2} \qquad \text{((VII 40)}$$

The field line has a separatrix if $K = \frac{2L_s B}{kB_o}$ and this separatrix has maximum width (the island width)

$$\Delta X_{is} = 2\left(\frac{B L_s}{k B_o}\right)^{1/2} \qquad \text{(VII 41)}$$

The field lines in the xy plane are shown in Fig. (VII 4).

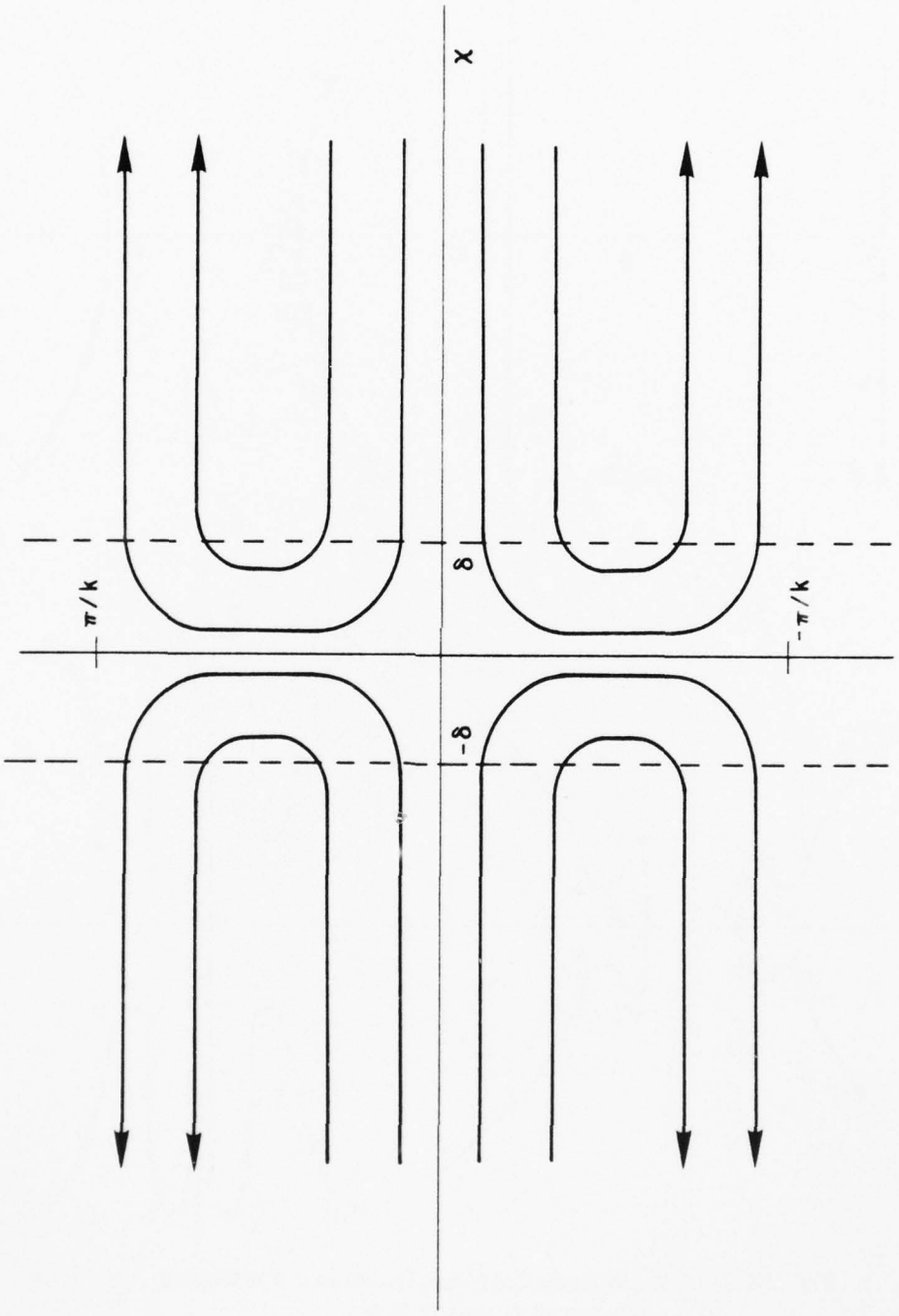

Fig. VII 1 — The velocity streamlines for a tearing motion.

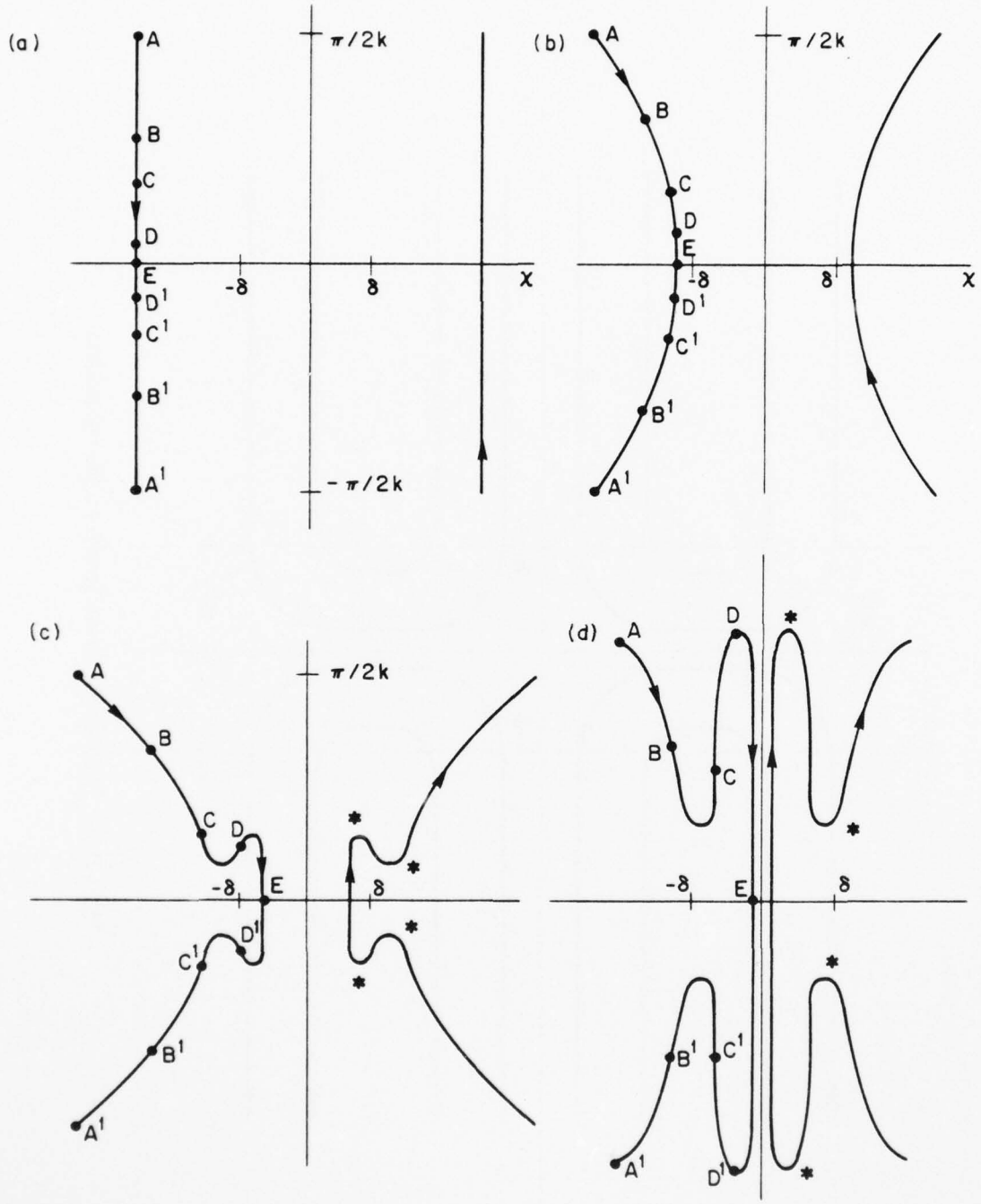

Fig. VII 2 — The magnetic field line, frozen into the tearing motion at successive times.

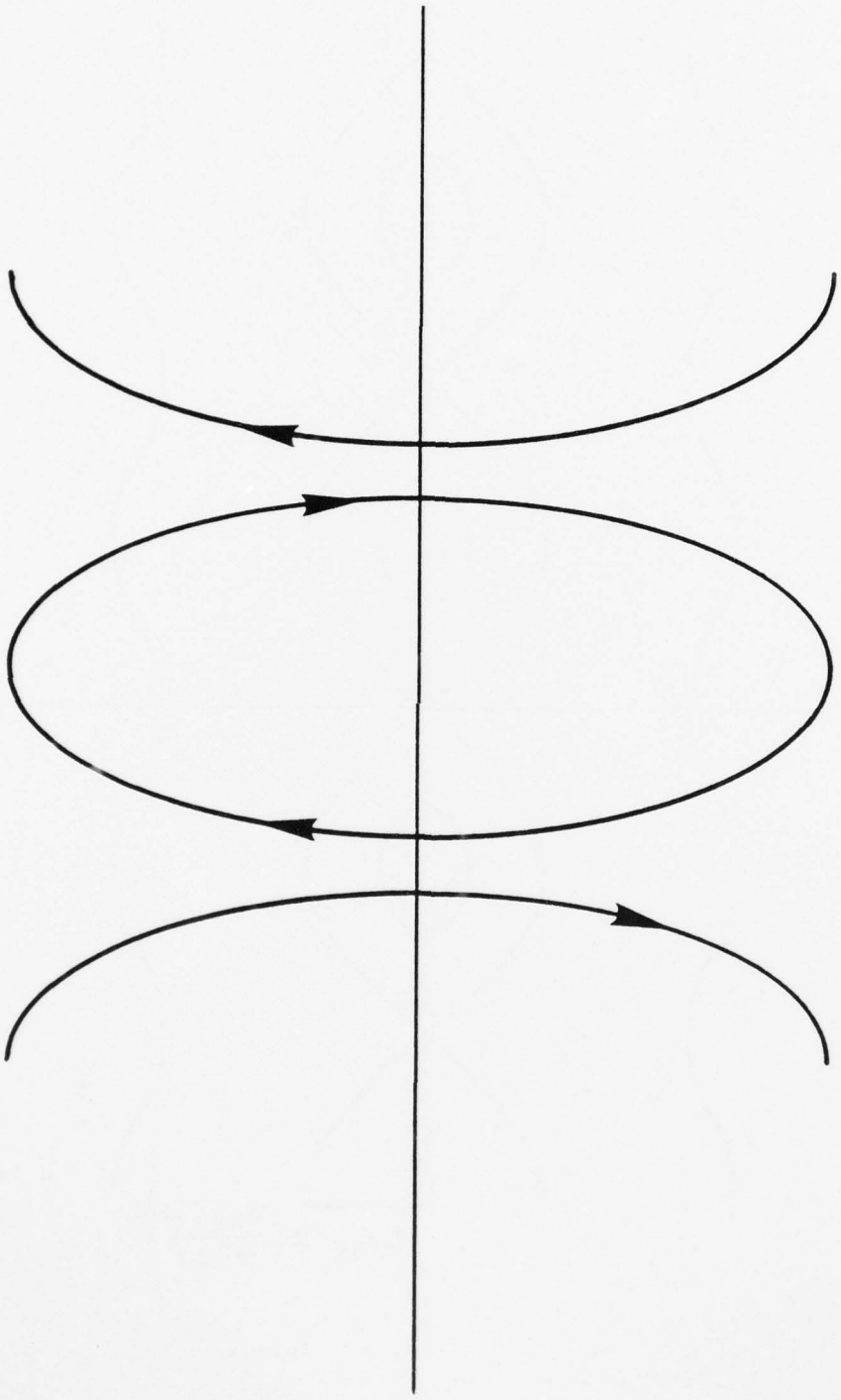

Fig. VII 3 — The field lines from Fig. 2c or d if reconnection is allowed.

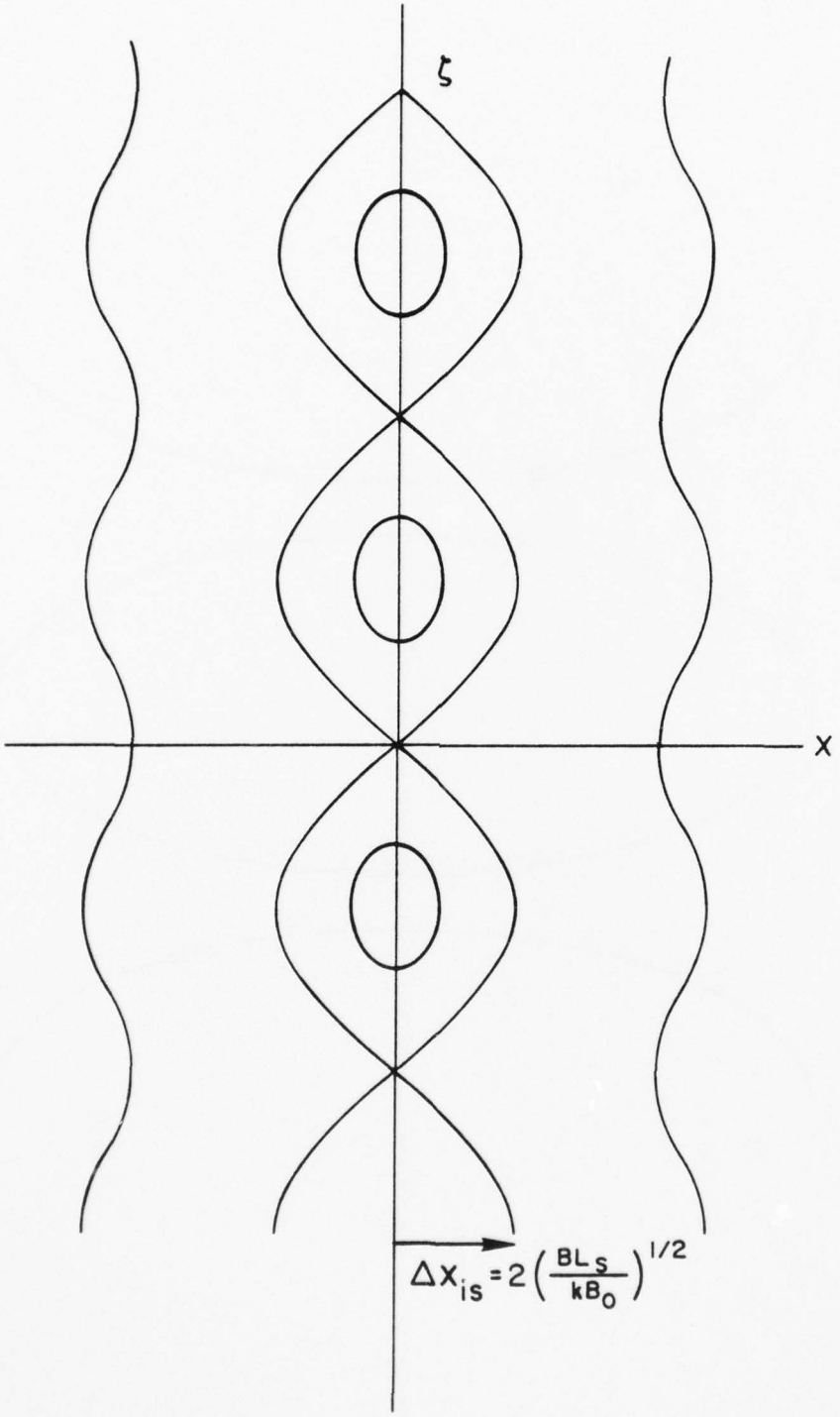

Fig. VII 4 — Magnetic island structure generated by a tearing mode.

VIII. Internal MHD Instabilities in Cylindrical Plasmas

In this section we discuss MHD instabilities in a cylindrical plasma with no free surface. As we will see shortly, the modes which we have discussed in the previous three chapters have simple analogs in cylindrical geometry. However there are also additional modes in cylindrical geometry which have no analog in slab geometry. Because this chapter is quite long, we subdivide it into six subchapters, VIII. A - VIII. F, which deal respectively with two dimensional MHD modes, ideal MHD modes with $m \geq 2$, ideal MHD modes with $m = 1$, resistive MHD modes with $m \geq 2$, resistive MHD modes with $m = 1$, and double tearing modes.

VIII. A - MHD Modes with Two Dimensional Structure

Recall from the last three chapters, that in slab geometry, the appropriate modes always had two dimensional structure in the plane perpendicular to B_{zo}. If $B_{zo} >> B_{\theta o}$ and $a << R$, (tokamak ordering) one might expect this to be valid in cylindrical geometry also. This is analogous to the analysis in the second part of Chapter IV where we examined two dimensional unstable modes in a cylindrical plasma with a free surface. Here, as we will see, two dimensional modes in a cylindrical plasma with no free surface are stable. However the analysis here is still useful to set the stage for a study of instabilities resulting from three dimensional or resistive effects.

In cylindrical geometry, all perturbed quantities vary as $\exp i(m\theta + kz)$. To make the transition to toroidal geometry we simply quantize k, that is $k \to n/R$, but neglect all other complications of the toroidal geometry. The perturbation is perpendicular to the ambient field wherever $mB_{\theta o}/r + nB_{zo}/R = 0$, so we expect unstable perturbations to be

in some way localized near this point (we assume here that B_{zo} is independent of r and is $>>B_{\theta o}$). If this is so, $k \approx m/r \quad B_{\theta o}/B_{zo} << m/r$ so that the variation in the θ direction is much more rapid than the variation in the z direction. Therefore, plasma motion will be approximately 2 dimensional in r and θ, quite analogous to the motion in slab geometry. Then $V_z = B_z = 0$, k is taken as a small quantity unless it multiplies B_{zo} and V_r, V_θ, B_r and B_θ are related by the incompressibility condition

$$\frac{1}{r}\frac{\partial}{\partial r} r V_r + \frac{im}{r} V_\theta = \frac{1}{r}\frac{\partial}{\partial r} r B_r + \frac{im}{r} B_\theta = 0 \qquad \text{(VIII 1)}$$

The next step then (analogous to the previous chapters) is to take the z component of the curl of the perturbed momentum equation, or

$$\frac{\gamma}{r}\left(\frac{\partial}{\partial r} r \rho_o V_\theta - \rho_o im V_r\right) = \frac{1}{c} \nabla \times \left(\underline{J} \times \underline{B}_o + \underline{J}_o \times \underline{B}\right)\Big|_z$$

$$= \frac{1}{c}\left\{(\underline{B}\cdot\nabla)\underline{J}_o + (\underline{B}_o\cdot\nabla)\underline{J} - (\underline{J}\cdot\nabla)\underline{B}_o - (\underline{J}_o\cdot\nabla)\underline{B}\right\}_z \qquad \text{(VIII 2)}$$

First look at the third and fourth terms on the right hand side of Eq. (VIII.2). Since B_{oz} is assumed to be constant, $(J\cdot\nabla)B_o = 0$. The fourth term is $- ikJ_oB_z$ which is small since both k and B_z are assumed small. The first term on the right is $\frac{1}{c} B_r \frac{dJ_{oz}}{dr}$ while the second is $(\frac{im}{r} B_{\theta o} + ikB_{zo})J_z$. However $J_z = \frac{c}{4\pi} \nabla \times B/_z$. Making use of Eq. (VIII. 1), Eq. (VIII. 2) reduces to

$$-\gamma\left(\frac{1}{r}\frac{\partial}{\partial r} r \rho_o \frac{1}{im}\frac{\partial}{\partial r}(r V_r) + \frac{\rho_o im}{r} V_r\right) =$$

$$\frac{1}{c}\left\{B_r \frac{\partial J_{oz}}{\partial r} + \frac{ic}{4\pi} F\left(-\frac{1}{r}\frac{\partial}{\partial r}\frac{r}{im}\frac{\partial}{\partial r} r B_r - \frac{im}{r} B_r\right)\right\} \qquad \text{(VIII 3)}$$

where

$$F = \frac{m B_{\theta o}}{r} + k B_{zo} \qquad \text{(VIII 4)}$$

Here, unlike the second part of Chapter IV, F depends on r in general.

To complete the description of linear modes in a cylindrical plasma in the tokamak ordering, an additional relation between V_r and B_r is required. This comes from Maxwell's equation

$$\gamma \underline{B} = - \underline{\nabla} \times \underline{V} \times \underline{B} - \frac{\eta c^2}{4\pi} \underline{\nabla} \times \underline{\nabla} \times \underline{B} \qquad \text{(VIII 5)}$$

To start we consider only ideal modes, so $\eta = 0$ in Eq. (VIII. 5) above. In this case

$$\gamma B_r = i F V_r \qquad \text{(VIII 6)}$$

Then inserting for B_r on the right hand side of Eq. (VIII. 3), we find after a bit of straight forward manipulation

$$\frac{1}{r}\frac{\partial}{\partial r} r^3 \left[\frac{F^2}{4\pi} + \rho_0 \gamma^2\right] \frac{\partial}{\partial r} V_r = (m^2 - 1)\left[\rho_0 \gamma^2 + \frac{F^2}{4\pi}\right] V_r + \gamma^2 r \frac{\partial \rho_0}{\partial r} V_r \qquad \text{(VIII 7)}$$

Equation (VIII. 7) above must be solved subject to the boundary condition that $V_r = 0$ at $r = a$ and V_r is well behaved for $r = 0$.

Near $r = 0$, Eq.(VIII. 7) reduces to

$$\frac{\partial}{\partial r} r^3 \frac{\partial V_r}{\partial r} = - r(1 - m^2) V_r \qquad \text{(VIII 8)}$$

so that the solutions have the form $V_r = r^n$. Solving for n (See Appendix), we find

$$n = -1 \pm m \qquad \text{(VIII 9)}$$

For $m \geq 2$, one root is well behaved at $r = 0$ and one is not. The solution which is well behaved at zero goes as r^{m-1} so that $V_r = 0$ there. Hence the center of the plasma does not move.

On the other hand, if $m = 1$, the well behaved solution for V_r is constant at $r = 0$. Let us now see what this implies for the motion of the plasmacenter. If $\underline{\hat{e}}_r$ is a unit vector in the r direction $V_r = \underline{V} \cdot \underline{\hat{e}}_r$. Near $r = 0$, V_r is a constant times $\cos(\theta + kz)$ and $\underline{\hat{e}}_r = \underline{\hat{e}}_x \cos\theta + \underline{\hat{e}}_y \sin\theta$. Therefore at $z = 0$, the velocity $\underline{V}$ is in the positive x direction, and at

AD-A071 099 NAVAL RESEARCH LAB WASHINGTON DC F/G 20/3
AN MHD INSTABILITY PRIMER.(U)
JUN 79 W MANHEIMER, C LASHMORE-DAVIES
UNCLASSIFIED NRL-MR-4000 NL

2 OF 2
AD
A071099

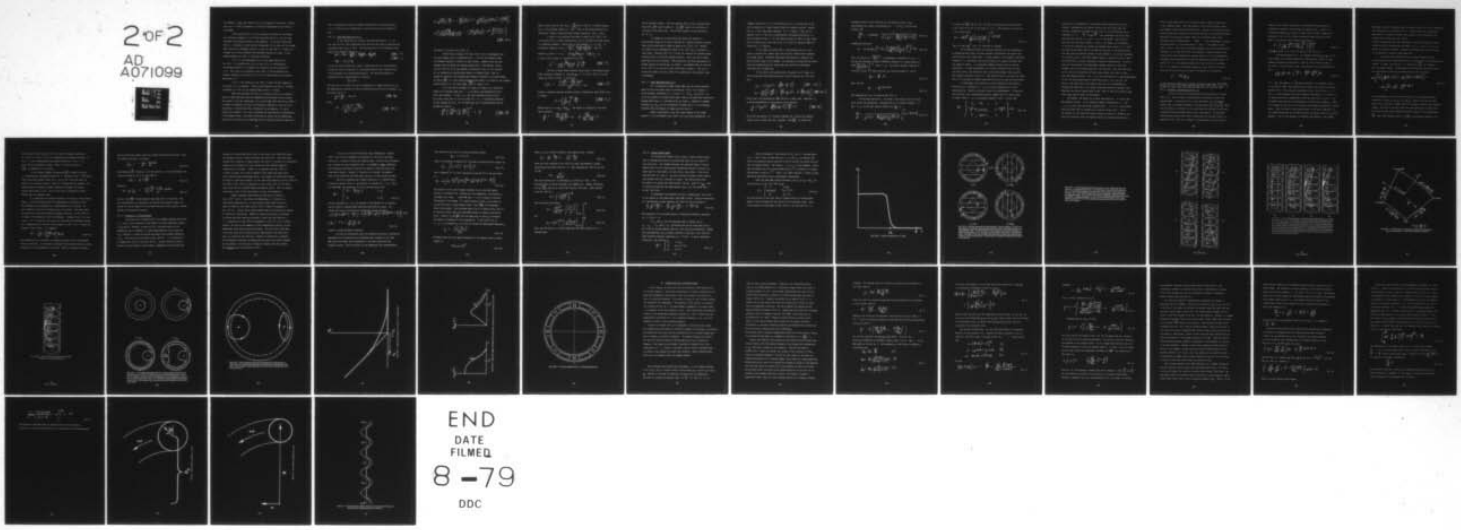

END
DATE
FILMED
8-79
DDC

for instance $z = \frac{\pi}{2k}$, the velocity $\underline{V}$ is in the negative y direction. Clearly then, an m = 1 mode corresponds to a helical displacement of the center of the plasma.

Since modes with $m \geq 2$ do not displace the center of the plasma, the cylindrical geometry is not crucial and modes with $m \geq 2$ are not very different from analogous modes in slab geometry. On the other hand modes with m = 1 represent a rigid helical displacement of the center of the plasma. Since there is no analogous motion in a slab, we find that m = 1 modes in a cylinder can be very different from anything occuring in a slab. We now examine whether Eq. (VIII. 7) predicts instability.

If $m \geq 2$, the coefficient of V_r on the right hand side of Eq. (VIII. 7) is positive for $\rho_o' < o$, so that if V_r is a monotonically increasing function of r as long as it is positive in the viscinity of r = 0. Thus there is no solution to Eq. (VIII. 7) which satisfies the boundary condition at the wall, $V_r(r = a) = 0$; hence there are no unstable modes with $m \geq 2$.

If m = 1, the solution to Eq. (VIII. 7) which is well behaved at the origin is V_r is constant. Since V_r must vanish at the wall, it vanishes everywhere, so there are no unstable modes with m = 1 either.

Hence the conclusion is that in a cylinder, there are no unstable modes in ideal MHD which have two dimensional structure and no free surface. The reason is that the coefficient of V_r on the right hand side of Eq. (VIII. 7) is always non negative, so that, as discussed in Chapter V, there can be no instability. However while this coefficient is not negative, it can be nearly zero wherever F = 0, that is wherever the perturbation is perpendicular to the ambient field. Thus small corrections to either the two dimensional structure of the mode, or to ideal MHD (that is resistive effects) might give

rise to instabilities which are somehow centered near the positions where F = 0. In the next five subsections, we will see that this is indeed the case.

VIII. B - Ideal MHD Modes with m ≥ 2

In this subsection we consider ideal MHD modes with m > 2. We deal with the full three dimensional mode structure and make no approximation concerning either B_θ/B_z of kr/m. The starting point is the linearized fluid equation and Maxwell's equation:

$$\gamma \rho_0 \underline{v} = -\underline{\nabla}\left(p + \frac{\underline{B}_0 \cdot \underline{B}}{8\pi}\right) + \frac{(\underline{B}\cdot\underline{\nabla})\underline{B}_0}{4\pi} + \frac{(\underline{B}_0\cdot\underline{\nabla})\underline{B}}{4\pi} \qquad \text{(VIII 10)}$$

$$\gamma \underline{B} = -\underline{\nabla} \times \underline{v} \times \underline{B}_0 \qquad \text{(VIII 11)}$$

for the two vector quantities $\underline{v}$ and $\underline{B}$. Consistent with our usual notation, a quantity without a subscript is a perturbed quantity and a quantity with a zero subscript is an equilibrium quantity. The perturbed pressure is eliminated by the incompressibility condition

$$\nabla \cdot v = 0$$

The idea now is to reduce this set of equations to a single equation for v_r. The manipulations involved in this are tedious and are set out in Appendix ____. The final result is

$$\frac{d}{dr} f \frac{dv_r}{dr} - h v_r = 0 \qquad \text{(VIII 12a)}$$

where

$$f = \frac{r^3 (\rho_0 \gamma^2 + F^2/4\pi)}{k^2 r^2 + m^2} \qquad \text{(VIII 12b)}$$

$$h = \frac{2k^2r^2}{k^2r^2+m^2}\frac{dP_o}{dr} + r\frac{k^2r^2+m^2-1}{k^2r^2+m^2}F^2 + \frac{2k^2r^3}{(k^2r^2+m^2)^2}\left[(kB_z)^2 - \left(\frac{mB_\theta}{r}\right)^2\right]$$

$$+\gamma^2\left[\frac{\rho_o r k^2 B_{\theta o}^2}{4\pi(k^2r^2+m^2)\left(\frac{F^2}{4\pi}+\rho\gamma_o^2\right)} - r^2\frac{d}{dr}\left(\frac{\rho_o}{k^2r^2+m^2}\right) + \rho_o r\frac{k^2r^2+m^2-1}{k^2r^2+m^2}\right]$$

(VIII 12c)

and where F is given by Eq. (VIII. 4).

Notice that as long as $\gamma^2>0$, Eq. (VIII. 12 a) is nonsingular and one could simply solve it numerically for γ. This is the approach taken by Freidberg (Physics of Fluids 13, 1812 (1970)). However there are many insights that can easily be obtained analytically. Specifically, notice that Eq. (VIII 12 a) is very similar in structure to Eq. (V. 17), derived in our discussion of gravitational modes in a sheared field. That is, regions of negative h are unstable and regions of positive h are stabilizing. As long as $\frac{dPo}{dr} < 0$, h will always be negative (for small γ) at least at the singular surface where F = 0 (of course $k^2B_z^2 - \frac{m^2B_\theta^2}{r^2} = 0$ where F = 0).

As in the case of g modes in a slab, for fixed $\gamma(\equiv\gamma_o)$ there will always be an unstable mode with $\gamma > \gamma_o$ as long as the eigenfunction $V_r(r)$ has a node between r = 0 and r = a. The first possibility then is that $V_r(r)$ has a node near F = 0 in the limit of $\gamma \to 0$. A calculation identical to that leading up to Eq. (V. 30) shows that such a localized mode will be unstable as long as

$$\frac{dP_o}{dr}\left\{\frac{rB_{zo}^2}{8\pi}\left(\frac{1}{g}\frac{dg}{dr}\right)^2\right\}^{-1} < \frac{1}{4} \qquad \text{(VIII 13)}$$

where we have used the fact that $q = \frac{rB_{zo}}{RB_{\theta o}}$ and $k = n/R$ for a toroidal plasma. Also, at the singular surface $q = -m/n$. This is the Suydam condition for instability (Suydam, Geneva UN Atomic Energy Conference, 1958 p. 1057).

A large q' can stabilize this mode, as shown in Eq. (VIII. 13). To see that this is a shear stabilization, let us calculate the shear length in cylindrical geometry. Recall that in slab geometry, $k_{\parallel} = k_y x/L_s$. In cylindrical geometry, then $k_{\parallel} = \frac{(B_o \cdot \nabla)}{|B_o|} = \frac{m/r\, B_{\theta o} + n/R\, B_{zo}}{(B_{\theta o}^2 + B_{zo}^2)1/2}$. Near the position r_s where $F = o$, $k_{\parallel} = \left[\frac{m}{r} \frac{B_{\theta o}}{[B_{\theta o}^2 + B_{zo}^2]^2} \quad \frac{1}{q}\frac{dq}{dr}\right]_{r_s} (r - r_s)$ so that if m/r is taken to correspond to k_y, then

$$L_s^{-1} = \frac{B_{\theta o}}{\left(B_{\theta o}^2 + B_{zo}^2\right)^{1/2}} \frac{1}{q}\frac{dq}{dr} \qquad \text{(VIII 14)}$$

Now let us relate these pressure driven modes to the gravitational modes discussed in Chapter V. Setting $d/dr = F = 0$ in Eq. (VIII. 12 a) and taking the limit $m^2 >> k^2 r^2$, it reduces to

$$\gamma^2 \rho_o r + \frac{\left(\alpha \frac{dP}{dr} + \frac{B_{\theta o}^2}{4\pi r}\right) k^2 r^2}{m^2} = 0 \qquad \text{(VIII 15)}$$

Clearly, a negative pressure gradient causes an instability whose growth rate is roughly

$$\gamma \sim \left(\frac{P_o'}{\rho_o r}\right)^{1/2} \frac{kr}{m} \qquad \text{(VIII 16)}$$

However since $F = 0$, $kr/m = B_{\theta o}/B_{zo}$. The radius of curvature of the field line is given by

$$\frac{1}{\underline{R}} = -\frac{(\underline{B}_o \cdot \underline{\nabla})\,\underline{B}_o}{|B_o|^2} = \frac{1}{r}\frac{B_{\theta o}^2}{B_{zo}^2 + B_{\theta o}^2}\,\underline{i}_r$$

and is directed outward. Thus the unstable mode is like a gravitational mode with $g \frac{\partial \rho_o}{\partial x}$ given roughly by $\frac{1}{\rho_o R} \frac{dP_o}{dx}$ where R is the radius of curvature of the field line. This is very similar to that derived in Eq. (V. 5).

To summarize, we have shown that modes very similar to gravitational modes can be driven unstable by a negative pressure gradient. These can be stabilized by shear as shown in Eq. (VIII. 13). However the plasma is not necessarially stable if Eq. (VIII 13) is violated at every point. Equation (VIII 13) is only the condition for unstable modes localized about a particular singular surface. There also may be gross modes which are not localized. This possibility has been investigated by Newcomb (Annals of Physics 10, 232 (1960)). He examined when the solution of Eq. (VIII 12 a) can have a node in the limit of small γ. One can of course also simply solve Eq. (VIII 12 a) numerically, the approach taken by Freidberg.

VIII. C - Ideal MHD Modes with m = 1

For a cylindrical plasma in ideal MHD, one can always determine mode structure and growth rates by solving Eq. (VIII. 12 a) subject to proper boundary conditions at r = 0 and r = a. If $B_{\theta o} \sim B_{zo}$ and $kr \sim m$, as in for instance a reversed field pinch, there is no particular distinction between modes with m = 1 and modes with all other m. However in tokamak ordering, $B_{\theta o} << B_{zo}$, $kr << m$, the behavior of modes with m = 1 is strikingly different from the behavior of modes with all other m.

Recall from Chapter V that only those regions of the plasma having $h < 0$ (h is defined in Eq. (VIII. 12 c) can drive instability. In

tokamak ordering for $m \geq 2$, the second term in h is so large that h can only be negative in a small region around the singular surface. However for m = 1, this term nearly vanishes. If k is equal to $-n/R$, then in general, for m = 1 and q(r) a monotonically increasing function of r, h will be negative from r = 0 to the radial position at which $q = 1/n$. Henceforth we specialize to the case of $n = 1$, so that the unstable region is within the q = 1 surface.

It was shown in Section VIII. A that motions with m = 1 are unique in another way, namely these are the only motions which displace the plasma center. Therefore these modes are expected to displace the entire central region of the plasma. We continue by calculating the growth rates and eigenfunctions for these modes and conclude by discussing physically what is happening.

In the limit of low growth rate, we neglect the γ^2 terms in h. Thus the equation describing the motion is still given by Eq. (VIII 12a) with

$$f = r^3\left(\rho_0\gamma^2 + \frac{B_{\theta 0}^2}{4\pi r^2}(g-1)^2\right) \qquad \text{(VIII 12b')}$$

$$h = \left(\frac{r}{R}\right)^2\left[2\frac{dP_0}{dr} + \frac{B_{\theta 0}^2}{r}(g-1)^2 + 2\frac{B_\theta^2}{r}(1-g^2)\right] \qquad \text{(VIII 12c')}$$

Notice that h is multiplied by $(r/R)^2$ which is a small term. Therefore, V_r is given approximately by the solution to the equation

$$\frac{d}{dr}\, r^3\left(\rho_0\gamma^2 + \frac{B_{\theta 0}^2}{4\pi r^2}(g-1)^2\right)\frac{dv_r}{dr} = 0 \qquad \text{(VIII 18)}$$

As we will see shortly, V_r is nearly constant for r within the singular surface, and is nearly zero for r outside. Thus $\frac{dV_r}{dr}$ is nearly zero

everywhere except in the viscinity of the singular surface $r \approx r_s$. Anticipating this result, and setting $q-1 = q'(r-r_s)$, we find from Eq. (VIII 18)

$$\frac{dv_r}{dr} = \text{constant} \times \frac{1}{r_s^3 \left(\rho_o \gamma^2 + \frac{B_{\theta o}^2 (r=r_s)}{4\pi r_s} \left[q'(r-r_s) \right]^2 \right)} \qquad \text{(VIII 19)}$$

Integrating once more,

$$V_r = K_1 \arctan \left[(r-r_s) \Big/ \left\{ \frac{4\pi \rho_o \gamma^2 r_s^2}{B_{\theta o}^2 (r=r_s)(q')^2} \right\}^{1/2} \right] + K_2 \qquad \text{(VIII 20)}$$

Thus, as long as $\gamma_o^2 << \frac{B_{\theta o}^2 (q')^2}{4\pi \rho_o}$, V_r approaches a constant for $r-r_s \to \pm \infty$ and the two different values are smoothly connected in a narrow region of width $\left[\frac{4\pi p_o \gamma^2 r_s^2}{B_{\theta o}^2 (r_s) q'^2} \right]^{1/2}$ about $r = r_s$. The proper boundary condition of course is $V_r(r=a) = 0$, which dictates the relation between K_1 and K_2

$$K_2 = -\frac{\pi}{2} K_1 \qquad \text{(VIII 21)}$$

Also, we find

$$K_1 = -\frac{1}{\pi} V_r(r=0) \qquad \text{(VIII 22)}$$

The eigenfunction $V_r(r)$ is shown in Fig. VIII. 1.

Now we must solve for γ. Of course γ must result from the h term which drives the instability. Assuming that V_r is constant between $r = 0$ and $r = r_s$, we find that another relation for $\frac{dVr}{dr}$ is

$$\frac{dV_r}{dr} = \frac{1}{\rho_o \gamma^2 r_s^3 + \frac{B_{\theta o}^2 (r=r_s) r_s}{4\pi} (q')^2 (r-r_s)^2} \int_0^r h(r) V_r(r=0) \qquad \text{(VIII 23)}$$

Of course the $\frac{dVr}{dr}$ from Eq. VIII. 23) must be consistent with that derived in Eq. (VIII 19 or 20) in the limit as $r \to r_s$. This allows us to solve for γ, the result being

$$\gamma = -\alpha(\pi)^{3/2} \frac{1}{\mathcal{B}_{\theta_0}(r=r_s)\, r_s^2\, g' \sqrt{\rho_0}} \int_0^{r_s} h(r)\,dr \qquad \text{(VIII 24)}$$

Thus, as long as $\int_0^{r_s} h(r) < 0$, the mode is unstable.

We now discuss briefly the physical mechanism of this instability. As emphasized many times, the most unstable perturbations are always those which bend the field lines least. In slab geometry, with boundary conditions imposed at $\pm \infty$, this means that the perturbation is somehow localized near the singular surface. In cylindrical geometry however there is another possibility. A rigid displacement of a cylinder certainly does not bend any field lines. The problem is that a rigid displacement cannot satisfy the boundary condition $V_r(r=a) = 0$. The question then is, can only the inner part of the cylinder be rigidly displaced but still not bend the field lines?

To investigate this question, we first examine the fluid motion. The motion V_r = constant for $r < r_s$ is of course something of an over-simplification. Clearly such motion cannot be incompressible. To describe more precisely this incompressible motion, imagine that in a narrow layer of width δ about $r = r_s$, V_r decreases linearly to zero. In this case

$$V_\theta = \left\{ \begin{array}{ccc} 0, & r<r_s, & V_r \\ -\frac{i\, r_s}{\delta} V_r, & r_s<r<r_s+\delta, & V_r \frac{r_s+\delta-r}{\delta} \\ 0, & r_s+\delta<r, & 0 \end{array} \right\} = V_r \qquad \text{(VIII 25)}$$

This motion is reminiscent of the tearing motion described in the last chapter. Assuming that the radial velocity goes as $\cos(m\theta + \frac{z}{R})$, the velocity streamlines are shown in Fig. (VIII 2) at four different axial positions, Z = 0, $\pi R/2$, πR and $3\pi R/2$. The streamlines are solid lines, while the two circles $r = r_s$ and $r = r_s + \delta$ are dashed. Also shown on each plot are three dots labled 1, 2 and 3. Dot number one corresponds to an initial position just inside the singular layer, where q = 1. Since the pitch of the field line is the same as the pitch of the perturbation, the same field line passes through all dots labeled 1. As the flow proceeds, for a time $\mathcal{L}_2$ and $\mathcal{L}_3$, the fluid element passes to positions 2 and 3, while the field line, of course, continues to interlace these points. In each of the four curves shown, the displacement between positions 1 and 2 and between 2 and 3 is the same except for a 90^o rotation. Thus the field line is not bent or stretched as the fluid races around, from front to back, near the singular surface. For $r < r_s$ the fluid motion is a rigid displacement in the $(r\theta)$ plane which does not bend field lines. For $r_s<r<r_s+\delta$, the pitch of the field line is the same as the pitch of the perturbation, allowing the field line to be rigidly displaced around the singular layer. Therefore the type of motion shown in Fig. (VIII 2) does not initially bend field lines and is likely to be unstable.

Now examine the motion for a field line which at $\mathcal{L} = 0$ is not near the singular surface. In the standard tokamak configuration, q < 1 for $r < r_s$, so this field line winds a tighter helix at $\mathcal{L} = 0$. The cylinder which the field line is initially on is dotted in Fig. VIII 2 and at the various Z's the field line passes through the points A. However, the field line does not enter the singular region at the same time any more,

since at some axial points it is initially closer, along a stream line, to the singular region. Thus some points of the field line whip around the singular region before other points do. Clearly, this involves considerable bending and stretching of the field line and is a stabilizing effect. Therefore as the motion proceeds, there is an opposing force, which increases with the displacement, rather like compressing a spring. The distortions of a field line with $q = 1$ and $q < 1$ are shown in Figs. (VIII 3 and 4). This lets us interpret somewhat the various effects which contribute to γ in Eq. (VIII 24). The integral h simply represents the average force which displaces the plasma, while the q' in the denominator represents the restraining force from the bending of the field lines. Of course if $q' = 0$, the analysis leading up to Eq. (VIII 24) is invalid. For $q' = 0$, however, the analysis leading up to Eq. (VIII 16) is still valid and we find that for zero shear, the growth rate is given by

$$\gamma^2 = \alpha P_o' / R^2 \rho_o' \qquad \text{(VIII 26)}$$

so that there is instability if P_o' and ρ_o' have the same sign. The growth rate in Eq. (VIII. 26) is much greater than that in Eq. (VIII. 24), so the presence of shear slows down these modes but does not stabilize them.

VIII D - Resistive Instabilities for $m \geq 2$

In this section we discuss resistive instabilities in a plasma with $m \geq 2$. The two types of instabilities are resistive g modes and tearing modes. In section VIII b, it was shown that in a cylindrical plasma, there are simple analogues to g modes where $g \frac{\partial \rho_o}{\partial x} \approx \frac{1}{\rho_o R} \frac{dP_o}{dr}$. Here R is the radius of curvature of the field lines and the sign is such that a negative pressure gradient gives rise to instability. In ideal MHD, these pressure driven modes could be stabilized by sufficient shear, as indicated in Eq. (VIII 13). However, in slab geometry, it was shown in

Chapter VI that finite resistivity could destabilize these modes by allowing the plasma to leak through the sheared field. Clearly, in cylindrical geometry, we expect the same result to apply, namely that, analogous to Eq. (VI 22), finite resistivity allows pressure driven modes to go unstable with a growth rate given by

$$\gamma \approx \left\{ \frac{1}{\rho_0 \mathcal{R}} \frac{dP_0}{dr} \left(\frac{m L_s}{r B_{\theta 0}} \right) \right\}^{2/3} \left(\frac{c^2 \eta}{\rho_0} \right)^{1/3} \qquad \text{(VIII 27)}$$

where $\mathcal{R}$ is given in Eq. (VIII 17) and L_s in Eq. (VIII 14).

The tearing mode for m > 2 in tokamak ordering ($B_{\theta o} << B_{zo}$, kr<<1) also follows in a straight forward way from analogous results in slab geometry discussed in Section VII. That is if the inertial terms in Eq. (VIII 3) are set equal to zero, the equation for the perturbed field gives

$$\frac{1}{r}\frac{\partial}{\partial r} r \frac{\partial}{\partial r} r B_r = \left(\frac{m^2}{r} + \frac{4\pi m}{cF} \frac{dJ_{oz}}{dr} \right) B_r \qquad \text{(VIII 28)}$$

if $k = {}^{-n}/_{R}$, the quantity $F = {}^{B_\theta}/_{r}\,(m-nq)$ vanishes at the singular surface $r = r_s$ where $q = {}^{m}/_{n}$. The procedure now is exactly as it was for the slab (Chapter VII). First calculate solutions for Eq. (VIII 28) for $r < r_s$ and $r > r_s$ which satisfy the proper boundary conditions at r = 0 and r = a. If these solutions are normalized to have the same value of B_r at $r = r_s$, in general there will be a discontinuity in slope as one crosses r_s. Then if Δ (defined in Eq. (VII 17)) is positive the plasma is unstable to tearing modes. Since the width of the tearing layer is very small compared to r_s the connection between the two MHD solutions can proceed exactly as in slab geometry. Thus to see whether a cylindrical equilibrium in the tokamak

ordering, is stable to tearing modes, one simply solves Eq. VIII 28 numerically and investigates the condition for $\Delta > 0$. Calculations such as these have been made by a variety of authors (For instance F with, Rutherford and Selberg, Phys. Fluids 16, 1054 (1973)).

Stated very qualitatively, the conclusion is that for sufficiently smooth current profiles, tearing modes are stable if $m \gtrsim 4$. For $m = 2$ or 3, the profile is typically unstable. However by tayloring the current profile, it is possible to stabilize these modes also.

We conclude this subsection with a simple physical picture illustrating the free energy which drives a tearing mode in an imcompressible plasma. To begin, take Eq.(VIII 3), multiply by $\frac{iV^*_r}{m}$ and integrate over the plasma volume. Integrating the second derivative terms by parts and neglecting the end point contributions, we find the result:

$$2\pi\gamma \int_0^a r dr \left[\rho_0 \left(|V_r|^2 + |V_\theta|^2 \right) + \frac{1}{4\pi} \left(|B_r|^2 + |B_\theta|^2 \right) \right] =$$

$$- 2\pi \int_0^a r dr \; \frac{\gamma}{mcF} \; \frac{d J_{oz}}{dr} |B_r|^2 \qquad \text{(VIII 29)}$$

In calculating Eq. (VIII 29) we have made use of the incompressibility condition to relate V_θ and B_θ to V_r and B_r. Notice that the left hand side of Eq. (VIII 29) is simply the rate of change of kinetic plus magnetic energy. The term on the right hand side then represents a driving term. This term can only drive instability in those regions of the plasma where $\frac{dJ_o}{dr}$ and F have opposite signs. If $\frac{1}{F}\frac{dJ}{dr}$ is everywhere positive, then

one can easily show from Eq. (VIII 28), that for boundary conditions $B_r = 0$ at $r = 0$ and $r = a$, B_r is a monotonically increasing function of r for $r < r_s$ and a monotonically decreasing function of r for $r > r_s$. Thus $\Delta<0$ and the plasma is stable. Hence $\Delta'>0$ can only arise if $\frac{1}{F}\frac{dJ}{dr} < 0$, somewhere in the plasma.

In the standard tokamak configuration $\frac{dJo}{dr}$ is negative and q(r) is a monotonically increasing function of r. Therefore since $F = \frac{B_\theta}{r}(m-nq)$, these terms have opposite signs for $m > nq$, or for radii less than the radius of the singular surface. Thus for a tearing mode in cylinder, the region inside the singular surface releases free energy; the region outside soaks some of it up. What is left over is deposited as Ohmic hearing near the singular layer.

It is instructive to examine physically the nature of this driving energy. Since the plasma motion is incompressible, the motion of each fluid element can be expressed as a displacement plus a rotation. We will consider for now the rotational part of the motion. The power input into rotation is the torque times the angular velocity. In Fig. (VIII 5) is shown a fluid element in polar co-ordinates between r and r + dr and θ and $\theta + d\theta$. To calculate the torque, we calculate the difference between the θ componentsof the force on the two edges at r and r + dr. Clearly one element of this torque $\underline{\tau} = \underline{r} \times \underline{\text{Force}}$ is

$$\underline{\tau} = \frac{\underline{i}_z}{\alpha c}\left(\frac{d J_{oz}}{dr} dr\right) B_r dr \qquad \text{(VIII 30)}$$

The problem now is to calculate the angular velocity of the fluid element about its own axis. To calculate the angular velocity about the axis, first subtract out the displacement of the axis. Then any variation of radial

velocity with polar angle θ must be a rigid rotation about the axis. Thus this angular velocity, Ω is simply

$$\underline{\Omega} = -\frac{i_z}{dr}\frac{\partial V_r}{\partial \theta} d\theta \qquad \text{(VIII 31)}$$

where negative $\frac{\partial V_r}{\partial \theta}$ implies $\underline{\Omega}$ is in the positive Z. In real notation, the relation between B_r and V_r in ideal MHD is

$$\gamma B_r = \frac{1}{m} F \frac{\partial V_r}{\partial \theta} \qquad \text{(VIII 32)}$$

Therefore

$$P = \underline{\tau} \cdot \underline{\Omega} = \frac{\gamma m B_r^2}{2r F} \frac{d J_{oz}}{dr} r\, dr\, d\theta \qquad \text{(VIII 33)}$$

so that F and $\frac{dJoz}{dr}$ having opposite sign means that P is positive. Now the interpretation is clear;when F and dJoz/dr have opposite signs, the torque on a fluid element is in the same direction as the rotation, thereby tending to increase the rotation.

VIII E - Internal m = 1 Tearing Modes

As we have seen in Chapter VIII C for tokamak ordering, modes with m = 1 can be driven unstable in ideal MHD by the three dimensional nature of the motion. However, as noted in VIII C the basic motion is two dimensional and it consists of a rigid displacement in the rθ plane for $r<r_s$, coupled to a rapid flow around the edge of the cylinder defined by $r \sim r_s$. This motion is illustrated in Fig. (VIII 2). It is instructive to compare Fig. (VIII 2) with Fig. (VII 1). Clearly these two types of motion are quite similar; in the former, a magnetized fluid collides and

bounces off a stationary fluid, while in the latter, two fluids with equal and opposite velocity collide and bounce off each other. Since the fluid motions are so similar, we might expect that this m = 1 motion in a cylindrical plasma is also unstable if finite resistivity (and therefore magnetic reconnection) is allowed. Indeed, as is apparent from Fig. (VIII 4), if there is shear, the frozen in magnetic field lines have sharp turns which provide strong restraining forces. The presence of resistivity allows the lines to break and reconnect, so that they would appear as in Fig. (VIII 6). The field in Fig. (VIII 6) (analogous to that in Fig. (VII 3)) has fewer sharp turns and thus provides weaker restraining forces. Thus for nonzero resistivity, there is more free energy to drive the instability.

Simpler diagrams illustrating the same point are shown in Figs. (VIII 7 and 8). For purely two dimensional m = 1 motion in a cylindrical plasma with $B_z = 0$, the frozen in field lines in the $(r\theta)$ plane are shown at four times in Fig. (VIII 7) (which is analogous to Fig. (VII 2)). Clearly sharp corners develop where the field has to stretch to follow the fluid motion. However if non-zero resistivity is allowed, the fields here will break and reconnect so that the field pattern at $t = t_4$ appears as in Fig. (VIII 8),(analogous to Fig. VII (3)). In these figures, the dots are the magnetic 0 point singularities (nulls); the two dimensional field lines circle these points. For the case of ideal MHD, no new null point can be produced and as complicated as the field line gets, it circles the dot only once. However if resistivity is present, the topological constraint is relaxed and new nulls (also called islands) can be produced. In this case an island is produced near the cylinder wall <u>opposite</u> from the direction of flow.

If $B_z \neq 0$, the field surfaces are three dimensional. Figures (VIII 7 and 8) can be regarded as projections of the field lines back into the Z = 0 plane for ideal and resistive MHD. The dots then correspond not to nulls, but now to magnetic axes. In ideal MHD in <u>three</u> dimensions the topological constraint preserves the number of times one field line winds about another. However if resistivity is present, new magnetic axes can be formed and the field lines can start to wind around new axes.

Now let us qualitatively discuss resistive m = 1 instabilities. As shown in Section (VIII c), the velocity is constant for $r > r_s$. Thus, for ideal MHD, the expression for B_r has the functional form

$$B_r = \begin{cases} F = \frac{B_\theta}{r}(q-1) & r < r_s \\ 0 & r > r_s \end{cases} \qquad \text{(VIII 34)}$$

Since B_r vanishes at $r = r_s$, the quantity Δ from Chapter VII is infinite and the theory of tearing modes described there does not apply. The growth rate must be calculated by solving the coupled equations

$$i\gamma\left(\frac{1}{r}\frac{\partial}{\partial r} r\rho_0 \frac{\partial}{\partial r}(rv_r) - \frac{\rho_0 v_r}{r}\right) = \frac{1}{c}\left\{B_r \frac{\partial J_{0z}}{dr} + \frac{cF}{4\pi}\left(-\frac{1}{r}\frac{\partial}{\partial r} r\frac{\partial}{\partial r}(rB_r) + \frac{B_r}{r}\right)\right\} \quad (a)$$

$$\gamma B_r = iFv_r + \frac{\gamma c^2}{4\pi}\frac{\partial^2}{\partial r^2} B_r \qquad \text{(VIII 35)}$$

subject to proper boundary conditions.

We will not follow this route, but instead will derive a qualitative expression for the growth rate by balancing power released in the outer MHD region with Ohmic power dissipated in the inner region near the singular surface. Since the motion is two dimensional and incompressible,

the velocity is the curl of a vector potential $\underline{Q}$ where

$$\underline{Q} = -i_r r V_r \underline{i}_z \qquad \text{(VIII 36)}$$

Then, as calculated in Chapter VII, the power liberated per unit length is:

$$P_F = \int \left(i r V_r^*\right) \cdot \underline{\nabla} \times \underline{F}\Big|_z d^2 r \qquad \text{(VIII 37)}$$

The Z component of ∇ x F was calculated in Section VIII A and the result is

$$P_F = -2\pi \int r dr \; \frac{\gamma r B^*}{F} \left\{ \frac{1}{c} B_r \frac{dJ_{oz}}{dr} + \frac{F}{4\pi} \left[-\frac{1}{r} \frac{d}{dr} r \frac{d}{dr} r B_r + \frac{B_r}{r} \right] \right\} \qquad \text{(VIII 38)}$$

The quantity in the curly brackets vanishes in the outer MHD region, exactly as in Chapter VII. However near the singularity, the bracket is no longer zero, since ideal MHD with $\gamma = 0$ is no longer an accurate description of the plasma. In a narrow region of width x_c the slope of B_r goes from zero to some constant value. Thus $\frac{d^2 B_r}{dr^2}$ is the dominant term in the bracket. The functional form of $B_r(r)$ is shown in Fig. (VIII 9) as the solid curve, while the ideal MHD solution is shown as the dotted curve. Clearly, B_r and $\frac{d^2 B}{dr^2}$ have the same sign, so that P_F is positive and energy is available to drive instability. If the value of B_r at $r = r_s - x_c$ is denoted B_{rc}, Eq. (VIII 38) yields the approximate expression,

$$P_F \approx \frac{\gamma r_s^3 \left| B_{rc} \right|^2}{2 x_c} \qquad \text{(VIII 39)}$$

The Ohmic power per unit length dissipated in the singular layer is given roughly by

$$2\pi r_s x_c \eta J_z^2 \qquad \text{(VIII 40)}$$

where J_z is the current flowing in the singular layer. However

$$J_z \approx \frac{c}{4\pi} \frac{B_{\theta c}}{x_c} \approx \frac{c r_s}{4\pi} \frac{B_{rc}}{x_c^2} \qquad \text{(VIII 41)}$$

where the first relation in Eq. (VIII 41) comes from Maxwell's current equation and the second from $\nabla \cdot B = 0$. Then combining Eq. (VIII 39 and 40) we find

$$\gamma \approx \frac{\eta c^2}{4\pi x_c^2} \qquad \text{(VIII 42)}$$

The only problem now is to determine x_c in terms of γ and η. The procedure here is exactly the same as in Chapter VII. Namely, substitute for the $\frac{d^2 B_r}{dr^2}$ term in Eq. (VIII 35a) from Eq. (VIII 35b). Then, exactly as in Eq. (VII 23),

$$x_c \approx \left\{ \frac{\rho \gamma \eta c^2}{(F')^2} \right\}^{1/4} \qquad \text{(VIII 43)}$$

This then gives the results

$$\gamma \approx \frac{(\eta c^2)^{1/3}}{(4\pi)^{2/3}} \left\{ \frac{(F')^2}{\rho_o} \bigg|_{r=r_s} \right\}^{1/3} \qquad \text{(VIII 44)}$$

and

$$x_c \approx (\eta c^2)^{1/3} \left\{ \frac{\rho}{4\pi (F')^2} \bigg|_{r=r_s} \right\}^{1/6} \qquad \text{(VIII 45)}$$

Thus, one can derive in a fairly simple way the basic results of m = 1 tearing modes.

VIII F - Double Tearing Modes

We conclude this chapter with a study of double tearing modes; that is tearing modes which are excited when there are two zeros of F near each other. For tokamak ordering, this generally means a current density which is not a monatonically decreasing function of radius, but which peaks at some radius, in other words a skin effect. This can be seen from Fig. 10 a and b). The solid curves are normal current density and poloidal field as a function of radius. The dotted curves show the effect of a narrow skin layer on both J and B_θ. Since $F = B_{\theta o}/r - kBz$, F clearly has basically the same behavior near r_c as the dotted curve in Fig. (VIII 10b).

To investigate the stability of such a configuration, first look at the regions of the plasma where ideal MHD is valid. Using the definition of F and Maxwells current equation, Eq. (VIII 28) can be reduced to

$$\frac{F}{r^2}\frac{d}{dr}r^3\frac{dB_r}{dr} = \frac{B_r}{r^2}\frac{d}{dr}r^3\frac{dF}{dr} + F\frac{m^2-1}{r}B_r \qquad \text{(VIII 46)}$$

This equation is to be solved subject to appropriate boundary conditions at r = 0 and r = a.

If r_{c1} and r_{c_2} are the positions where F vanish, and if $r_{c1} - r_{c_2} \ll r_c$, then $r \sim r_c$, the second term on the right hand side of Eq. (VIII 46) is much smaller than the first, and can be neglected. Making this approximation, one can easily construct a solution to Eq. (VIII 46) which satisfies boundary conditions at r = 0 and r = a and is everywhere continuous. The solution is

$$B_r = \begin{cases} 0 & r < r_{c2} \\ F & r_{c2} < r < r_{c1} \\ 0 & r_{c1} < r \end{cases} \qquad \text{(VIII 47)}$$

This is analogous to the solution for B_r for m = 1 tearing modes. If ρ_o, η and F' have the same value at $r = r_{c1}$ and r_{c2}, an analysis like that in the previous section gives Eq. (VIII 44 and 48) for growth rate and size of singular region. (Of course $x_c << r_{c1}-r_{c2}$ is also assumed). Notice that the growth rate for a skin current goes as $\eta^{1/3}$, whereas for a normal tearing mode it goes as $\eta^{3/5}$. Since η is a small quantity, a double tearing mode grows much faster than a conventional tearing mode.

Since the ideal MHD relation between V_r and B_r is $\gamma B_r = iFV_r$, the solution for B_r in Eq. (VIII 47) gives

$$V_r = \begin{cases} 0 & r < r_{c2} \\ \text{constant} & r_{c2} < r < r_{c1} \\ 0 & r_{c1} < r \end{cases} \qquad \text{(VIII 48)}$$

The flow pattern is then that which is characteristic of tearing modes, namely a fluid collides with and recoils off a stationary fluid. Such a flow pattern is illustrated in Fig. (VIII 1) for the case of m = 4.

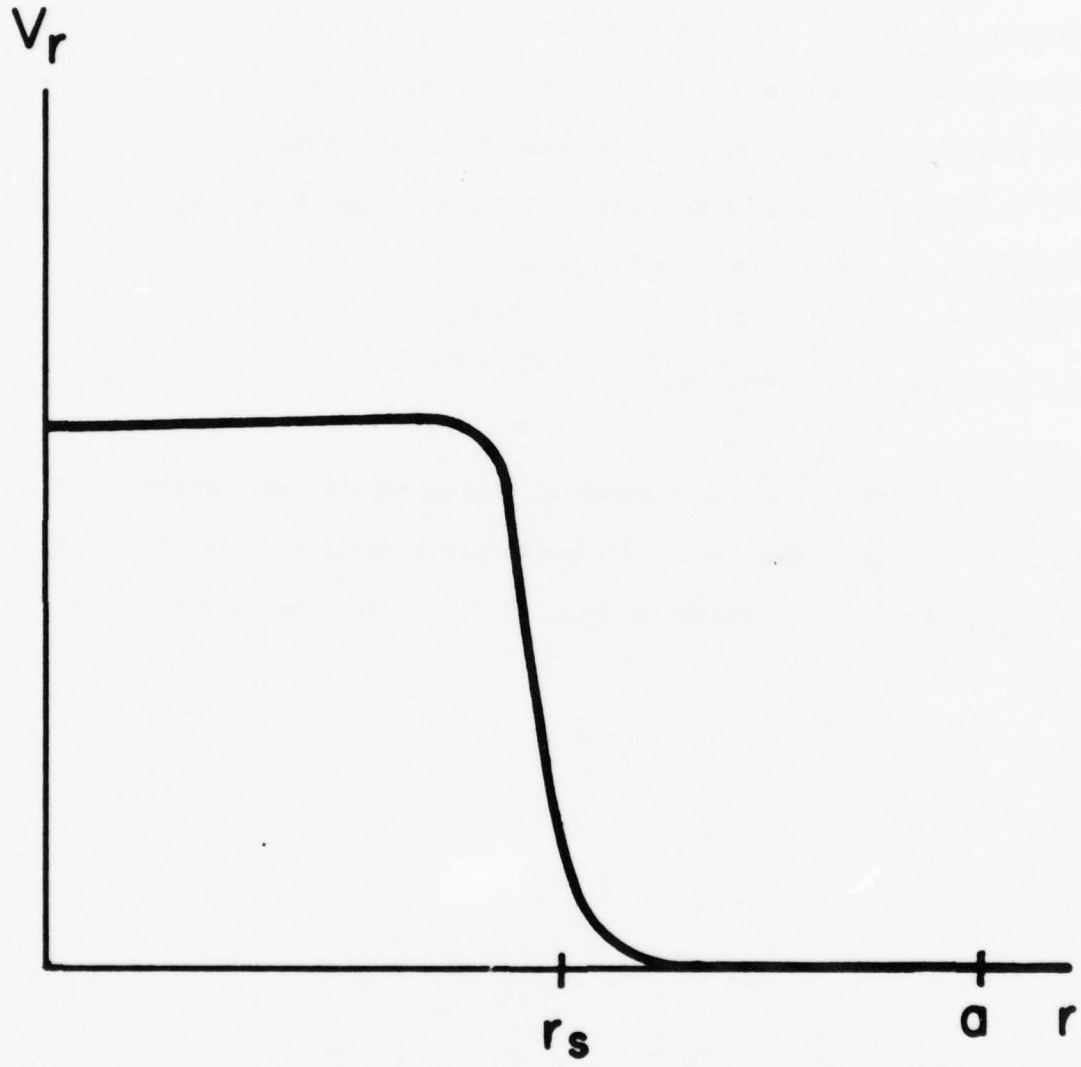

Fig. VIII 1 — A plot of $V_r(r)$ for an m = 1 mode.

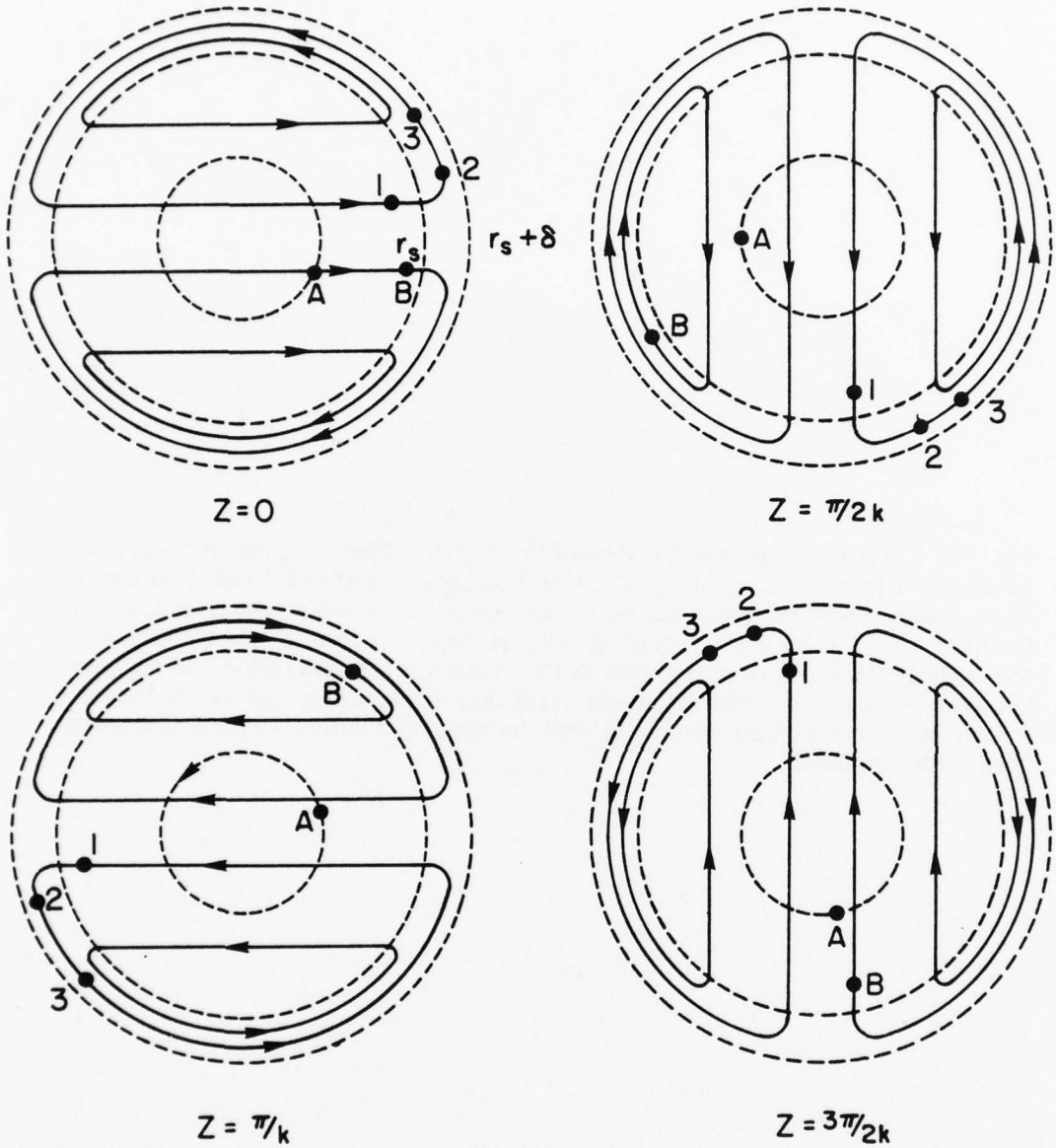

Fig. VIII 2 — The flow pattern at four axial positions. The dots labeled 1, 2, and 3 are intersections of a field line, having the same pitch as the flow, with these four planes at three different times. The points labeled A are intersections of a field line having $q < 1$ with these four planes. At Z = 0, point A is closer along a stream line to the separation region. Therefore it will enter this region first and will race around the cylinder before it does so at other axial positions. This will lead to considerable bending and stretching of the field line.

Fig. VIII 3 — A three dimensional view of the motion of two neighboring field lines having q = 1 (same pitch as the flow). The field lines are red and the flow pattern is blue. A solid field line means it is near the front of the cylinder, dotted means near the back. At t = 0 (a) the field lines in front of the cylinder are convected towards the separation region. At t_1, (b) they both enter the separation region and whip around the cylinder in opposite directions. At t_2 (c) they are continuing around the edge. Finally at t_3 (d) they have both re-entered the main rigid body flow, and now are in back of the cylinder.

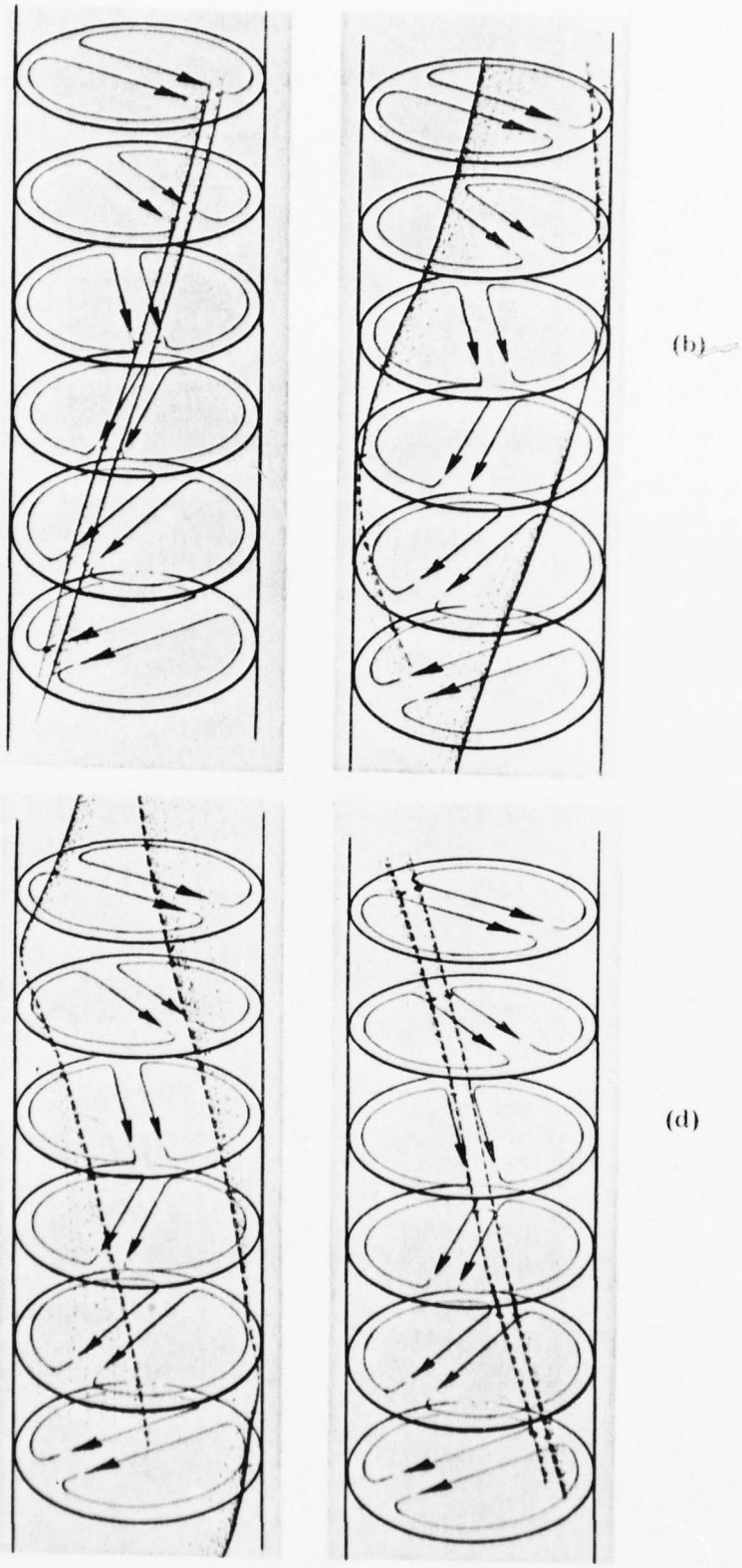
(a)
(b)
(c)
(d)

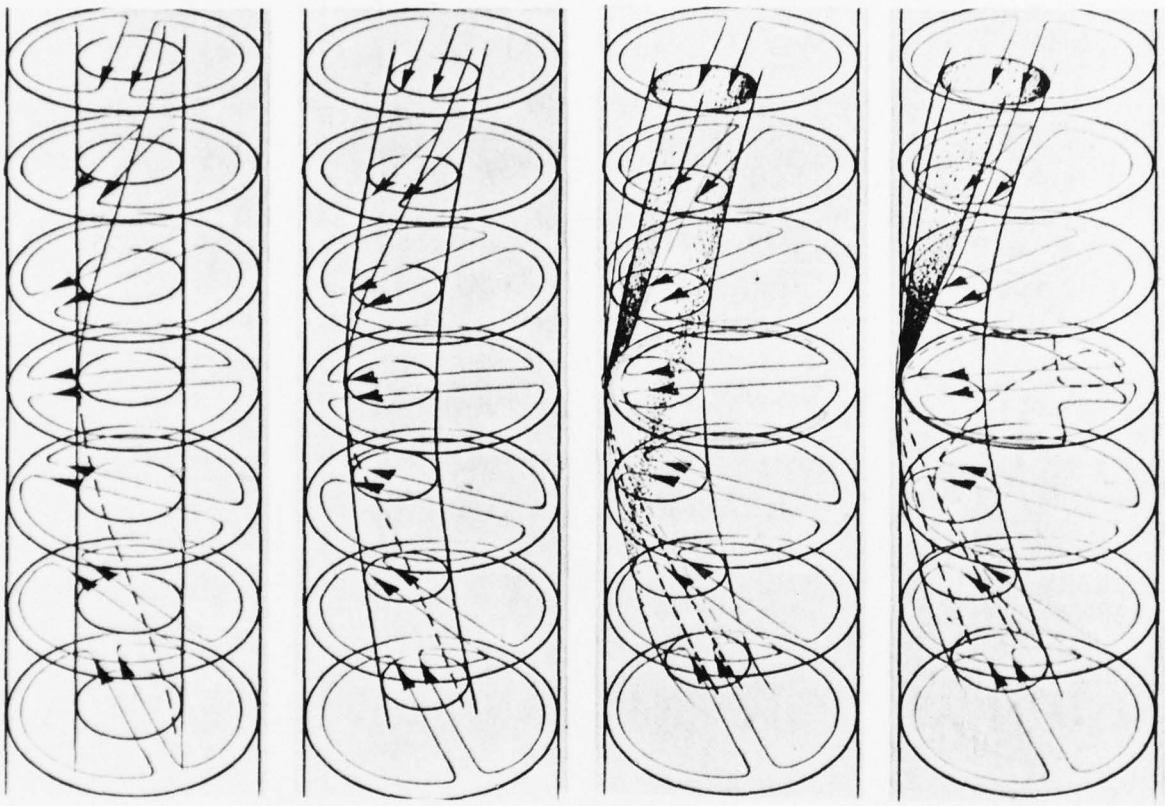

(a) (b) (c) (d)

Fig. VIII 4 — A three dimensional plot of a field line having higher pitch ($q < 1$) than the flow pattern. At $t = 0$, the field line wraps around the inner cylinder shown in (a). At $t = t_1$, (b) this cylinder convects like a rigid body (in the $r\theta$ plane) with the main flow and the field line continues to wrap around it. At $t = t_2$ (c), the field line enters the separation region at one point and begins to whip around, while most of the field line just continues to move as a rigid body. At $t = t_3$, (d) more of the field line has entered the separation region and the first part of the field line to enter the separation region has re-emerged out the other side of the cylinder. Clearly the field line is contorted much more than in Fig. VIII 3.

(Page 120 Blank)

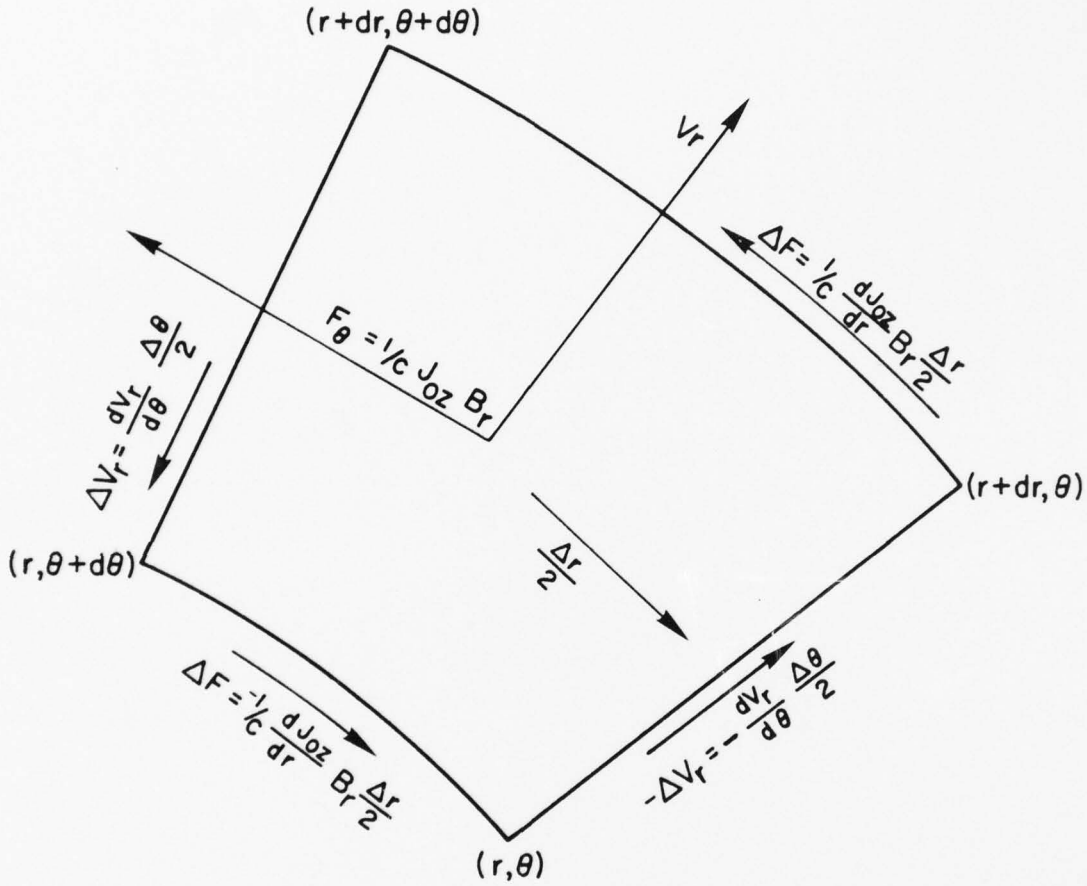

Fig. VIII 5 — A fluid element in cylindrical co-ordinates illustrating how $\partial J_{oz}/\partial r$ can give rise to a torque which enhances the rotation.

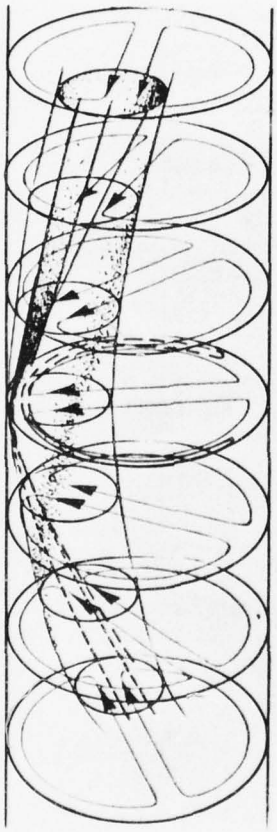

Fig. VIII 6 — The field pattern, analogous to Fig. VIII 4c if magnetic reconnection is allowed.

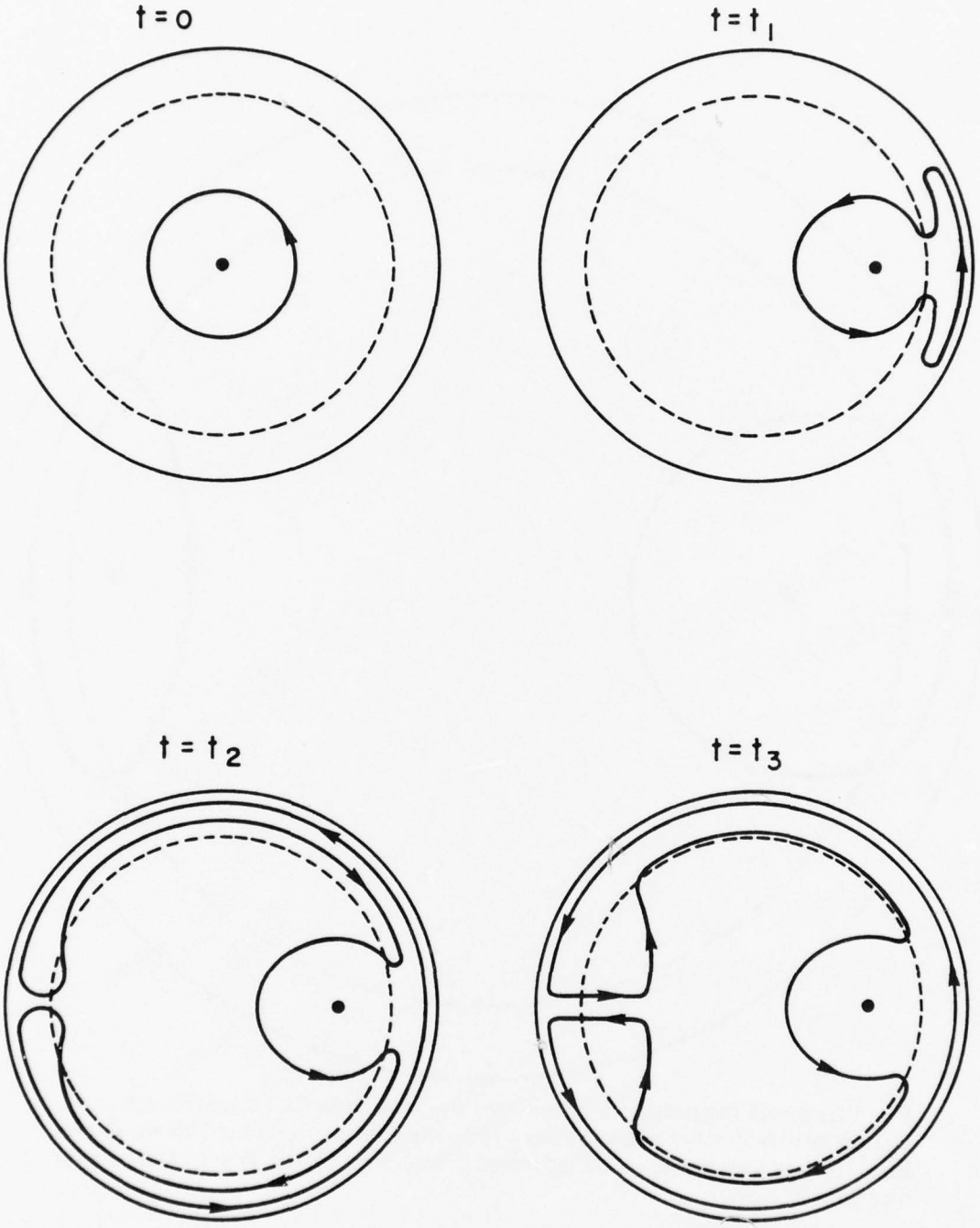

Fig. VIII 7 — A two dimensional field line in the r,θ plane which is frozen into the flow given by Eq. VIII 25. The field line is shown at four different times. Notice that it is rapidly convected around the separation layer and re-emerges into the main flow on the other side of the circle. At $t = t_3$ fields of opposite sign are forced next to each other in the separation layer and along a horizontal diameter on the left side of the circle.

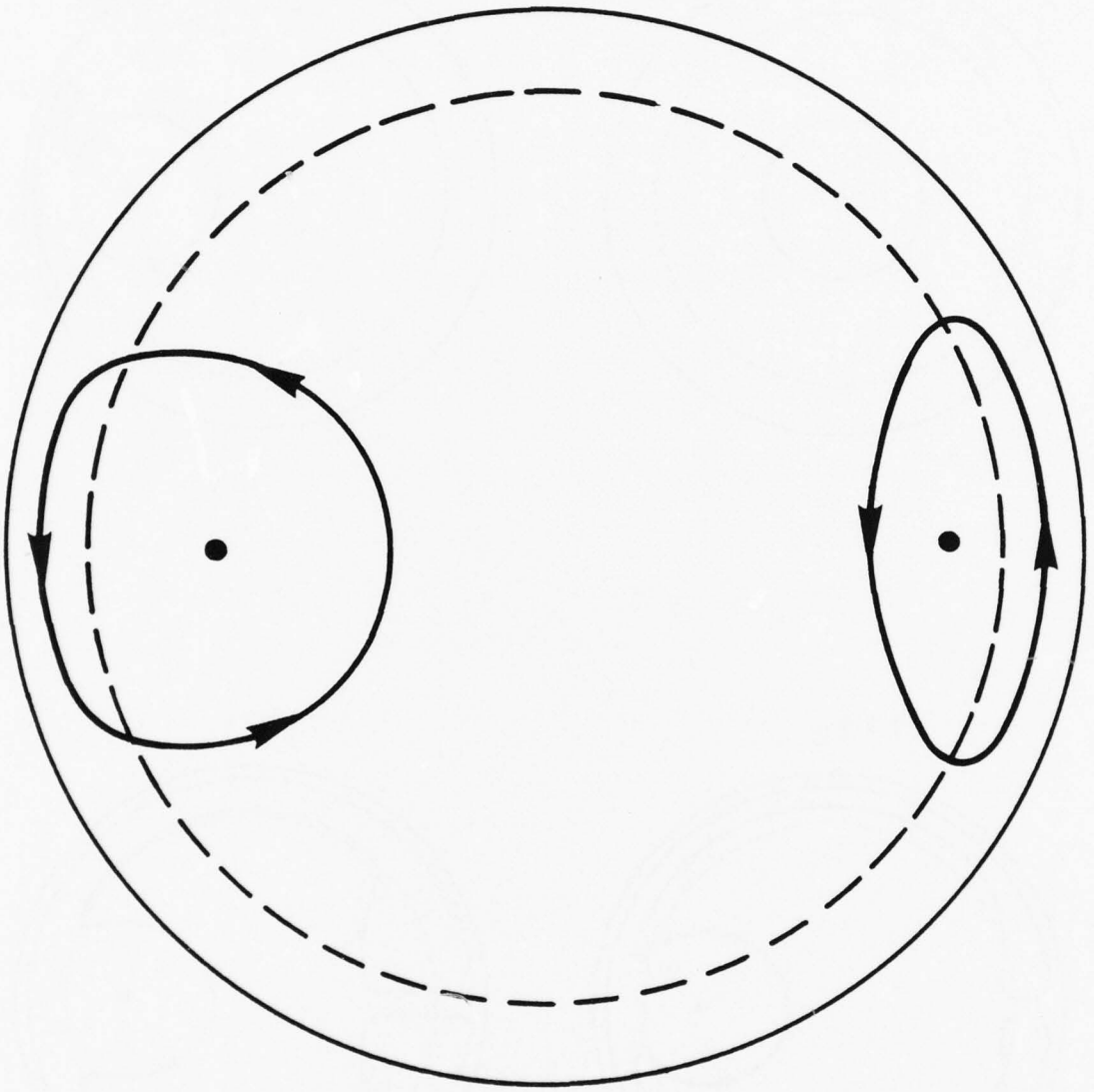

Fig. VIII 8 — If the resistivity is non zero the nearby field of opposite sign can diffuse into each other and annihilate each other leaving the field pattern shown here. Notice a magnetic island is formed in the circle on the side opposite to the direction of flow.

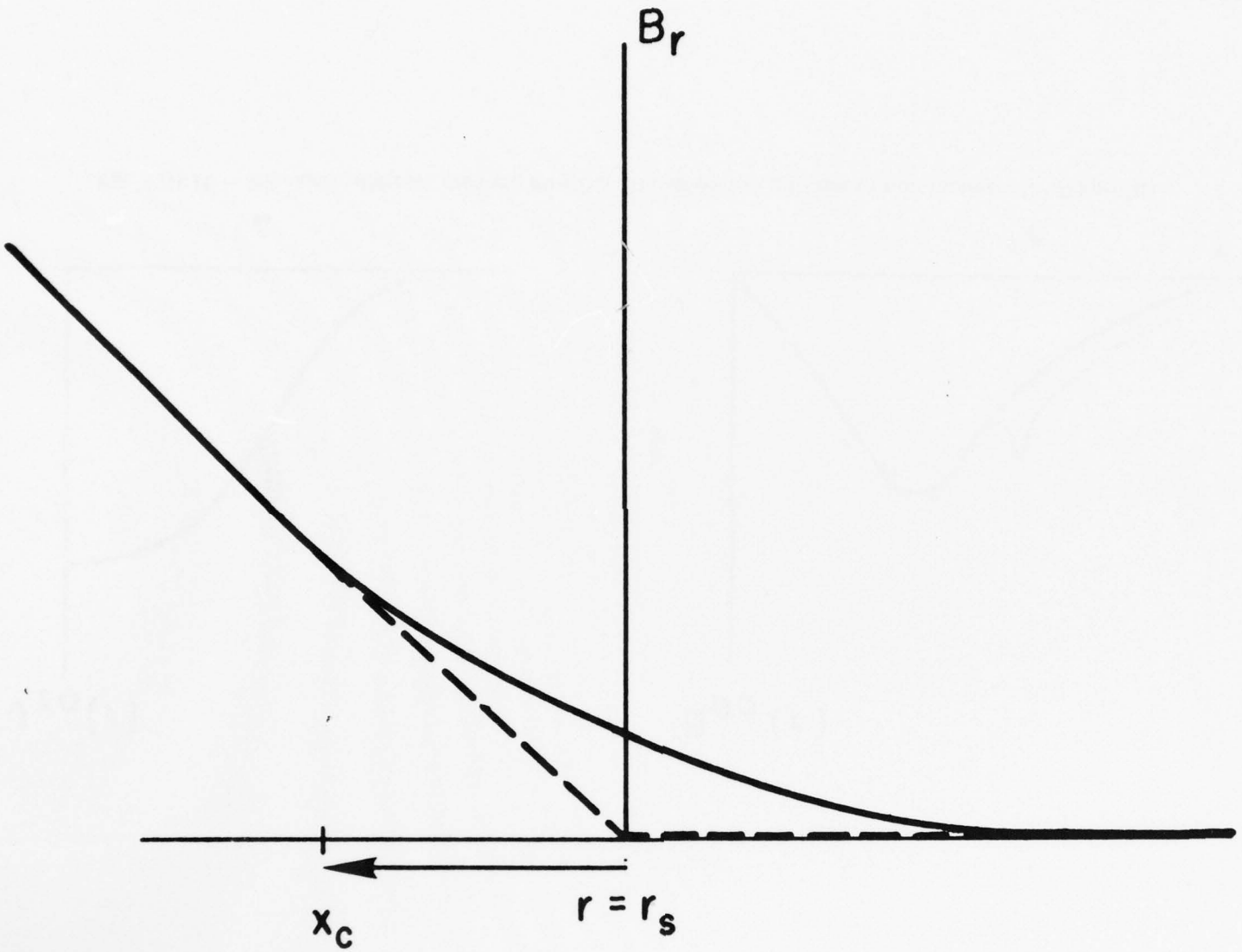

Fig. VIII 9 — A plot of B_r as a function of r for an m = 1 tearing mode.

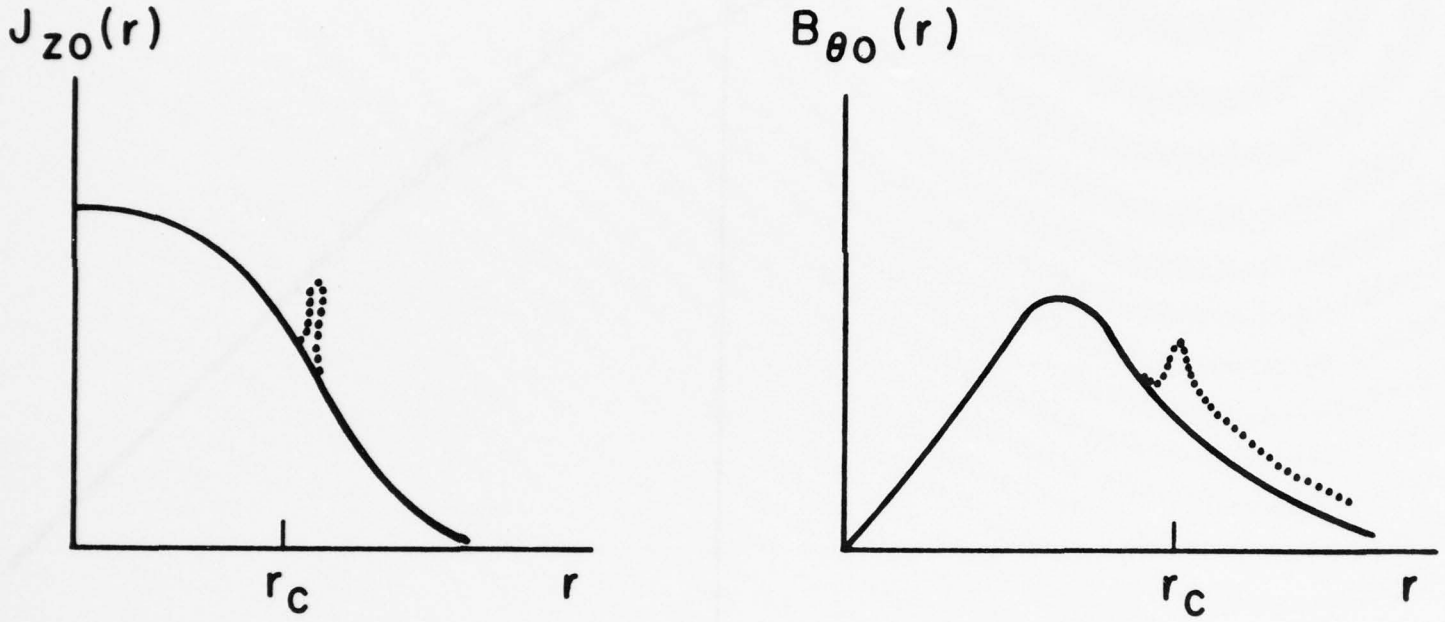

Fig. VIII 10 — Schematic diagram showing how the skin effect can give rise to non-monotonic q(r) profile.

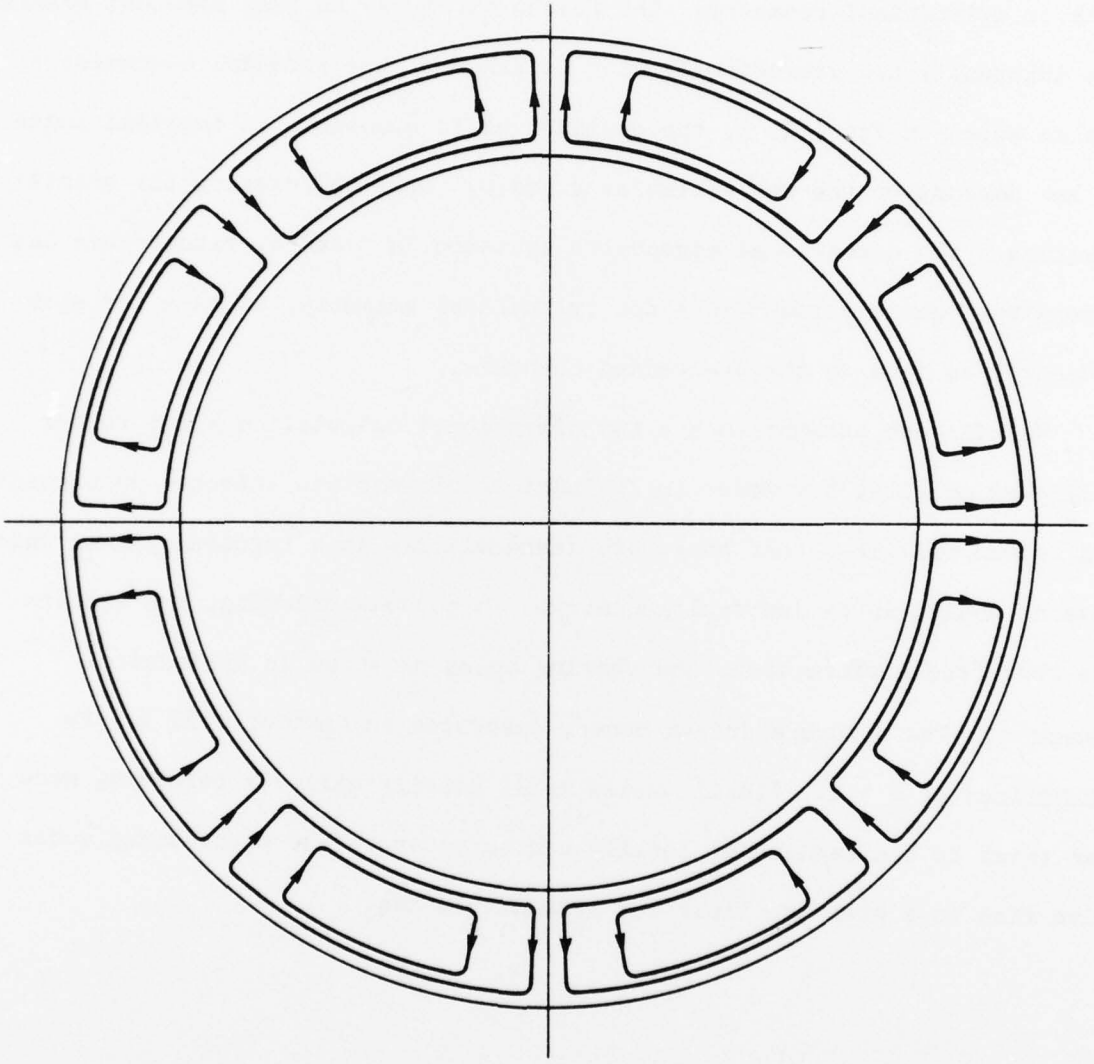

Fig. VIII 11 — The flow pattern for an m = 4 double tearing mode.

IX. Instabilities in a Toroidal Plasma

In this chapter, we just touch upon the question of MHD instabilities in toroidal geometry. The actual calculations of relevant instabilities has many more mathematical complications than the equivalent calculations in slab or cylindrical geometry. The reason of course is that toroidal plasmas are inherently two dimensional. For instance if the toroidal co-ordinates are as shown in Fig. IX. 1, the equilibrium is symmetric in toroidal angle ζ, but depends on the two variables r and θ. Thus calculating the stability involves a two dimensional eigenvalue equation in r and θ, rather than one dimensional calculations (in r for cylindrical geometry, or in x for slab geometry) as done in the preceeding chapters.

We will not attempt such a two dimensional calculation here; rather will examine first how modes in cylindrical plasmas are affected by toroidicity, and second will show that there are instabilities in a toroidal plasma which have no analog in cylindrical geometry. In tokamak ordering, the results are that free surface modes and tearing modes exist as in cylindrical geometry. The pressure driven modes, described in Chapter VIII b, are stabilized of $q > 1$. Finally a new mode, usually called a balooning mode, can exist in the regions of locally bad curvature. These balooning modes give rise to a pressure limit for tokamak plasmas.

We now examine these points more thoroughly. In the tokamak ordering, $a \ll R$, $B_\theta \ll B_z$, and all toroidal effects will be small by a factor of at least a/R. However in deriving the equations for modes with two dimensional structure in cylindrical geometry (Eqs. (IV 35) or (VIII 7)), all

terms of order a/R were neglected. Therefore, any instabilities which exist in this approximation for a cylindrical plasma should also exist in toroidal geometry if a<<R. The relevant instabilities are then the free surface modes described in Chapter IV and the tearing modes described in Chapter (VIII. d-f). However, as pointed out in Chapter (VIII. a), a plasma with no free surface and with zero resistivity is stable to modes with two dimensional structure. Now let us examine the pressure driven modes discussed in Chapter (VIII. b). These modes were driven by a pressure gradient, and as is apparent from Eq. (VIII.12c), the driving term is multiplied by $k^2r^2 \sim (r/R)^2$. However toroidal effects are also of this order, so that these pressure driven modes can be strongly affected. Calculation of the exact stability condition is mathematically involved and was first given by Mercier and also by Shafranov.

We will give here a plausible argument which gives the correct result, namely the pressure driven modes in a tokamak are stabilized if $q \equiv \frac{rB_{zo}}{RB_{\theta o}} > 1$.

Recall that Chapter V speculated that the effective gravity arose from forces acting on the fluid which originate in the geometrical complexities of $\underline{B}_o$ which had no analog in slab geometry. This was confirmed in Chapter VIII. b where the gravity was related to the curvature of field lines in cylindrical geometry. We will use this result to calculate the appropriate gravity for a toroidal plasma. Here, there are three geometrical effects which give rise to an average force having no analog in slab geometry. The first and second are forces due to the curvature of both the toroidal and poloidal field, the third is the outward force due to the fall off in toroidal field strength with major radius. This latter is clearly a geometrical effect since it is not balanced directly by a change in plasma

pressure. The average force on a particle arising from the curvature of the field lines is

$$\underline{F}_c = M v_{\parallel}^2 \frac{(\underline{B}_o \cdot \underline{\nabla})\underline{B}_o}{B_o^2} \qquad \text{(IX. 1)}$$

while the force on a particle resulting from the gradient of the strength of the toroidal field is

$$F_G = \frac{M v_{\perp}^2}{2} \frac{\underline{\nabla} |B_{zo}|}{|B_{zo}|} \qquad \text{(IX. 2)}$$

Adding up the forces on all particles, and using the fact that $\langle \frac{1}{2} v_{\perp}^2 \rangle = \langle v_{\parallel}^2 \rangle \equiv v_i^2$ for an isotropic plasma, we find that the effective gravitational force $\underline{g}$ is given by

$$\underline{g} = - v_i^2 \left(\frac{(\underline{B}_o \cdot \underline{\nabla}) B_o}{|B_o|^2} + \frac{\nabla |B_{zo}|}{|B_{zo}|} \right) \qquad \text{(IX. 3)}$$

Let us first calculate the $(\underline{B}_o \cdot \underline{\nabla})\underline{B}_o$ term above. To do so, let introduce cylindrical co-ordinates, shown in Fig. (IX. 2). Here ζ is the same angle as in Fig. IX. 1. The components of the field in cylindrical co-ordinates are

$$B_\zeta = B_{zo} \frac{R_o}{R} \qquad \text{(a)}$$

$$B_z = B_{\theta o} \frac{(R - R_o)}{\left[(R-R_o)^2 + z^2\right]^{1/2}} \qquad \text{(b)} \qquad \text{(IX. 4)}$$

$$B_R = B_{\theta o} \frac{z}{\left[(R-R_o)^2 + z^2\right]} \qquad \text{(c)}$$

Then after some algebra, one can make use of the expression for $(\underline{B}_o \cdot \underline{\nabla})\underline{B}_o$ in cylindrical co-ordinates to give the result

$$(\underline{B}_o \cdot \underline{\nabla})\underline{B}_o = \left\{ \frac{-B_{\theta o}^2 (R - R_o)}{(R-R_o)^2 + Z^2} - \frac{B_{zo}^2 R_o^2}{R^3} \right\} \underline{i}_R + \left\{ \frac{-B_{\theta o}^2 Z}{(R-R_o)^2 + Z^2} \right\} \underline{i}_z \qquad \text{(IX. 5)}$$

where we have included only the components in the Rz plane. In Eq. (IX. 5), the first term multiplying $\underline{i}_R$ and the $\underline{i}_z$ part clearly arise from the curvature of the poloidal field; the second term multiplying $\underline{i}_R$ arises from the curvature of the toroidal field.

Now pressure driven modes can occur when the density (or pressure) gradient is anti parallel to g. However the density gradient is in the negative r direction (here r is given in Fig. IX 1). Using the fact that

$$r = \left[(R-R_o)^2 + Z^2 \right]^{1/2} \qquad \text{(a)}$$

$$\underline{i}_r = \underline{i}_R \cos\theta + \underline{i}_z \sin\theta \qquad \text{(b)}$$

$$\theta = \arctan Z/(R-R_o) \qquad \text{(c)} \qquad \text{(IX. 6)}$$

we find

$$\left[(\underline{B}_o \cdot \underline{\nabla})\underline{B}_o \right] \cdot \underline{i}_r = - \frac{B_{\theta o}^2}{r} - \frac{B_{zo}^2 R_o^2 \cos\theta}{(R_o + r\cos\theta)^3} \qquad \text{(IX. 7)}$$

Similarly

$$\hat{i}_r \cdot \frac{1}{|B_{z_0}|} \nabla |B_{z_0}| = -\frac{\hat{i}_R \cdot \hat{i}_r}{R} = -\frac{\cos\theta}{R_0 + r\cos\theta} \qquad \text{(IX. 8)}$$

Thus our final expression for g is

$$\underline{g} \cdot \underline{\hat{i}}_r = V_i^2 \left[\frac{\frac{B_{\theta_0}^2}{r} + \frac{B_{z_0}^2 R^2 \cos\theta}{(R_0 + r\cos\theta)^3}}{\frac{B_{z_0}^2 R^2}{(R_0 + r\cos\theta)^2} + B_{\theta_0}^2} + \frac{\cos\theta}{R_0 + r\cos\theta} \right] \qquad \text{(IX. 9)}$$

Assuming that $B_{\theta o} << B_{zo}$, we find

$$\underline{g} \cdot \underline{\hat{i}}_r = V_i^2 \left[\frac{B_{\theta_0}^2}{r B_{z_0}^2} + \alpha \frac{\cos\theta}{R_0 + r\cos\theta} \right] \qquad \text{(IX. 10)}$$

The first term in the bracket of Eq. (IX. 10) is simply from the curvature of the field line in cylindrical geometry. The second is from the curvature and gradient of the toroidal field. It is a larger term than the first, but it nearly averages to zero over poloidal angle θ. In order to see the effect of this term, expand the denominator in powers of $\frac{r\cos\theta}{R}$ and average over θ. The result is

$$\langle \underline{g} \cdot \underline{\hat{i}}_r \rangle = \frac{V_i^2 B_{\theta_0}^2}{r B_{z_0}^2} (1 - q^2) \qquad \text{(IX. 11)}$$

Thus for $q>1$, the averaged g changes sign and is negative. Since $\frac{dn_o}{dr}$ and $\frac{dP_o}{dr}$ are also negative the effect of the gravity is no longer destabilizing. Therefore, tokamaks, which are characterized by $q>1$, are stable to pressure

driven modes. Reversed field pinches however, which have $q<1$, are potentially unstable to pressure driven modes in ideal MHD if the shear is not great enough, and are also potentially unstable to resistive g modes no matter what the shear is.

We close this chapter by qualitatively examining the problem of balooning modes in tokamaks. Notice that the gravity, $\underline{g}\cdot\underline{i}_r$ in Eq. (IX. 10) is the sum of two terms, one of which is constant along the field line and one which varies along a field line. The latter nearly averages to zero along a field line because of the cos θ in the numerator. However, in tokamak ordering the maximum value of this latter term is much larger than the value of the former ($\frac{2Rq^2}{r}$ larger, to be precise). This naturally brings up the following question: Can a mode be localized along a field line so that it only sees the positive, destabilizing, values of $\underline{g}\cdot\underline{i}_r$ (around $\theta\approx 0$) and not the negative, stabilizing, values? We will see that such instabilities can indeed be generated if the plasma pressure is too high. These are usually called balooning modes, probably in comparison to the behavior of a baloon of varying thickness. Imagine a baloon whose thickness varies around its surface, also imagine a second baloon of uniform thickness equal to the average thickness of the first. Say that someone is too weak to pop the second baloon; he might still be able to blow up and pop the first, because it blows out much more easily where the surface is thin.

This is then analogous to an MHD instability in a tokamak picking out the most unstable (outer) region and localizing itself there. Of course, it is not so simple for a mode to localize itself along a field line. Any disturbance which is localized along a field line is also setting up shear Alfven waves, which tend to give a positive frequency V_A^2/L^2 where L is the

characteristic length of the disturbance along the field line and V_A is the Alfven speed. The distance L is given roughly by $(2\pi)^{-1}$ times the distance along the field line between $\theta = -\pi/2$ and $\theta = \pi/2$, or $L \approx Rq_{/2}$. The maximum growth rate is given roughly by the maximum value of g divided by the gradient scale length, taken here as $1/r$. The plasma can only be stable if the outward motion forced by the gravity does not overcome the resistance to field line bending, or if

$$\frac{g}{L_n} \sim \frac{2V_i^2}{Rr} < k_{\parallel}^2 V_A^2 \sim \frac{4V_A^2}{R^2 q^2} .$$

This gives rise to an approximate limit on the total β of a tokamak of $\beta = \frac{V_i^2}{V_A^2} \lesssim \frac{2r}{Rq^2}$.

Now let us show how this basic result can be obtained more rigorously. If we assume slab geometry with all perturbed quantities varying as (z)exp i ky, $\underline{B}_o$ uniform and in the z direction, the density gradient in the x direction, and g varying with z, an analysis similar to that which led to Eq. (V.17) gives the result

$$\left(-\gamma\rho_o - \frac{B_o^2}{4\pi\gamma}\frac{\partial^2}{\partial z^2}\right) V_x + \frac{1}{\gamma}\frac{\partial \rho_o}{\partial x} g(z) V_x = 0 \qquad \text{(IX. 12)}$$

Specializing to a tokamak, where $\frac{\partial}{\partial z} = \frac{1}{Rq}\frac{\partial}{\partial \theta}$ and $g(z) = 2\frac{V_i^2 \cos\theta}{R}$, we find that Eq. (IX. 12) reduces to

$$\left\{-\frac{V_A^2}{R^2 q^2}\frac{d^2}{d\theta^2} + \gamma^2 - \frac{2V_i^2 \cos\theta}{RL_n}\right\} V_x(\theta) = 0 \qquad \text{(IX. 13)}$$

where L_n is the gradient scale length.

Notice that the last term in the parentheses is periodic in θ with period 2π. However the solution for $V_x(\theta)$ must also be periodic with the same periodicity, since V_x must be a single valued function of θ. Thus γ is determined by the condition that solutions to Eq. (IX. 13) exist which are periodic in θ with period 2π. An approximate criterion for unstable roots can be derived as follows. If $\gamma = 0$, the solutions to Eq. IX are oscilliatory between $-\pi/2 < \theta < \pi/2$ and are exponentially growing and damping for $\pi/2 < |\theta| < \pi$. Imagine a solution for V localized between $-\pi/2$ and $\pi/2$ and which damps to a very small value between say $\pi/2 < \theta < \pi$. Then the solution for V_x between $-\pi/2$ and $\pi/2$ does not affect the solution for V_x betweem say $3\pi/2$ and $5\pi/2$. The condition for a solution to Eq. (IX. 4) with zero γ is simply the condition for localized roots between the turning points, or according to WKB theory,

$$\int_{-\pi/2}^{\pi/2} d\theta \; \frac{V_i}{V_A} \, g \left(\frac{2R}{L_n} \cos\theta \right)^{1/2} = \pi/2 \qquad \text{(IX. 15)}$$

The eigenfunction is as shown in Fig. (IX. 3). Notice that between $\pi/2 < \theta < \pi$, V_x gets so small that it does not affect the value of V_x in $3\pi/2 < \theta < 5\pi/2$, where V_x gets large again. Using the fact that $\int_{-\pi/2}^{\pi/2} \sqrt{\cos}\, d\theta =$ we find that the plasma is unstable if

$$\frac{V_i^2}{V_A^2} > \qquad \text{(IX. 16)}$$

This condition then puts a limit on the maximum pressure which can be stably confined in a tokamak. If the plasma is unstable, growth rates can be calculated in an analogous way by setting

$$\oint d\theta \left(\frac{2 V_i^2 q^2 \cos\theta}{R L_n V_A^2} - \gamma^2 \right)^{1/2} = \pi \qquad \text{(IX. 17)}$$

The problem of balooning modes in sheared fields, and with nonzero resistivity is much more complicated and is still under active investigation.

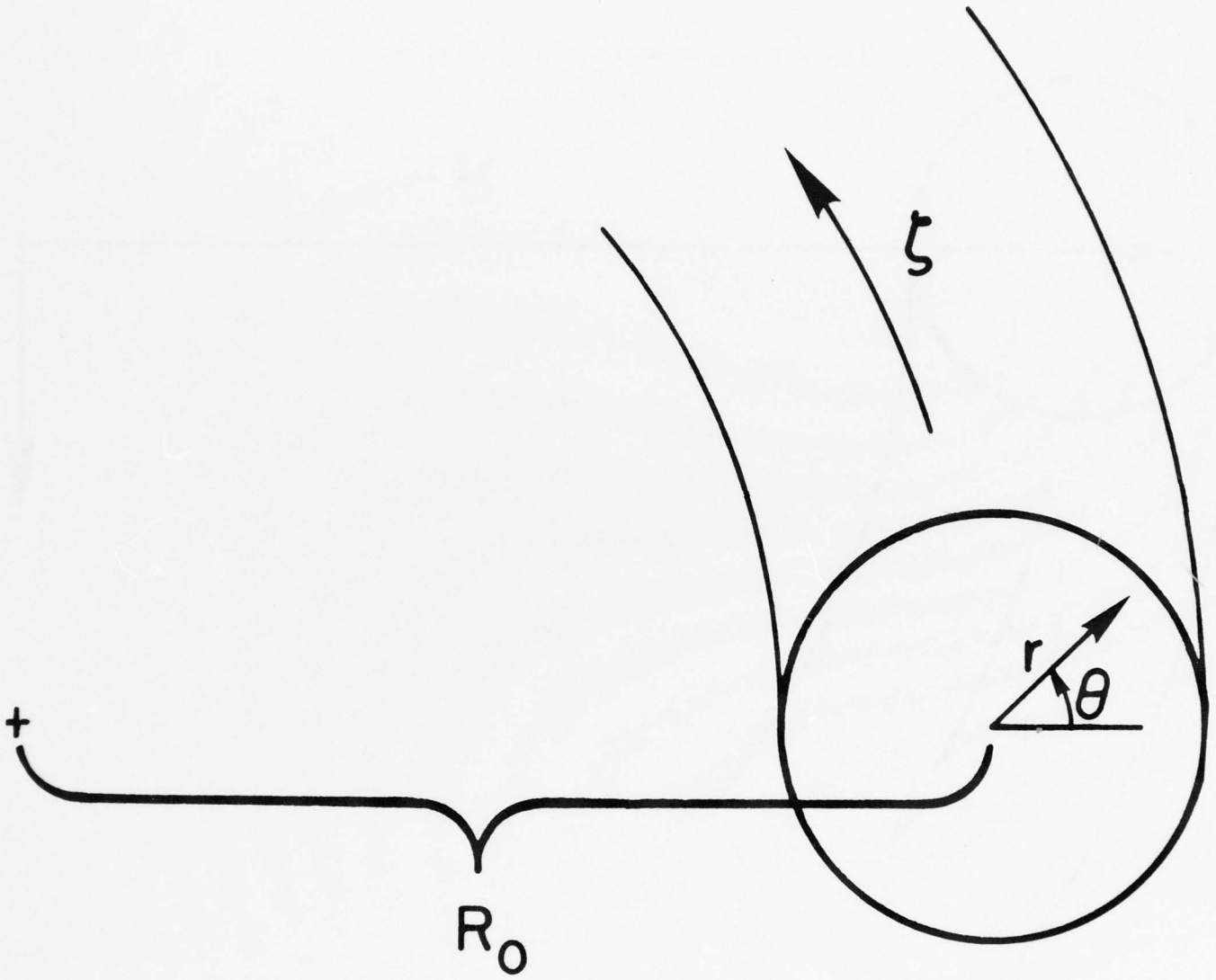

Fig. IX 1 — The toroidal co-ordinate r, θ, and ζ.

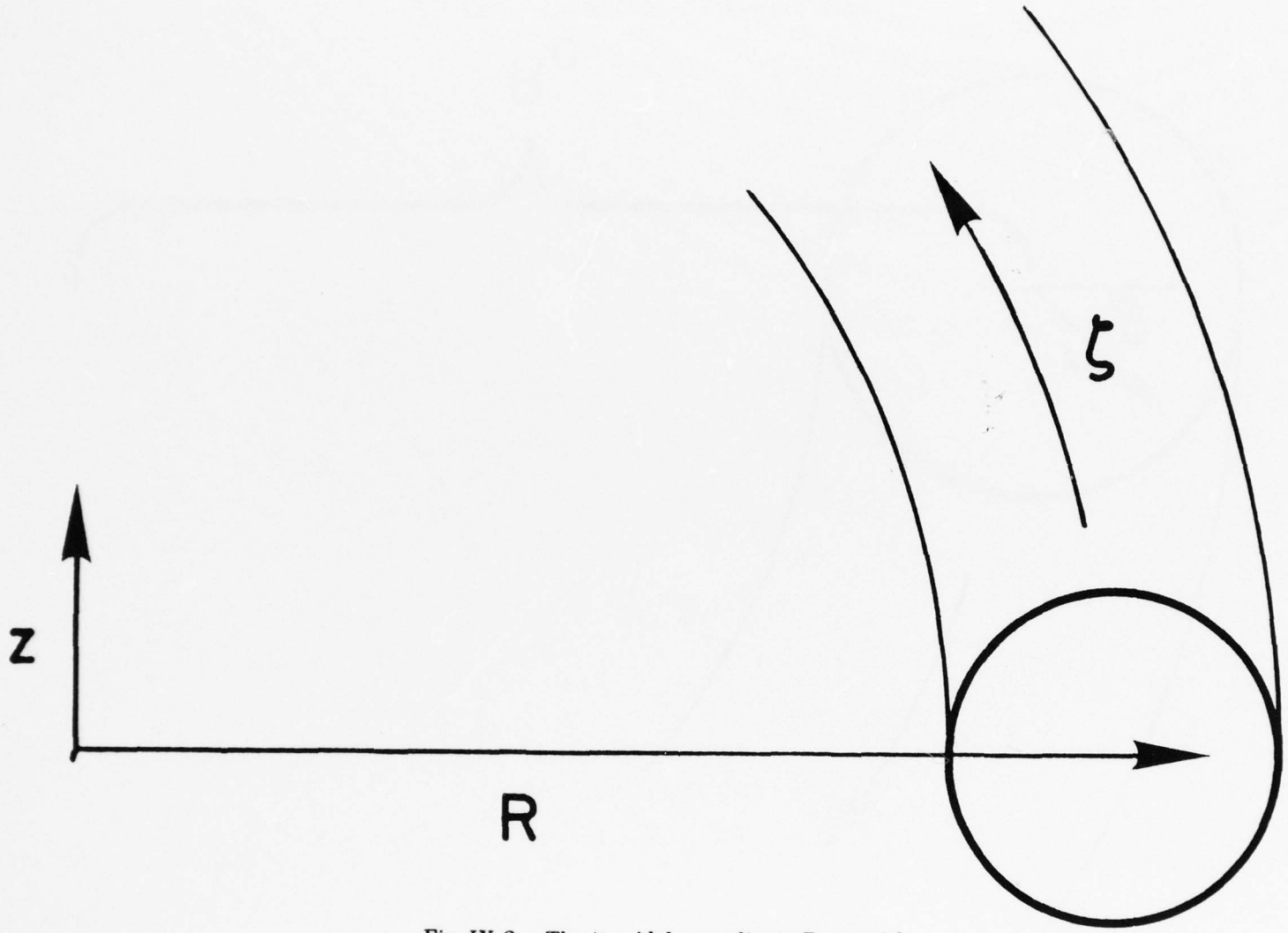

Fig. IX 2 — The toroidal co-ordinate R, z and ζ.

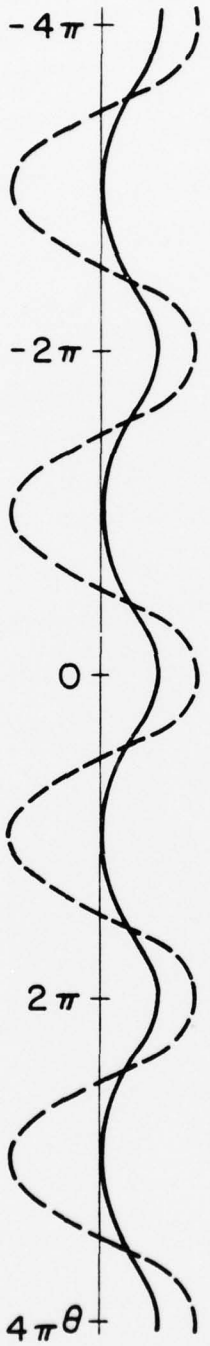

Fig. IX 3 — The eigenfunction (dotted curve) and local wave number squared (solid curve) for ballooning modes in a tokamak.